國 立 交 通 大 學

生物科技研究所
碩士論文

利用飽和定點突變方法探討酵母菌氧化鯊烯環化酵素內

Tyr707 和 Tyr710 對反應過程中 B 環形成的影響

Site-Saturated Mutagenesis Approach to Investigate the Influences of Tyr707 and Tyr710 within *Saccharomyces cerevisiae* Oxidosqualene-Lanosterol Cyclase to the B-ring Formation during the Polycyclization Processes

研 究 生：王采婷

指導教授：吳東昆 博士

中華民國 九十七年七月

Site-Saturated Mutagenesis Approach to Investigate the Influences of Tyr707 and Tyr710 within *Saccharomyces cerevisiae* Oxidosqualene-Lanosterol Cyclase to the B-ring Formation during the Polycyclization Processes

研究生：王采婷　　Student: Tsai-Ting wang

指導教授：吳東昆 博士　　Advisor: Dr. Tung-Kung Wu

國 立 交 通 大 學

生物科技研究所

碩士論文

A Thesis

Submitted to Department of Biological Science and Technology

College of Science

National Chiao Tung University

in partial Fulfillment of the Requirements

for the Degree of

Master

in

Biological Science and Technology

July, 2008

Hsinchu, Taiwan, Republic of China

中華民國九十七年七月

利用飽和定點突變方法探討酵母菌氧化鯊烯環化酵素內 Tyr707 和 Tyr710 對反應過程中 B 環形成的影響

學生：王采婷　　指導教授：吳東昆　博士

國立交通大學　生物科技研究所碩士班

摘要

(3*S*)-2,3-氧化鯊烯((3*S*)-2,3-oxidosqulaene)可經由不同的環化酵素催化而產生各式各樣的三萜類化合物，這複雜的環化反應在這半世紀以來一直令有機及生物化學家為之著迷。在酵母菌及哺乳類動物中，氧化鯊烯環化酵素(oxidosqualene-lanosterol cyclase, ERG7)催化(3*S*)-2,3-氧化鯊烯產生具有四個環的羊毛硬脂醇(lanosterol)，透過所謂的"椅形-船形-椅形" (chair-boat-chair)的折疊方式。這個複雜的環化/重組反應機制包括一開始氧化鯊烯的環氧基被質子化而斷裂，接著由碳陽離子-π 電子作用 (cationic-π interaction)所引導的四個環的環化反應和一連串氫化基及甲基的重排，以及最後具有高度專一性的去質子化步驟。在此我們利用飽和定點突變的方法，來探討酵母菌的氧化鯊烯環化酵素內 Tyr707 以及 Tyr710 這兩個被高度保留的芳香性胺基酸，在酵素催化反應的過程中所扮演的角色。經由產物的分析，我們在 $ERG7^{Y707X}$ 的突變株中，分離出先前從未被發表過的雙環新產物(9*R*,10*S*)-polypoda-8(26),13*E*,17*E*,21-tetraen-3β-ol，以及其他因改變最後的去質子化位置而造成的產物。因此我們推測 Tyr707 在環化機制中可能是扮演穩定雙環 C-8 碳陽離子以及最終的羊毛硬脂醇 C-8/C-9 碳陽離子中間物的角色。將這個位置的胺基酸替換成其他胺基酸則會干擾整個環化/重組反應的過程，因而導致環化不完全的雙環產物以及其他改變最後去質子化位置的產物產生。另外在 $ERG7^{Y710X}$ 方面，由飽和定點突變分析顯示，在某幾個突變點中產生了羊毛硬脂醇及兩個因改變最後的質子化位置而造成的產物，parkeol 和 9β-lanosta-7,24-dien-3β-ol。此外，在 Tyr710Arg 的突變株中也產生了兩個單環的產物， achilleol A 和 camelliol C。而所有突變點中只有 Tyr710Pro 使

氧化黨烯環化酵素失去活性，且沒有任何產物產生。由這些實驗結果，我們推測 Tyr710 可能透過與 Trp390 作用來影響單環 C-10 碳陽離子中間物的穩定性，並且在維持蛋白質的結構及活性區的形狀上有所貢獻。

Site-Saturated Mutagenesis Approach to Investigate the Influences of Tyr707 and Tyr710 within *Saccharomyces cerevisiae* Oxidosqualene-Lanosterol Cyclase to the B-ring Formation during the Polycyclization Processes

Student: Tsai-Ting Wang Advisor: Dr. Tung-Kung Wu

Institute of Biological Science and Technology

Naitonal Chiao Tung Unversity

Abstract

The enzymatic cyclization of acyclic 2,3-oxidosqualene to polycyclic triterpenoids is one of the most complicated biochemical reactions that captured the interest of organic chemists and biochemists for over half a century. In fungi and mammals, oxidosqualene-lanosterol cyclase (ERG7) converts (*3S*)-2,3-oxidosqualene to the tetracyclic sterol precursor lanosterol via the so called "chair-boat-chair" conformation. The postulated cyclization/rearrangement reaction encompasses oxirane ring protonation and cleavage, cationic/π interaction-directed consecutive tetracyclic ring cyclization, 1,2-shifted hydride and methyl groups rearrangement, and final highly specific deprotonation step. Site-saturated mutagenesis experiments were carried out on two highly conserved aromatic residues, Tyr707 and Tyr710, of *Saccharomyces cerevisiae* ERG7 to investigate their functional roles in the oxidosqualene cyclization/rearrangement reaction. A novel bicyclic intermediate, (9*R*,10*S*)-polypoda-8(26),13*E*,17*E*,21-tetraen-3β-ol, with several altered deprotonation products were isolated from the ERG7^{Y707X} mutants. It indicates that the Tyr707 residue may play an important role in stabilizing both the bicyclic C-8 cation and the final lanosteryl C-8/C-9 cationic intermediate. On the other hand, the site-saturated mutagenesis of ERG7^{Y710X} revealed that two altered deprotonation products, parkeol and

9β-lanosta-7,24-dien-3β-ol as well as lanosterol, were produced in several mutants. Besides, the Tyr710Arg mutant produced two monocyclic products, achilleol A and camelliol C, and only the Tyr710Pro mutant lost the cyclase activity. These results suggested that Tyr710 may influence the stability of the monocyclic C-10 cationic intermediate through the interaction with Trp390 and play a role in preserving the cyclase structure and the conformation of active site.

誌謝(Acknowledgement)

兩年的研究所生涯，轉眼間即將隨著這本論文的誕生而劃上句點。回想當初對一切都還懵懵懂懂的我，經過兩年的淬鍊與成長，如今也要畢業了。這兩年的生活，酸甜苦辣，不在話下。而這本論文能順利完成，要感謝的人實在是太多了，如果沒有你們，我大概也無法順利地取得這紙畢業證書，簡短的隻字片語實在難以表達出我的感激之意，僅在此列出，獻上我最由衷的感謝。

最首要感謝的人是吳東昆老師，感謝您這兩年的教誨與指導，如果不是您當初收留了沒有任何生物背景的我，我也不會有今天。謝謝您一直包容身體很虛的我，也提供我們一個自由的研究環境讓我們發揮。而在您這兩年的教誨下，我也學習到實驗的精神與積極的態度，及許多待人處事的道理。另外也感謝李耀坤教授、袁俊傑教授與鄭建中教授對這篇論文的指教，使本論文能更加完善有系統。也特別感謝清大貴儀中心彭菊蘭女士在 NMR 上所提供的協助。

再來要感謝實驗室的程翔學長與媛婷學姐，感謝你們在這兩年來一直帶領著我一步步的學習，並且幫忙我解決各種實驗上的疑難雜症，以及在實驗上及知識上無私的傳授。學長的嚴謹與學姊的開朗積極一直都是 OSC 組的兩大支柱，在此也恭賀學長順利畢業。另外感謝文暄學姊，用心的帶著剛進實驗室的我做實驗；感謝晧宇學長特地從台北跑回來帶我一起通銀染。感謝晉豪學長在 GC-MS 操作上的指導與協助；文鴻學長總像個大哥哥一樣關心著每個人，跟你討論實驗總是能獲益良多；感謝裕國學長在生活上的關心與照顧；感謝衣鵑學姊在我壓力很大時，總是有耐心的聽我抱怨，並提供我許多照顧身體的方法。感謝同學文祥幫忙處理畢業相關的事宜，讓我省了不少麻煩；另外也謝謝小高這兩年來幫忙我各種大大小小的雜事與苦力；感謝亦諄、天昶、禕庭及育勳在這一年來的幫忙及對實驗室大小雜務的付出，及其它學弟妹們在口試期間的幫忙。總之，謝謝各位實驗室夥伴們在這兩年來的陪伴與包容。另外也特別謝謝宗哥在我最無助的時候陪伴著我，帶給我許多的歡笑。

當然也要特別感謝默默支持我、關心我的家人們，你們永遠是我最大的精神支柱，伴我度過這兩年在異地的求學之路。

另外也感謝好友馨慧的關心與陪伴，在我壓力極大時幫助我度過那些難熬的時光；還有又仁在我寫論文遇到瓶頸時提供的建議；以及盧叔、唯聖、敏書在最後這段日子給我的支持與鼓勵，在此也預祝你們都能順利畢業。

謝謝所有曾關心、幫助過我的人。僅以此論文獻給你們。

Table of Contents

Abstract (Chinese) I

Abstract (English) III

Acknowledgement V

Table of Contents VI

List of Figures IX

List of Tables X

List of Schemes XI

Chapter 1 Introduction 1

1.1 Triterpenoids and Steroids 1

1.2 Triterpene Synthases 5

1.3 Overview of the Enzymatic Polycyclization: Oxidosqualene-Lanosterol Cyclase and Squalene-Hopene Cyclase 8

1.3.1 The Hypothesis for Triterpene Synthetic Mechanism 8

1.3.2 Oxidosqualene-Lanosterol Cyclase (OSC) 11

1.3.3 Squalene-Hopene Cyclase (SHC) 17

1.4 Bicyclic Triterpenoids 21

1.5 The Amino Acid Sequence Alignment of (Oxido-)squalene Cyclase 25

1.6 Research Goal 28

Chapter 2 Materials and Methods 31

2.1 Materials 31

2.2 Methods 38

2.2.1 The Construction of Recombinant Plasmids 38

2.2.2 Preparation of Competent Cell (CBY57 and TKW14C2) 41

2.2.3 Ergosterol Complementation (expression mutated ERG7 gene in yeast strain TKW14C2) 42

2.2.4 Plasmid Shuffle and Counter Selection (expression mutated ERG7 gene in yeast strain CBY57) 43

2.2.5 Extracting Lipids and Column Chromatography 43

2.2.6 Acetylating Modification and Argentic Column Chromatography 44

2.2.7 $AgNO_3$-impregnated Silica Gel Chromatography 45

2.2.8 Deacetylation Reaction of the Modified Compounds 45

2.2.9 GC-MS Column Chromatography Condition 45

2.2.10 Molecular Modeling 46

Chapter 3 Results and Discussions 47

3.1 Functional Analysis of Tyr707 within *S. cerevisiae* ERG7 47

3.1.1 Site-Saturated Mutagenesis of Tyr707 47

3.1.2 Identification and Characterization of the Novel Product 52

3.1.3 Proposed Cyclization/Rearrangement Mechanism of TKW14C2 Expressing $ERG7^{Y707X}$ 56

3.1.4 Analysis of the $ERG7^{Y707X}$ Mutants with the ERG7 Homology Modeling 58

3.2 The Double Mutagenesis of $ERG7^{F699M/Y707H}$ and $ERG7^{F699M/Y707Q}$ 64

3.3 Functional Analysis of Tyr710 within *S. cerevisiae* ERG7 66

3.3.1 Generation of Site-Saturated Mutants of Tyr710..... 66

3.3.2 Lipid Extraction, Column Chromatography and Product Characterization. 68

3.3.3 Proposed Cyclization/Rearrangement Mechanism of TKW14C2 Expressing ERG7^{Y710X}..... 71

3.3.4 Analysis of the ERG7^{Y710X} Mutants with the ERG7 Homology Modeling..... 72

Chapter 4 Conclusion..... 76

Chapter 5 Future Perspective 80

Chapter 6 Reference..... 81

Appendix 1 85

Appendix 2 86

Appendix 3 87

List of Figures

Fig. 1-1 The structures of (a) isoprene (b) the basic ring system of steroids.....1

Fig. 1-2 The sterol biosynthetic pathway.....4

Fig. 1-3 The product diversity of triterpene synthases.....5

Fig. 1-4 Cyclization of oxidosqualene to the protosteryl and dammarenyl cations.....7

Fig. 1-5 The hypothetic model proposed by Johnson.....9

Fig. 1-6 Griffin's aromatic hypothesis model.....10

Fig. 1-7 The structure of human OSC with Ro 48-8071.....15

Fig. 1-8 The structure of human OSC with lanosterol.....15

Fig. 1-9 The X-ray crystal structure of *A. acidocaldarius* SHC.....18

Fig. 1-10 Stereo view of the active-site of *A. acidocaldarius* SHC.....20

Fig. 1-11 Cyclization of oxidosqualene with chair-chair conformation to form bicyclic triterpene compounds from bicyclic cation.....21

Fig. 1-12 Cyclization of squalene to form bicyclic triterpene compounds from bicyclic cation.....22

Fig. 1-13 Bicyclic products obtained by the mutated *A. acidocaldarius* SHCs.....24

Fig. 1-14 Amino acid sequence alignment of ERG7, CAS, SHC genes.....27

Fig. 1-15 The human OSC strucute with lanosterol.....29

Fig. 2-1 QuikChange site-directed mutagenesis strategies.....41

Fig. 2-2 The acetylation modification.....44

Fig. 3-1 The strategies of two selection method using TKW14C2 and CBY57 strains....48

Fig. 3-2 The TLC analysis of the unknown compound.....52

Fig. 3-3 GC analysis of the NSL extracts derived from ERG7^{Y707Gly}.....52

Fig. 3-4 The mass spectra of all products of ERG7^{Y707X} mutants.....53

Fig. 3-5 The structure and the NOE correlation of the unknown compound.....54

Fig. 3-6The homology models of wild-type ERG7 and ERG7^{Y707X} complexed with lanosterol.....61

Fig. 3-7 The product patterns of ERG7^{Y710Gly}, ERG7^{Y710Ile} and ERG7^{Y710Arg} mutants GC analysis and their mass patterns.....69

Fig. 3-8 The homology models of ERG7^{Y710X} mutants coupled with wild-type ERG7.....75

List of Tables

Table 2-1 QuikChange Site-Directed Mutagenesis Kit PCR composition.....39

Table 2-2 Reaction conditions for PCR mutagenesis reaction.....39

Table 2-3 QuikChange Site-Directed Mutagenesis PCR products digestion.....39

Table 3-1 The site-saturated mutants of *S. cerevisiae* ERG7^{Y707X} and its viability in TKW14C2 and CBY57 strains.....49

Table 3-2 The product profile of *S. cerevisiae* TKW14 expressing ERG7^{Y707X} site-saturated mutants.....50

Table 3-3 NMR assignments for (9*R*,10*S*)-polypoda-8(26),13*E*,17*E*,21-tetraen-3β-ol for dilute CD_2Cl_2 solution.....54

Table 3-4 The distance of Tyr707 to C-8 in the homology models complexed with bicyclic C-8 cation and lanosterol, respectively.....63

Table 3-5 The genetic selection results and the product profiles of the ERG7$^{F699M/Y707H}$ and ERG7$^{F699M/Y707Q}$ double mutants.....64

Table 3-6 The site-saturated mutants of *S. cerevisiae* ERG7^{Y710X} and its viability in TKW14C2 and CBY57 strains.....67

Table 3-7 The product profile of *S. cerevisiae* TKW14 expressing ERG7^{Y710X} site-saturated mutants.....70

List of Schemes

Scheme Ⅰ The proposed cyclization mechanism of OSC.....12

Scheme Ⅱ Proposed mechanism for concerted C-ring expansion/D-ring formation by Hess.....13

Scheme Ⅲ The proposed cyclization mechanism of SHC.....17

Scheme Ⅳ The proposed cyclization/rearrangement mechanism occurred in the ERG7^{Y707X} site-saturated mutants.....57

Scheme Ⅴ The proposed cyclization/rearrangement mechanism occurred in the ERG7^{Y710X} site-saturated mutants.....71

Chapter 1 Introduction

1.1 Triterpenoids and Steroids

Terpenes are a large class of hydrocarbons, which derived biosynthetically from units of isoprene (Fig. 1-1a). The basic molecular formula of terpene is $(C_5H_8)_n$, where n is the number of linked isoprene units. There are many types of terpenes, including monoterpenes ($C_{10}H_{16}$), sesquiterpenes ($C_{15}H_{24}$), diterpenes ($C_{20}H_{32}$), triperpenes ($C_{30}H_{48}$), and tetraterpenes ($C_{40}H_{64}$). Terpenoids are oxygen-containing compounds which derive from terpenes, and they constitute the largest group of natural products. The acyclic triterpene, squalene, is an important metabolic precursor of sterols, steroid hormones, and related membrane components.

The lipid components obtained from plants and animals contain an important group of compounds known as steroids. Steroids are derivatives of the perhydrocyclopentanophenanthrene ring system (Fig. 1-1b), usually has an alkyl group on C17.[1] Steroids are important biological regulators that show many physiological effects in living organisms. They include the sex hormones, adrenal cortical hormones, the bile acids, vitamin D and sterols, and exist in plants, animals and fungi.

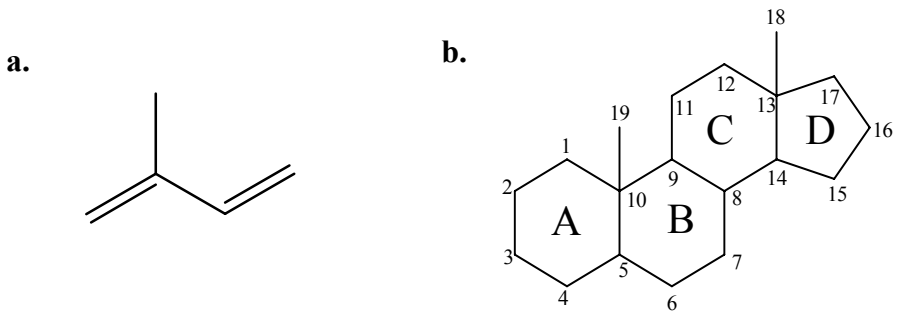

Figure 1-1 The structures of (a) isoprene (b) the basic ring system of steroids.

Cholesterol is the most important sterol in vertebrates. It is a primary component of the cell membranes and serves as an intermediate in the biosynthesis of most of the important steroids. Therefore, it is essential to life. Cholesterol circulates in the bloodstream and is synthesized by the liver and several other organs. However, high levels of blood cholesterol have been implicated in the development of arteriosclerosis and in heart attacks that occur when cholesterol-containing plaques block arteries of the heart. On the other hand, for those who suffer from the genetic disease "familial hypercholesterolemia" (FH), other means of blood cholesterol reduction are required.

Cholesterol and other steroids are generally biosynthesized from acetyl coenzyme A. It was converted to isoprene units firstly, and condensed to a linear molecule with 30 carbons, squalene, which is the substrate of squalene-hopene cyclase in bacteria. Squalene was further epoxidized to 2,3-oxidosqualene, which is the cyclization precursor of lanosterol, also leading to cholesterol in animals and ergosterol in fungi. In the biosynthetic pathway, the rate limiting step is controlled by 3-hydroxy-3-methylglutaryl-coenzyme A (HMG-CoA) reductase, which catalyzed the reduction of HMG-CoA to form mevalonic acid (Fig. 1-2). HMG-CoA reductase is also the target of the statin class of cholesterol-lowering drugs.[2] Clinical trials of statin treatments have revealed significant reductions in cardiovascular mortality and morbidity that are associated with lowering cholesterol levels.[3] However, statins also reduce the levels of some non-sterol intermediates (e.g. isoprenoids, dolichol and ubiquinone) synthesized through the 'second messenger pathway' of the cholesterol synthetic pathway and cause adverse clinical events.[4,5] On the other hand, inhibitors of oxidosqualene-lanosterol cyclase (OSC) as anticholesteraemic drugs act downstream of farnesyl-pyrophosphate in the cholesterol pathway and do not interfere with the synthesis of isoprenoids and coenzyme Q. Therefore, the enzyme OSC represents a novel target for cholesterol-lowering drugs. [6]

Oxidosqualene-lanosterol cyclase, which is encoded by *ERG7* gene, catalyzes the

cyclization of linear 2,3-oxidosqualene to lanosterol, the first sterol to be formed in the pathway (Fig. 1-2). It is another crucial step in the sterol biosynthesis, and it also as the target in the development of antifungal and hypocholesterolemic drugs. The reaction mechanism catalyzed by OSC is a very complicated and highly selective reaction which encompasses protonation, cyclization, rearrangement of methyl groups and hydrides shift, and final deprotonation. The product, lanosterol, which has seven chiral centers, reveals the highly regio- and stereochemical specificity of the oxidosqualene-lanosterol cyclase. Therefore, current researches focused on OSC and try to elucidate the structure-function relationships of this enzyme. It might provide more useful information for developing appropriate antifungal and hypocholesterolemic drugs.

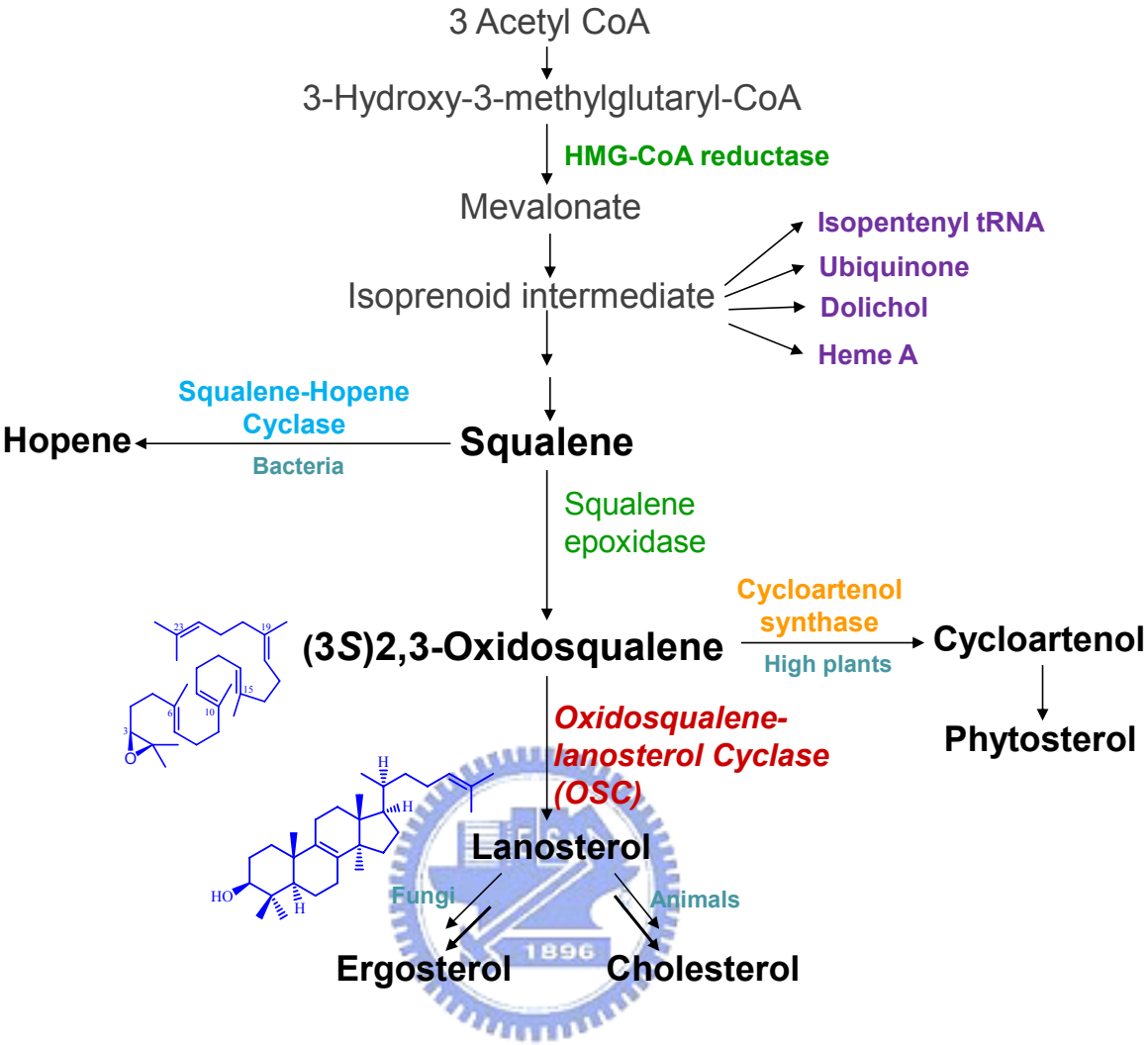

Figure 1-2 The sterol biosynthetic pathway

1.2 Triterpene Synthases

The triterpenoids are a large and structurally diverse group of natural products derived from squalene or other acyclic 30-carbon precursors.[7] The unusually complex and flexible reaction mechanism generates these ring systems and results in over 100 distinct triterpenoid skeletons. The enzymes that catalyze these reactions are known as triterpene synthases and can be categorized as squalene cyclases or oxidosqualene cyclases, which convert squalene and oxidosqualene to diverse triterpenes and triterpene alcohols, as shown in Figure 1-3. The enzymatic cyclization of squalene or oxidosqualene to polycyclic triterpenoids is one of the most complicated biochemical reactions that captured the interest of organic chemists and biochemists for over half a century.

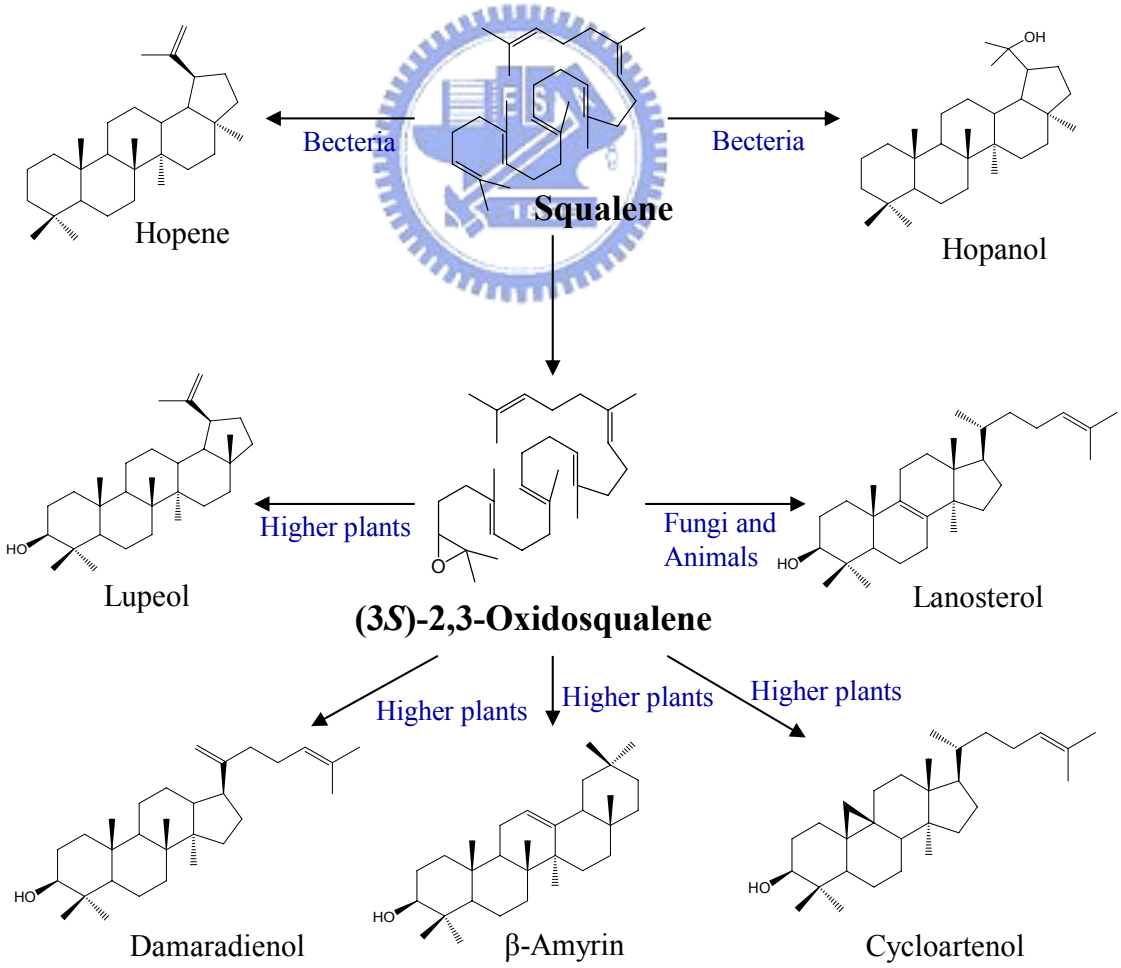

Figure 1-3 The product diversity of triterpene synthases.

There is a general mechanism among these enzymes, involving: 1) binding of the

polyolefinic substrate in a folded conformation, 2) initiation of the reaction by protonation of a double bond (squalene) or an epoxide (2,3-oxidosqualene), 3) ring formation, 4) skeletal rearrangement by 1,2-methyl and hydride shifts in some cases, and 5) termination by deprotonation or addition of water.[8] However, there are still many differences in their mechanisms. The enormous skeletal diversity found among the triterpenes is the result of different cyclization reactions that lead to varied carbocyclic skeletons, hydride and methyl shifts, and different cation-quenching steps.

The substrate in these enzymes is pre-folded into two different conformations. In squalene-hopene cyclases, the binding substrate squalene is pre-folded into all-chair conformation. However, there are two folding types within oxidosqualene cyclases, chair-chair-chair and chair-boat-chair (Fig. 1-4). Although the chair-boat-chair conformation is more common in oxidosqualene cyclases (ex: oxidosqualene-lanosterol cyclase and cycloartenol synthase), some enzymes in this family such as lupeol synthase and β-amyrin synthase folded the substrate in a chair-chair-chair conformation.

The different substrate prefolded conformation results in the formation of different intermediate cations. These species-dependent cyclization products can be categorized into two types, protosteryl and dammarenyl cation. The difference between the two major intermediate cations is the conformation of B-ring. In protosteryl cationic pathway, a six-membered B-ring boat form was produced, whereas the chair form of B-ring was found in the dammarenyl cationic pathway (Fig. 1-4).

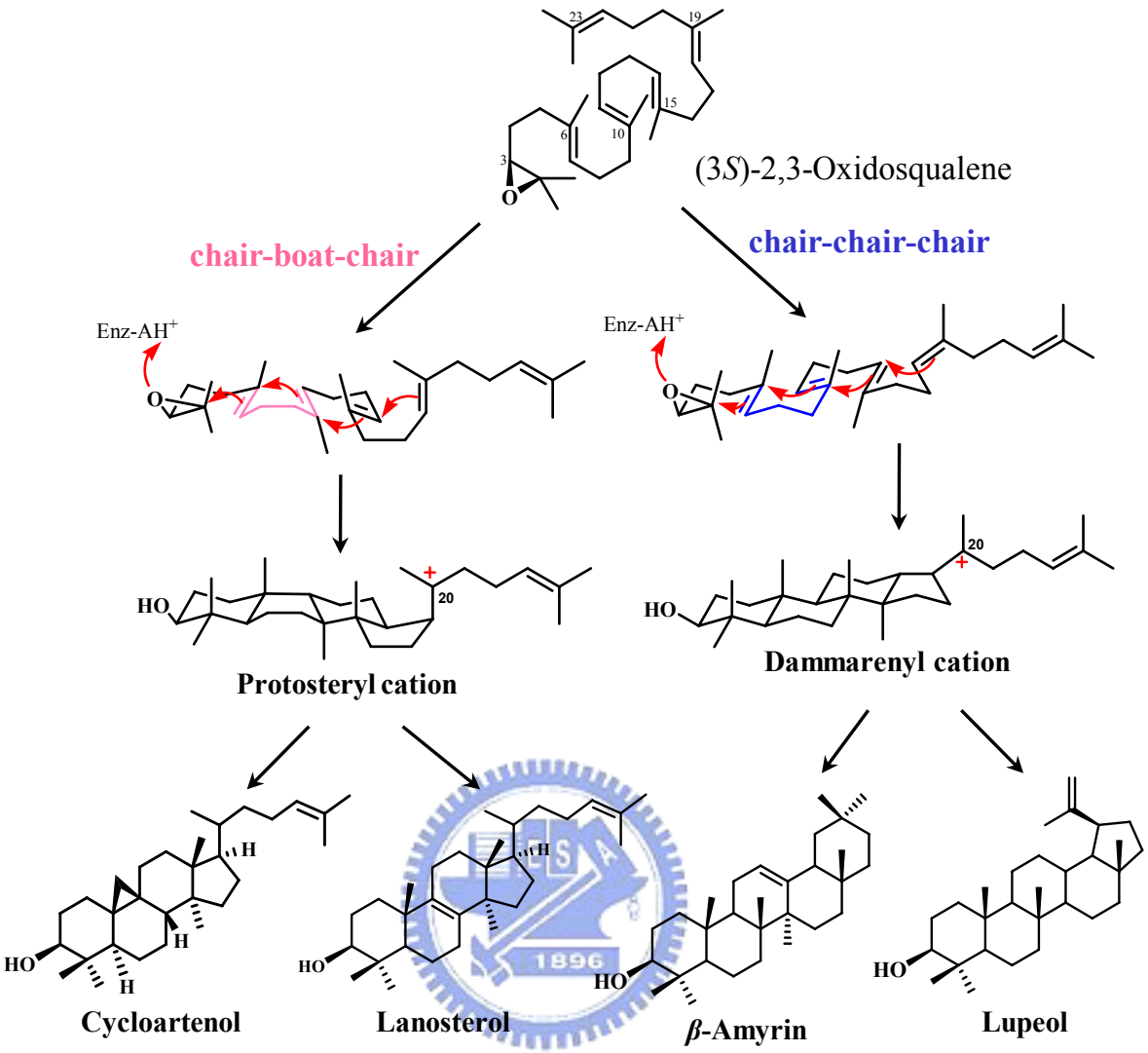

Figure 1-4 Cyclization of oxidosqualene to the protosteryl and dammarenyl cations.

1.3 Overview of the Enzymatic Polycyclization: Oxidosqualene-Lanosterol Cyclase and Squalene-Hopene Cyclase

Amoung all of the triterpene synthases, oxidosqualene-lanosterol cyclase (OSC) and squalene-hopene cyclase (SHC) are two which have been accessible enough to support extensive study of their mechanistic details. Oxidosqualene-lanosterol cyclase is readily available from native mammalian liver or yeast; while squalene-hopene cyclase is the most accessible SC that a recombinant expression source has provided material for structural work and mechanistic study.[9-14] Thus, we described the mechanism and structural information of these two cyclases in the following section to prvide an insight to the triterpene synthesis.

1.3.1 The Hypothesis for Triterpene Synthetic Mechanism

In the early 1950s, Ruzicka and co-workers deduced that all $C_{30}H_{50}O$ triterpene alcohols known by that time were biosynthesized similarly, and they proposed the biogenetic isoprene rule, a set of governing principles that could explain the biosynthesis of each triterpene skeleton.[15-18] As a general mechanism, all-*trans* squalene or oxidosqualene is activated by cationic attack. A cascade of cation-olefin cyclizations then generates a cyclic carbocation, which can rearrange and cyclize further. Antiperiplanar shifts terminated by proton loss then yield a neutral species. This rule has been refined from several decades of research. Consequently, the biogenetic isoprene rule is the most credible origin of the enzyme-mediated cyclization of squalene or oxidosqualene.[19]

In the OSC catalyzed triterpenoid cyclization, the production of four new rings in one high-yielding, stereoselective step from acyclic polyenes is hardly achieved without the help of the enzyme to overcome the unfavorable entropy of activation. In 1987, Johnson *et al*. proposed a concept of cation-stabilizing auxiliaries for the cyclization of 2,3-oxidosqualene.

The enzyme could possibly provide external negative point-charge sites which would stabilize developing cationic centers in the substrate by ion pairing (Fig. 1-5).[20] The axial delivery of negative point-charges in the hypothetic model also accounts for the boat ring-B as well as the non-Markownikov ring-C cyclization. The direction that the negative point-charges is delivered to *pro*-C-8 determines whether the A/B/C ring configuration is *trans*,*anti*,*trans* or *trans*,*syn*,*trans*. In the enzyme that produces dammarane triterpenoids, these point charges are considered to be on the β-face (axial) of *pro*-C-8 of the reacting substrate; in the case of the enzyme which product is the protosteryl type, the critical point charges are delivered, instead, to the *α*-face (Fig. 1-5). Therefore the boat closure of the B-ring could be promoted by delivery of a point charge to the *α*-face at pro-C-8, thereby lowering the activation energy of the boat form relative to the chair closure. On the other hand, the anti-Markovnikov closure of the C-ring may be favored by delivery of a point charge at *pro*-C-13. Further, such charge deliver to the β-face at *pro*-C-10 may be important in enhancing the rate and efficiency of the overall cyclization process.[21-23]

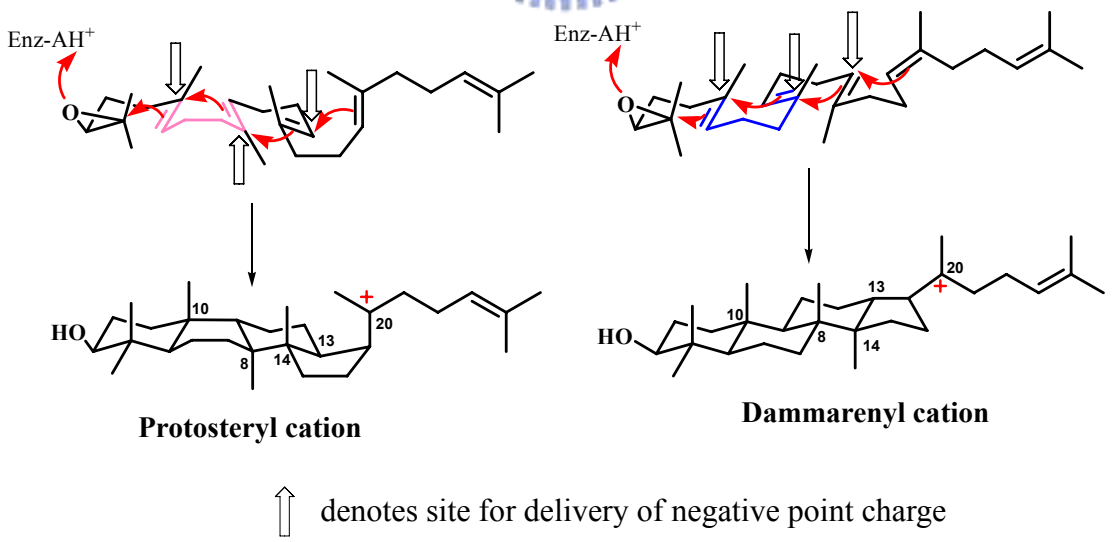

Figure 1-5 The hypothetic model proposed by Johnson.

However, a carbocation in close proximity to a carboxylate might be expected to react irreversibly to form an ester. Alternatively, the aromatic ring could readily guide cation formation without providing such a reactive site. Besides, due to the substrate is quite hydrophobic, the active site would be expected to be hydrophobic.[24]

In previous research, it is believed that cation will bind to the π-face of an aromatic ring through a surprisingly strong, noncovalent interaction, that is, the cation-π interaction. [24,25] It has been reported that unusually large amounts of tyrosine and tryptophan are highly conserved in most oxidosqualene cyclase known to date.[26,27] Thus, Griffin et al. proposed an aromatic hypothesis for cyclase active-site structure. In this hypothesis, the electron-rich aromatic side chains of the aromatic residues such as Phe, Tyr, or Trp, serve to stabilize the cationic transition states and/or high-energy intermediates along the cyclization/rearrangement pathway via cation-π interactions.[26,27] The direction of the aromatic residues is the same as the negative point-charges proposed in the Johnson's hypothesis model (Fig. 1-6).

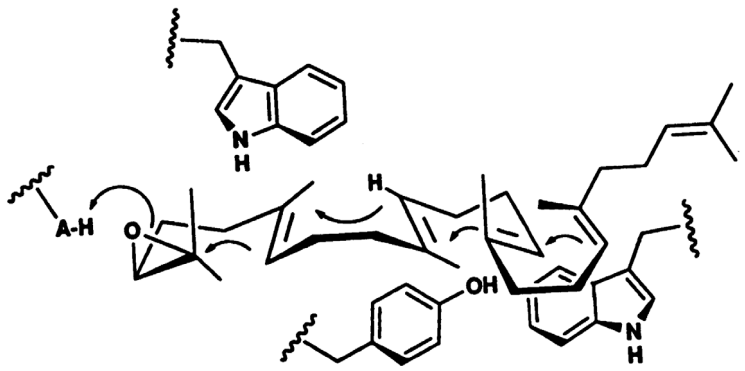

Figure 1-6 Griffin's aromatic hypothesis model. The highly conserved aromatic residues in the active site cavity might stabilize the cationic intermediates during the cyclization cascade.[27]

1.3.2 Oxidosqualene-Lanosterol Cyclase (OSC)

Oxidosqualene-lanosterol cyclase (EC 5.4.99.7; also called lanosterol synthase) exist widely in animals and fungi, which converts linear (3*S*)-2,3-oxidosqualene into tetracyclic lanosterol through a highly stereoselective cyclization reaction. In OSC, the substrate is pre-folded in a chair-boat-chair conformation. The mechanism includes the initiation of the cyclization cascade which by protonated the epoxide ring of 2,3-oxidosqualene,[28] and the subsequent cyclization of four-rings to form the 6.6.6.5-fused tetracyclic protosteryl C-20 cation with a pseudoaxial 17β-side chain. [29,30] Then it followed by skeletal rearrangement of two hydride and two methyl group (H-17α→20, H-13α→17α, CH_3-14β→13β, CH_3-8α→14α), and further deprotonation of lanosteryl C-8/C-9 cation generated the product lanosterol, which is a 6.6.6.5-fused tetracyclic triterpene alcohol with a double bond between C-8 and C-9 position (Scheme I).[29-31]

It is abundantly clear that tight enzymatic control of substrate conformation is a requirement for the highly selective formation of products such as lanosterol or hopene. Oxidosqualene-lanosterol cyclase shows a highly specificity on the substrate recognition that it only accepted the (3*S*)- and not the (3*R*)-enantiomer of 2,3-oxidosqualene as a substrate.[32] Since oxidosqualene is quite stable in neutral media and even in glacial acetic acid at room temperature for up to one day, a more powerful Brønsted acid is required for sufficiently strong epoxide activation to promote cyclization.[33] Site-directed mutagenesis experiments identified a highly conserved aspartic acid as an essential residue for catalysis,[34,35] which is thought to play the role of the proton donor for epoxide activation. The X-ray structure determined by Thoma et al. also confirmed Asp455 is the catalytic acid in human OSC.[6] However, because epoxides are more readily protonated than alkenes, the Brønsted acidity of the OSC catalytic acid appears to be lower than that of SHC, potentially in order to enable the enzyme to discriminate between the olefin and epoxide sides of its natural substrate.[8,36,37]

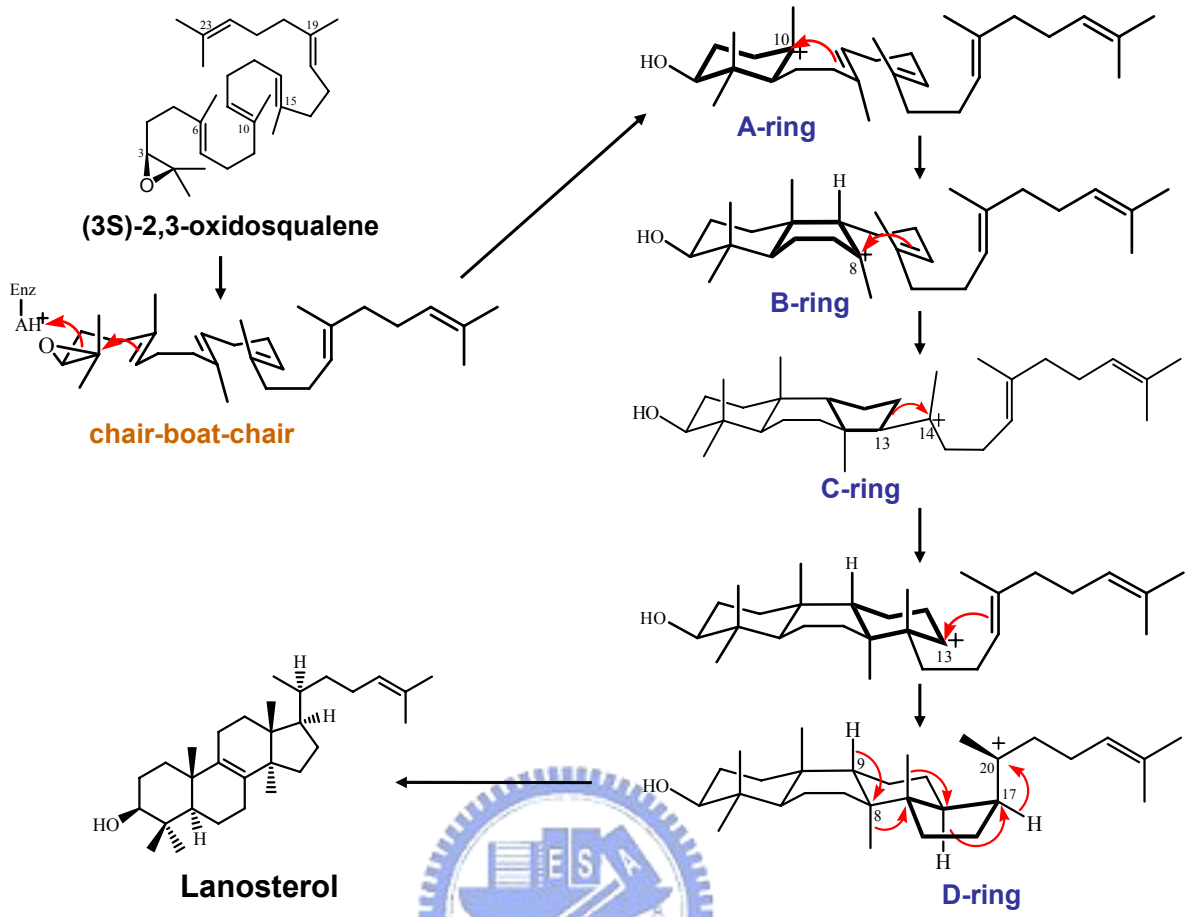

Scheme I The proposed cyclization mechanism of OSC. The number system of lanosterol is used to denote the position of cation.

The enzyme-catalyzed polycyclization reactions are thought to proceed through a series of discrete, conformationally rigid, partially cyclized carbocationic intermediates.[38] It is now accepted that the oxirane cleavage and the A-ring formation are concerted in oxidosqualene cyclization.[34,39] Previously, formation of B-ring as a boat conformer is thought to occur very rapidly and probably concerted with A-ring formation.[13,19] However, a density functional study for the formation of the A and B rings in the oxidosqualene cyclase pathway found two intermediates located on the reaction pathway during the formation of the B ring, indicated the formation of A and B rings was not concerted.[40]

After formation of a 6.6 bicyclic A/B-ring system, it is believed that the six-membered C-ring is formed by initial ring closure to a tricyclic Markovnikov tertiary cation with a five-membered C-ring, then followed by ring expansion to a six-membered C-ring to generate a 6.6.6-fused tricyclic anti-Markovnikov secondary cation.[13,41] Site-directed mutagenesis and substrate-analogue studies of oxidosqualene also afford numerous partially cyclized 6.6.5-fused tricyclic products, which are formed from a thermodynamically favored teriary cation, provide further evidence for a five-membered C-ring closure followed by a ring expansion.[13,41-43] However, it still remains controversial how the C-ring process overcomes the energy barrier required to expand the tertiary carbocation to the thermodynamically less stable secondary carbocation.[44,45] On the basis of *ab initio* calculations, Hess proposed that the 6.6.5 tricyclic Markovnikov tertiary cation (**1**) is the first intermediate in the cascade of the cyclization reactions, and that conversion of **1** to **2** might instead involve expansion of the C-ring in concert with the formation of the five-membered D-ring in **4**, *via* transition state structure **3** (Scheme Ⅱ). [44,45]

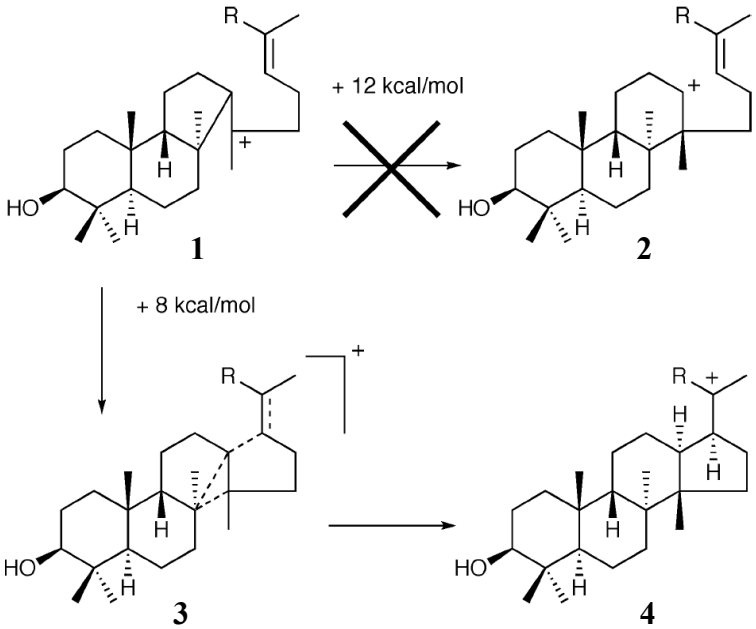

Scheme Ⅱ Proposed mechanism for concerted C-ring expansion/D-ring formation by Hess.[44,45]

Corey and Virgil demonstrated that the D ring closure during lanosterol formation produces a protosteryl cation with the 17β-oriented side chain by analogue of 2,3-oxidosqualene.[29,30] In this case, the initially formed conformation of the protosteryl C-20 cation can lead to the natural C-20*R* configuration via a small (<60°) rotation around the C-17 —C-20 bond. Further, the β-orientation of the side chain at C-17 is thought to facilitate the control of configuration at C-20 in lanosterol formation, since the protosteryl cation is generated in the correct geometry for hydride migration and the C-17—C-20 bond rotation is restricted by the steric bulk of the 14β-methyl substituent.[46]

In 2004, Thoma *et al*. have succeeded in determining the long-awaited structure of human OSC in complex with the reaction product lanosterol and it provided an important additional snapshot of the triterpene polycyclization cascades (Fig. 1-7a).[6]

The crystal structure revealed that human OSC is a monomer which consists of two (α/α) barrel domains that are connected by loops and three smaller β-structures. The large active-site cavity is located in the centre of the molecule between domains 1 and 2 (Fig. 1-7a). Human OSC is a monotopic membrane protein that attached to the membrane from one side rather than spanned the lipid bilayer.[47] The membrane-inserted surface consists of a plateau 25 Å in diameter and a channel that leads to the active-site cavity. This channel is supposed to allow the substrate oxidosqualene to enter the hydrophobic active site but a constriction site separates it from the active-site cavity (Fig. 1-7b). [6]

The X-ray structure of human OSC revealed that Asp455 (Asp456 of *S. cerevisiae* ERG7) is the catalytic acid to initiate the cyclization reaction by protonating the epoxide group of 2,3-oxidosqualene, and its acidity is further increased by hydrogen-bonding to Cys456 and Cys533. In addition, the highly conserved basic residue, His232, and its hydrogen-bonding partner, Tyr503, are thought to be involved in the termination of cyclization reaction by protonating the C-8/C-9 lanosterol cation (Fig. 1-8). [6]

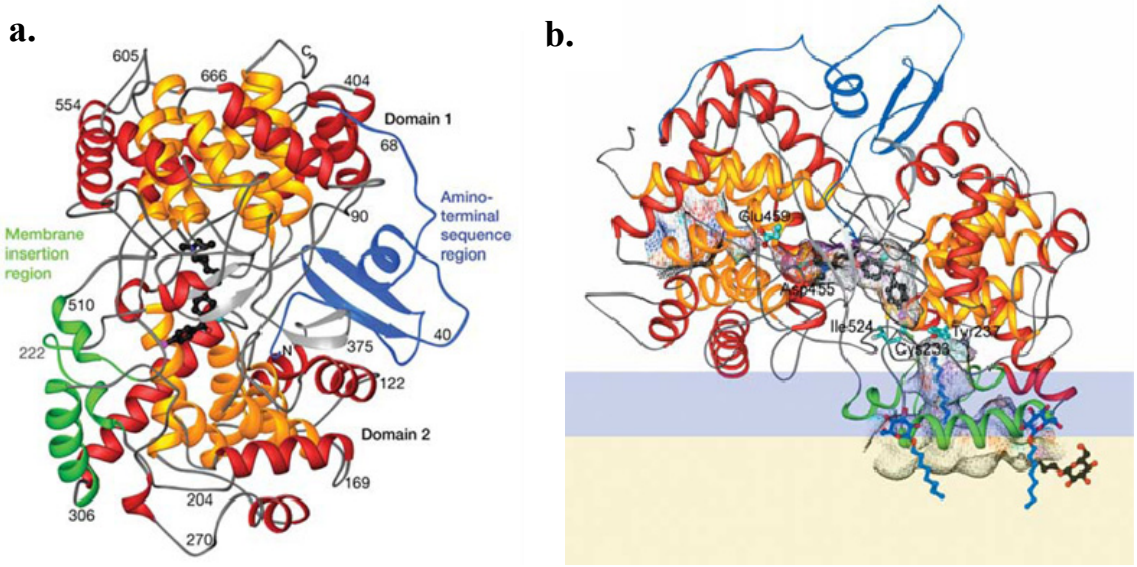

Figure 1-7 The structure of human OSC with Ro 48-8071. (a)The bound inhibitor (black) indicates the location of the active site. (b)Two channels lead to the enzyme surface: one is hydrophobic to the membrane insertion site and one is polar. [6]

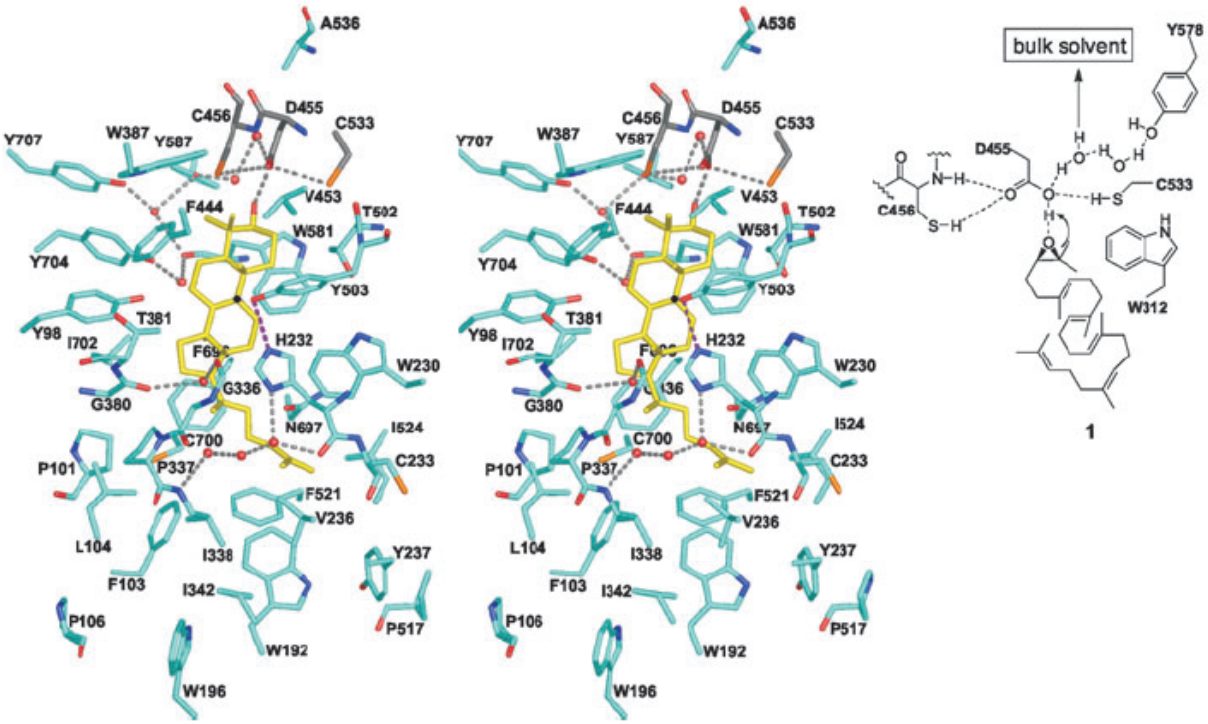

Figure 1-8 Human OSC (turquoise) with lanosterol (yellow). Highlighted are polar residues around the catalytic acid Asp455 (dark gray), structural water molecules (red spheres), and polar interactions (gray dashes). [6,8]

Coupled with the crystal structure of OSC, the mutagenesis studies can give intimate structural details of the catalytic mechanism of the enzyme-templated ring forming reactions of oxidosqualene cyclization. In Recent years, the site-saturated/directed mutagenesis experiments on the putative active site residues with *S. cerevisiae* ERG7, including Trp232, His234, Phe445, Tyr510 and Phe699 were carried out.[42,43,48-51] The products produced in these mutants provide the mechanistic evidence for the formation of the 6.6.5-fused tricyclic Markovnikov cation and the rearrangement track of protosteryl cation during the cyclization of oxidosqualene. Moreover, the results also demonstrate the catalytic plasticity of OSC, and subtle changes in the catalytic environment may have stereoelectronic effects that leading to formation of the structurally diverse product profiles.[31]

1.3.3 Squalene-Hopene Cyclase (SHC)

Prokaryotic squalene-hopene cyclase (SHC; EC 5.4.99.17) converts squalene to the pentacyclic hopene skeleton. It binds squalene in the all-chair conformation, and initiates the cyclization cascade by protonating the terminal double bond. The cyclization reaction produces the 6.6.6.6.5-fused pentacyclic hopanyl C-22 carbocation, which undergoes either proton elimination or addition of water to produce a 5: 1 mixture of hopene and hopanol (Scheme Ⅲ).[31] The cyclization reaction catalyzed by SHC is similar to that of OSC, but skeletal rearrangement reactions observed on lanosterol biosynthesis are not involved. The ring enlargement reactions are also involved in the polycyclization cascades in SHC. It is now accepted that the 5-membered C- and/or D-rings are formed according to the Markovnikov rule prior to the ring expansion into the corresponding anti-Markovnikov 6-membered C-and/or D rings.[14]

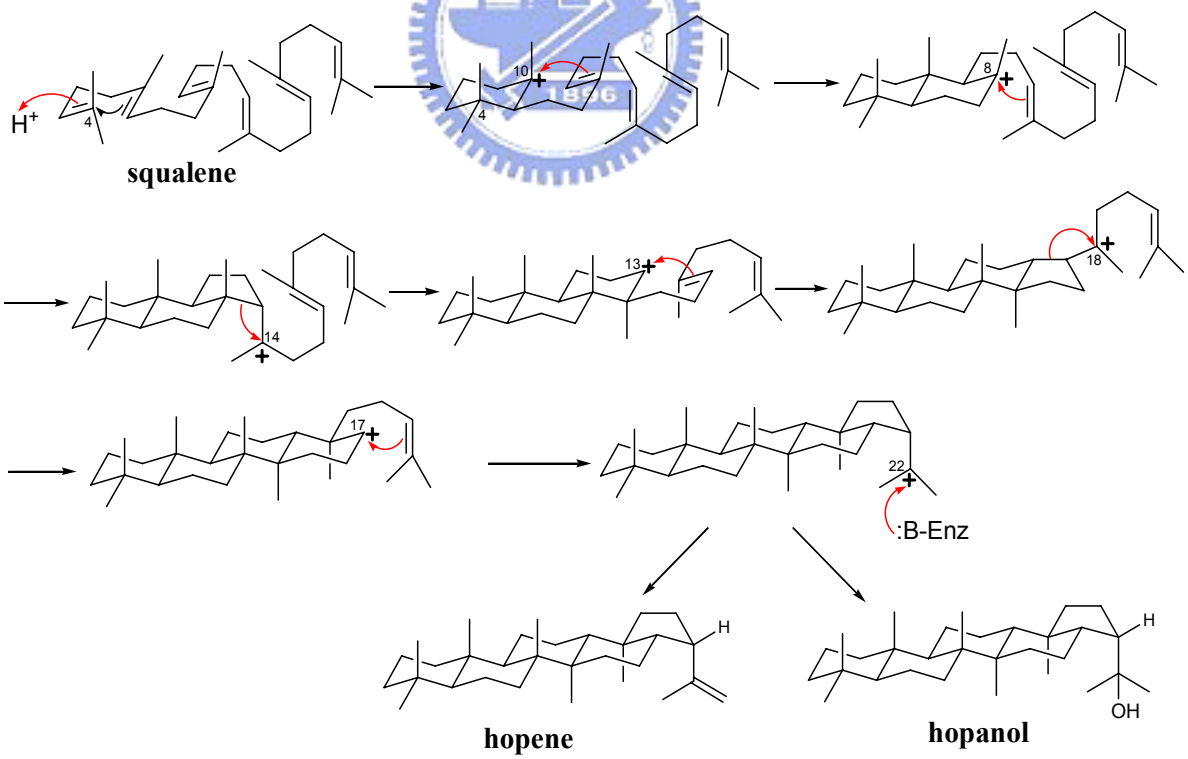

Scheme Ⅲ The proposed cyclization mechanism of SHC.

However, the bacterial SHCs displayed very low substrate specificity. They can cyclize not only the natural substrate, but also both enantiomers of oxidosqualene, and regular polyprenols.

In 1997, Wendt et al. first reported the X-ray crystal structure of *A. acidocaldarius* SHC. The crystal structures of the monotopic membrane-bound 72 kDa protein revealed an α–helix-rich dumbbell-shaped homodimer containing a large central cavity as the putative active site (Fig. 1-9).[11,12,31] The active-site of the enzyme is located in the central cavity, consisting of an extended central hydrophobic section lined with conserved aromatic residues, and the top and bottom sections of the cavity are formed by polar hydrogen networks around Asp376 and Glu45, which are thought to participate in the initial protonation and in the final deprotonation reaction, respectively.[13]

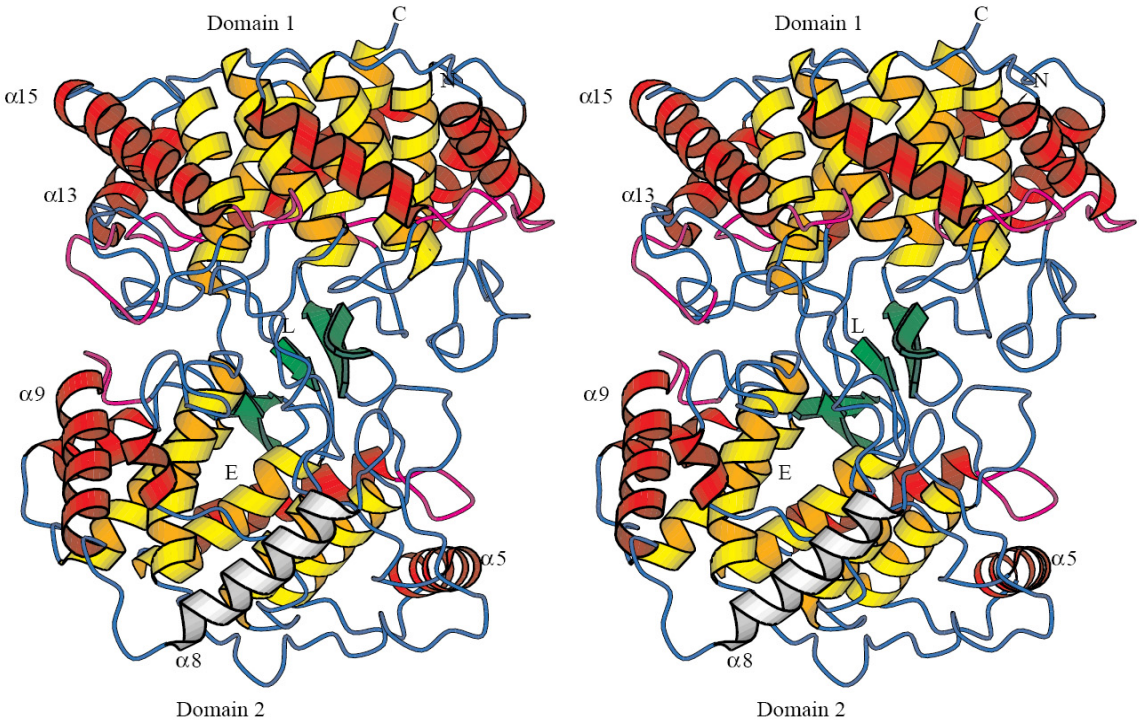

Figure 1-9 The X-ray crystal structure of *A. acidocaldarius* SHC. Color code: internal (yellow) and external (red) barrel helices, β structure (green), QW-motifs (purple), and *α*8 in the nonpolar plateau (white). N and C denote the NH2- and COOH-termini; L: inhibitor position; and E: channel entrance.[11]

The amino acid sequences of the squalene cyclase and 2,3-oxidosqualene cyclases are 20 to 26% identical, and they share a highly-conserved unique sequence repeat, called QW motif, which is represented by the specific amino acid repeats [(K/R)(G/A)X_{2-3}(F/Y/W)(L/I/V)$_3X_3QX_{2-5}$GXW].[52] The aromatic amino acids enriched QW motifs in OSCs and SHCs are now thought to stabilize the enzyme structure by connecting surface α-helices during the highly exergonic polyene cyclization reaction.[31,53,54]

Another characteristic motif in SHCs is the DXDDTA motif, which corresponds to the VXDCTA motif of eukaryotic OSCs.[55] It was first reported by Poralla's group that carried out the mutagenesis experiments for the acidic residues of the $D_{374}XD_{376}D_{377}$TA motif of *A. acidocaldarius* SHC.[56] According to the X-ray crystallographic data[11,12] and the mutagenesis experiments[57] of SHC, it was suggested that the DXDDTA motif is responsible for protonation on the terminal double bond to initiate the polycyclization.[14]

Crystal structures of SHC coupled with the site-directed mutational data have provided a wealth of mechanism information between the active site residues and the substrate (Fig. 1-10). Asp376 in SHC is the general acid that initiates the cyclization cascade by protonating the terminal double bond. The Asp313 and Asp447 residues may function to enhance the Asp376 acidity,[14] and the hydrogen-bonded Asp374:Asp377 pair has been suggested to accommodate the positive charge on the Asp376:His451 pair, prior to proton transfer.[13] The kinetic data indicated Trp312 and Trp169 may function in the binding with the substrate rather than cation-π interaction, and Trp489 may have the functions of both stabilization of C-10 cation and substrate binding. Phe365 is proposed to stabilize bicyclic carbocation *via* the interaction between the intermediary cation and the π-electrons of Phe365. Tyr612 and Tyr609 may function to place Asp377 and Phe365 at the correct positions in the enzyme cavity and to enrich the negative charge of Asp377 and the π-electrons of F365. The function of Tyr420 is likely to be assigned for stabilization of the C-8 cation, because the high yielded bicyclic products in its mutants. Further, the function of Glu45 has been presumed to be

responsible for the final deprotonation reaction, and the crystal structure also indicated that there is enough space in the cavity to accommodate the water molecule with hydrogen-bonding water network, which is in turn fixed by Glu45 and Gln262.[14,58]

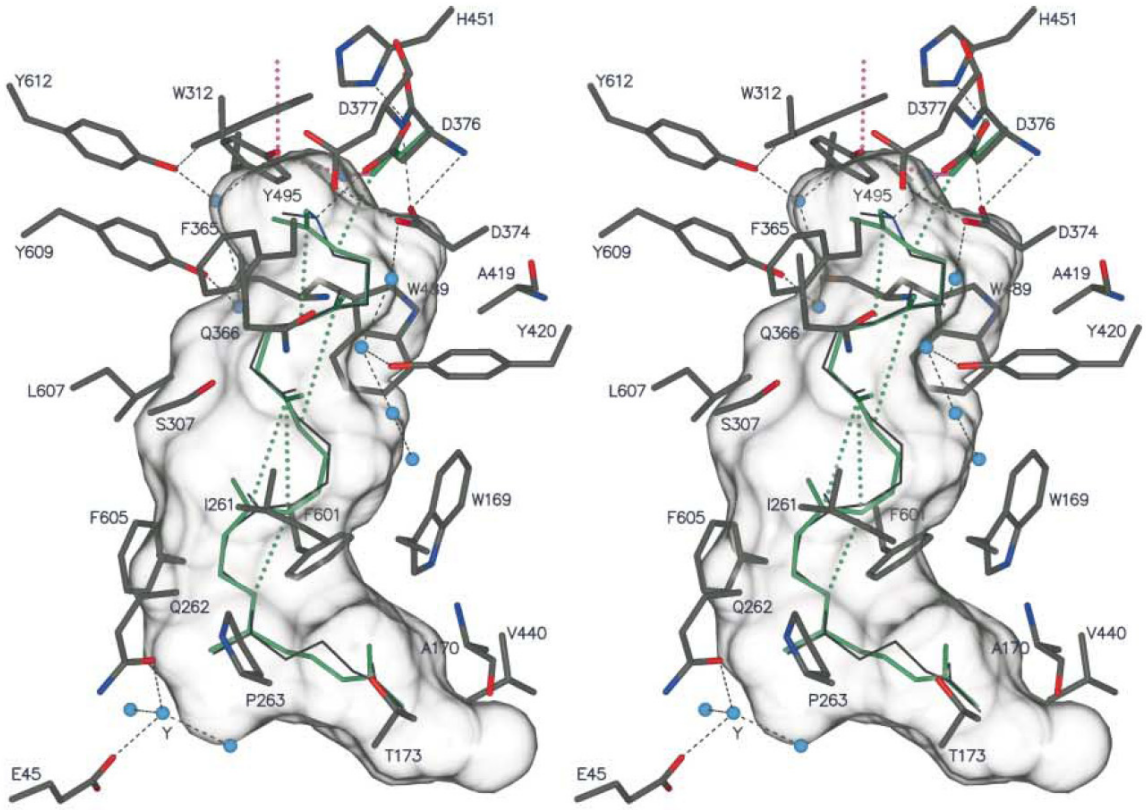

Figure 1-10 Stereo view of the active-site of *A. acidocaldarius* SHC. The squalene model (green) indicated the first four carbocation additions to double bonds (green dots) that run through cations at C2, C6, C10, C14-C15, and C19 to yield the 6-6-6-5 tetracycle. The observed 2-azasqualene is represented by thin dark lines. [58]

1.4 Bicyclic Triterpenoids

Most triterpenoids are 6-6-6-5 tetracycles, 6-6-6-6-6 pentacycles, or 6-6-6-6-5 pentacycles, but mono-, bi-, tri- and acyclic triterpenoids have also been isolated from native sources or generated by mutant forms.

The known bicyclic triterpenoids which are supposed to be derivatives of 2,3-oxidosqualene are polypoda-8(26),13,17,21-tetraen-3-ol (**5**)[59], polypoda-7,13,17,21-tetraen-3-ol (**6**)[60] and polypoda-13,17,21-trien-3,8-diol (**7**)[61], which were found in *Cratoxylum cochinchinense* (**5** and **6**) and *Pistacia* resins (**7**). They are thought to be products that result from quenching chair-chair bicyclic C-8 carbocation by deprotonation of H26 (**5**) or H7 (**6**), or by water addition (**7**) (Fig. 1-11). These compounds have not been experimentally verified to be products of oxidosqualene cyclase, but no plausible alternative origin has been proposed. Interestingly, although B-ring boat folding also appears in oxidosqualene cyclase, the known bicyclic $C_{30}H_{50}O$ triterpenoids are only chair-chair derivatives.

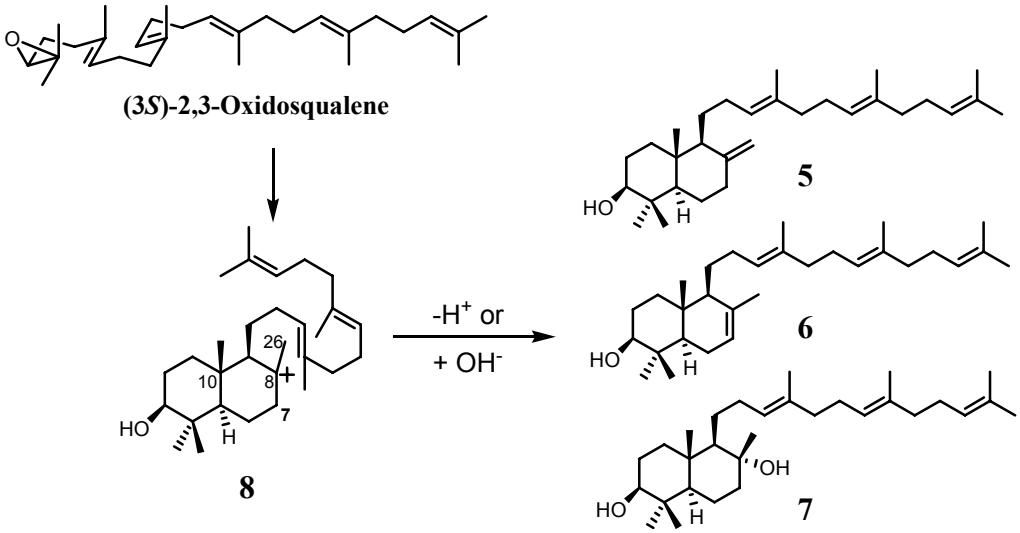

Figure 1-11 Cyclization of oxidosqualene with chair-chair conformation to form bicyclic triterpene compounds from bicyclic cation (**8**).

Some bicyclic triterpenoids, 7,13,17,21-polypodatetraene (*γ*-polypodatetraene)(**9**)[62], 8(26),13,17,21-polypodatetraene (*α*-polypodatetraene)(**10**)[62], 13,17,21-polypodatrien-8-ol (**11**)[63], and neopolypodatetraene A (**12**)[14,64] are considered to be squalene cyclization products which were derived from the chair-chair bicyclic cation intermediate via immediate deprotonation or water addition, or through several 1,2- shifts of hydrides and a methyl group before deprotonation (Fig. 1-12). The *α*-(**10**) and *γ*-polypodatetraene(**9**) were first isolated from the fresh leaves of *Polypodium fauriei* and *Lemmaphyllum microphyllum* for **9**, and *Polystichum ovatopaleaceum* and *P. polyblephalum* for **10**, respectively.[62] **9** was also been found in moss *Floribundaria aurea* subsp[65]; and **11** was first isolated from the fern *Polypodiodes*; whereas **12** has been merely generated by *A. acidocaldarius* SHC mutant F365A[64]. Compounds **9** and **10** have also been obtained from *A. acidocaldarius* SHC mutants.[14] In addition, (+)-*α*-polypodatetraene (**10**) and (+)-*γ*-polypodatetraene (**9**) have also been synthesized successfully. [66]

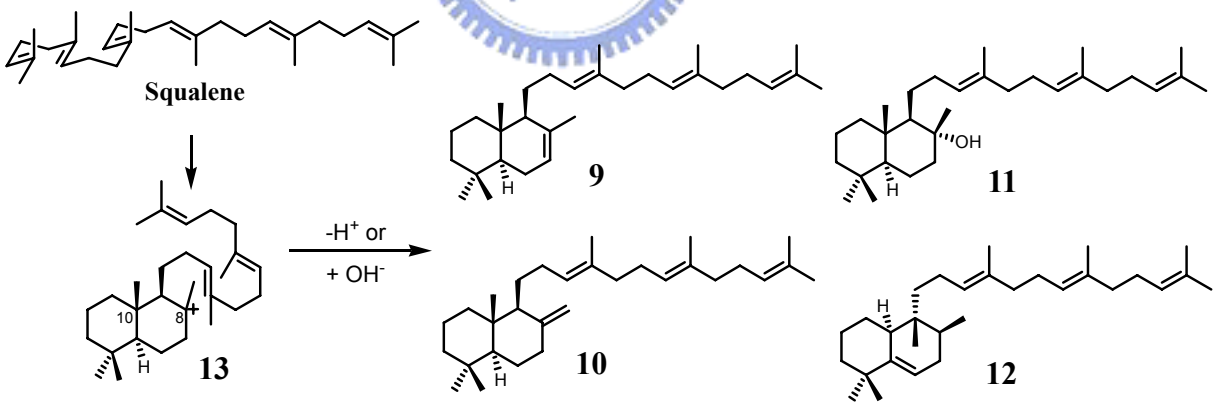

Figure 1-12 Cyclization of squalene to form bicyclic triterpene compounds from bicyclic cation (**13**).

In the triterpene cyclization, whether the mechanism is a "concerted" or "stepwise" process still confused most scientists. The cyclization of squalene and (3*S*)-2,3-oxidosqualene was originally considered as a full concerted process because of the failure to trap or

otherwise detect any intermediates.[16] The isolation of these abortive cyclization products may provide indirect evidence that the polycyclization is a *stepwise* process which proceeds via a series of partially cyclized carbocationic intermediates.[38] In 1984, Bohr et al. first isolated a bicyclic triterpenoid (**7**) that the structure and absolute stereochemistry of which are fully consistent with its formation by interception of the bicyclic carbocation on OSC postulated as an intermediate in the cyclization of the chair-chair-chair conformation of (3*S*)-2,3-oxidosqualene.[61] It provided an indirect evidence that the cyclization of B-ring may not concert with C-ring. In 1985, Nishizawa's experiments also supported the stepwise mechanism of a biomimetic olefin cyclization by trapping of mono-, bi-, and tri-cyclic cationic intermediates.[67]

However, Kronja *et al*. argued that the product composition is not very indicative of the reaction mechanism; either a stepwise or a concerted polycyclization can yield acyclic and polycyclic products. He further suggested an extended participation involving at least two double bonds in a biomimetic reaction of a squalene derivative according their kinetic measurements, and indicated a conceted biomimetic polycyclization.[68] In contrast, recently, Hess *et al.*, by using a density functional computational study, found two intermediates located in the oxidosqualene-lanosterol cyclase reaction pathway during the formation of the B ring, provided an evidence that the formation of the A and B rings was not concerted, although they were be found to be very shallow and perhaps would not lead to formation of a viable intermediate on the enzymatic pathway.[40]

In the field of mutagenesis studies, the abortive products coupled with the structure information and kinetic analysis can give a detailed description of the functional role of a specific residue. Bicyclic products can be obtained from various mutants of *A. acidocaldarius* SHC (Fig. 1-13).[14] There are significant accumulations of two bicyclic products in F365A mutant, indicating that Phe365 is critical to the completion of the polycyclization and that the π-electron of this side chain may stabilize the transient C-8 carbocation (hopene numbering).

This finding also suggested that the Phe365 residue is close to the C-8 cation in the enzyme cavity. It is noteworthy that the formation of **12** may be achieved by a series of 1,2-shifts of hydrides and a methyl group in an antiparallel fashion that trigger the deprotonation at C-6.[14,64]

In the mutants of Tyr609, bicyclic **9** and **10** were also appeared. However, the yields of the bicyclic compounds were different. The higher yield of 96% for **9** and **12** by F365A, than that of *ca.* 50% by Y609A and less than 10% of **10** by Y609F, suggesting that the bicyclic carbocation stabilization may have been achieved mainly by the π-electrons of Phe365 with the aid of Tyr609.[54,69,70] Further, the mutants of Tyr612 produced bicyclic product **9**, but only with a little amount (6%), indicating that Tyr612 may work to place Phe365 at the most favorable positions for cyclization catalysis and enrich the π-electrons of Phe365.[54]

On the other hand, some mutants of Tyr420 afforded bicyclic **9** and **10** in a significant yield. Tyr420 and Tyr609 are located on the wall of the catalytic cavity in a mirror-image position, thereby, pointing to ring B of hopene.[12] The accumulation of bicyclic products in Tyr420 mutants suggested that the major function of Tyr420 is to stabilize the bicyclic cation intermediate formed during the cyclization cascade.[70,71,72] In addition, the Leu607 mutants gave significant amounts of bicyclic **9** and **10**, indicating that the steric bulk size at position 607 is critical to the optimal folding of the chair form for the B-ring; the most appropriate bulk size of Leu gives rise to perfect contact around the B-ring formation site.[72,73] (Note: there may some other products besides the bycyclic products in these mutants, but they are not described herein.)

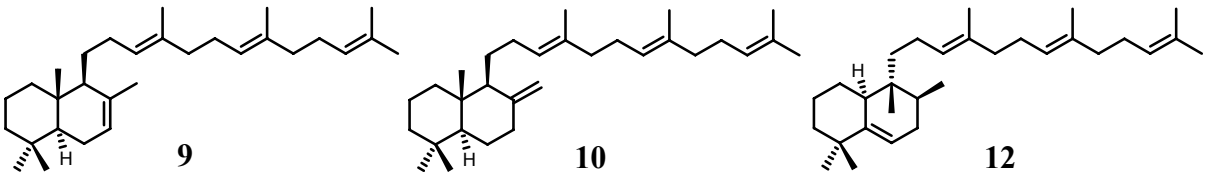

F365A, Y420A/S, L607K, Y609A/C/L/S, Y612A/L | **Y420A/G/F, Y609F** | **F365A**

Figure 1-13 Bicyclic products obtained by the mutated *A. acidocaldarius* SHCs.

1.5The Amino Acid Sequence Alignment of (Oxido-)squalene Cyclase

Rapidly advancing technology in molecular biology has facilitated isolating the genes for triterpene synthases from numerous biological species. Comparison of the sequence similarities among the known prokaryotic and eukaryotic cyclases permitted researchers to deduce the putative active sites responsible for the polycyclization reaction.

Sequence alignment coupled with molecular modeling as well as protein crystallography will provide enormous information for understanding this complicated reaction. The available X-ray structural information of *A. acidocaldarius* SHC and human OSC to date also give a perspective view of the active site. Combining these information with site-directed mutagenesis studies, many of functional important residues will be identified.

In order to investigate the functional residues in the active site cavity of oxidosqualene cyclases, we used the program of Clustal W to produce multiple sequence alignment of the following enzymes: *H. sapiens* ERG7: P48449, *S. cerevisiae* ERG7: P38604, *A. thaliana* CAS: NP_178722, *A. acidocaldarius* SHC: BAA25185. All of them were obtained from the Protein Data Bank (PDB) in NCBI. The result of sequence alignment was shown in below (Fig. 1-14).

```
H.s. ERG7        MTEGTCLRRRGGPYKTEPATDLGR--WRLNCERGR--------QTWTYLQDERAGREQTG 50
S.c. ERG7        -MTEFYSDTIG---LPKTDPRLWR---LRTDELGR--------ESWEYLTPQQAANDPPS 45
A.t. CAS         -MWKLKIAEGGSPWLRTTNNHVGRQFWEFDPNLGTPEDLAAVEEARKSFSDNRFVQKHSA 59
A.a. SHC         --------------------------------------------------MAEQLVEAP-- 9

                                                                          *
H.s. ERG7        LEAYALGLDTKNYFKDLP----------KAHTAFEGALN-GMTFYVGLQAED-GHWTGDY 98
S.c. ERG7        TFTQWLLQDPK-FPQPHPERNK----HSPDFSAFDACHN-GASFFKLLQEPDSGIFPCQY 99
A.t. CAS         DLLMRLQFSRENLISPVLPQVKIEDTDDVTEEMVETTLKRGLDFYSTIQAHD-GHWPGDY 118
A.a. SHC         -------------------------------AYARTLDRAVEYLLSCQKDE-GYWWGPL 36
```

```
H.s. ERG7     GGPLFLLPGLLITCHVA---RIPLPAGYREEIVRYLRSVQLP-DGGWGLHIEDKSTVFGT 154
S.c. ERG7     KGPMFMTIGYVAVNYIAG---IEIPEHERIELIRYIVNTAHPVDGGWGLHSVDKSTVFGT 156
A.t. CAS      GGPMFLLPGLIITLSITGALNTVLSEQHKQEMRRYLYNHQNE-DGGWGLHIEGPSTMFGS 177
A.a. SHC      LSNVTMEAEYVLLCHILD----RVDRDRMEKIRRYLLHEQRE-DGTWALYPGGPPDLDTT 91

H.s. ERG7     ALNYVSLRILGVGPDDPD--LVRARNILHKKGGAVAIPSWGKFWLAVLNVYSWEGLNTLF 212
S.c. ERG7     VLNYVILRLLGLPKDHPV--CAKARSTLLRLGGAIGSPHWGKIWLSALNLYKWEGVNPAP 214
A.t. CAS      VLNYVTLRLLGEGPNDGDGDMEKGRDWILNHGGATNITSWGKMWLSVLGAFEWSGNNPLP 237
A.a. SHC      IEAYVALKYIGMSRDEEP--MQKALRFIQSQGGIESSRVFTRMWLALVGEYPWEKVPMVP 149

H.s. ERG7     PEMWLFPDWAPAHPSTLWCHCRQVYLPMSYCYAVRLSAAEDPLVQSLRQELYVEDFASID 272
S.c. ERG7     PETWLLPYSLPMHPGRWWVHTRGVYIPVSYLSLVKFSCPMTPLLEELRNEIYTKPFDKIN 274
A.t. CAS      PEIWLLPYFLPIHPGRMWCHCRMVYLPMSYLYGKRFVGPITSTVLSLRKELFTVPYHEVN 297
A.a. SHC      PEIMFLGKRMPLNIYEFGSWARATVVALSIVMSRQPVFPLPERARVP--ELYETDVPPRR 207

H.s. ERG7     WLAQRNNVAPDELYTPHSWLLRVVYALLN-----LYEHHHS-AHLRQRAVQKLYEHIVAD 326
S.c. ERG7     FSKNRNTVCGVDLYYPHSTTLNIANSLVV-----FYEKYLRNRFIYSLSKKKVYDLIKTE 329
A.t. CAS      WNEARNLCAKEDLYYPHPLVQDILWASLHKIVEPVLMRWPG-ANLREKAIRTAIEHIHYE 356
A.a. SHC      RGAKGG----------GGWIFDALDRALHG-----YQKLSVHPFRRAAEIRALDWLLERQ 252

H.s. ERG7     DRFTKSISIGPISKTINMLVRWYVDGPASTAFQEHVSRIPDYLWMGLDGMKMQGTNGSQI 386
S.c. ERG7     LQNTDSLCIAPVNQAFCALVTLIEEGVDSEAFQRLQYRFKDALFHGPQGMTIMGTNGVQT 389
A.t. CAS      DENTRYICIGPVNKVLNMLCCWVED-PNSEAFKLHLPRIHDFLWLAEDGMKMQGYNGSQL 415
A.a. SHC      AGDGSWGGIQPP-WFYALIALKILDMTQHPAFIKGWEGLELYGVELDYGGWMFQASISPV 311

H.s. ERG7     WDTAFAIQALLEAGGHHRPEFSSCLQKAHEFLRLSQVPDNPP-DYQKYYRQMRKGGFSFS 445
S.c. ERG7     WDCAFAIQYFFVAGLAERPEFYNTIVSAYKFLCHAQFDTECV---PGSYRDKRKGAWGFS 446
A.t. CAS      WDTGFAIQAILAT--NLVEEYGPVLEKAHSFVKNSQVLEDCPGDLNYWYRHISKGAWPFS 473
A.a. SHC      WDTGLAVLALRAAG---LPADHDRLVKAGEWLLDRQIT--VPGDWAVKRPNLKPGGFAFQ 366
```

```
H.s. ERG7     TLDCGWIVSDCTAEALKAVLLLQEK--CPHVTEHIPRERLCDAVAVLLNMRNPD----GG 499
S.c. ERG7     TKTQGYTVADCTAEAIKAIIMVKNSPVFSEVHHMISSERLFEGIDVLLNLQNIGSFEYGS 506
A.t. CAS      TADHGWPISDCTAEGLKAALLLSKVP-KAIVGEPIDAKRLYEAVNVIISLQNAD----GG 528
A.a. SHC      FDNVYYPDVDDTAVVVWALNTLRLP------DERRRRDAMTKGFRWIVGMQSSN----GG 416

H.s. ERG7     FATYETKRGGHLLELLNPSEVFGDIMIDYTYVECTSAVMQALKYFHKRFPEHRAAEIRET 559
S.c. ERG7     FATYEKIKAPLAMETLNPAEVFGNIMVEYPYVECTDSSVLGLTYFHKYF-DYRKEEIRTR 565
A.t. CAS      LATYELTRSYPWLELINPAETFGDIVIDYPYVECTSAAIQALISFRKLYPGHRKKEVDEC 588
A.a. SHC      WGAYDVDNTSDLPNHIPFCD-FG-EVTDPPSEDVTAHVLECFG-------SFGYDDAWKV 467

H.s. ERG7     LTQGLEFCRRQQRADGSWEGSWGVCFTYGTWFGLEAFACMGQTYRDGTACAEVSRACDFL 619
S.c. ERG7     IRIAIEFIKKSQLPDGSWYGSWGICFTYAGMFALEALHTVGETYEN---SSTVRKGCDFL 622
A.t. CAS      IEKAVKFIESIQAADGSWYGSWAVCFTYGTWFGVKGLVAVGKTLKN---SPHVAKACEFL 645
A.a. SHC      IRRAVEYLKREQKPDGSWFGRWGVNYLYGTGAVVSALKAVGIDTREP----YIQKALDWV 523

H.s. ERG7     LSRQMADGGWGEDFESCEERRY--LQSAQSQIHNTCWAMMGLMAVRHPDIEAQ--ERGVR 675
S.c. ERG7     VSKQMKDGGWGESMKSSELHSY--VDSEKSLVVQTAWALIALLFAEYPNKEVI--DRGID 678
A.t. CAS      LSKQQPSGGWGESYLSCQDKVYSNLDGNRSHVVNTAWAMLALIGAGQAEVDRKPLHRAAR 705
A.a. SHC      EQHQNPDGGWGEDCRSYEDPAY--AGKGASTPSQTAWALMALIAGGRAESEAAR--RGVQ 579

                                        *  *
H.s. ERG7     CLLEKQLPNGDWPQENIAG-VFNKSCAISYTSYRNIFPIWALGRFSQLYPERALAGHP 732
S.c. ERG7     LLKNRQEESGEWKFESVEG-VFNHSCAIEYPSYRFLFPIKALGMYSRAYETHTL---- 731
A.t. CAS      YLINAQMENGDFPQQEIMG-VFNRNCMITYAAYRNIFPIWALGEYR--CQVLLQQGE- 759
A.a. SHC      YLVETQRPDGGWDEPYYTGTGFPGDFYLGYTMYRHVFPTLALGRYKQAIERR------ 631
```

Figure 1-14 Amino acid sequence alignment of *H. sapiens* (H.s.) ERG7, *S. cerevisiae* (S.c.) ERG7, *A. thaliana* (A.t.) CAS, and *A. acidocaldarius* (A.a.) SHC. The highly conserved residues are marked with black and gray boxes. The asterisks denote Tyr99, Tyr707 and Tyr710 residues in *S. cerevisiae* ERG7, respectively.

1.6 Research Goal

There are a lot of triterpenoid products have been found in oxidosqualene cyclase, involving monocyclic, bicyclic, tricyclic, tetracyclic and pentacyclic triterpene skeletons. However, the known bicyclic triterpene alcohols so far are chair-chair, trans-decalin derivatives.[19] The enzymatically produced bicyclic triterpene alcohols derived from a chair-boat bicyclic cation has never been found.

Among the triterpene synthetic processes, the B-ring moiety is always a focal point that interested most researchers. In squalene-hopene cyclases (SHCs), the B-ring exists in the native products all with chair conformation, while it folds into boat type in oxidosqualene-lanosterol cyclase (OSC). It seems that B-ring is favor to adopt in the energetically unfavorable boat conformation in OSC. The inconsequent formation was suggested to be achieved by enzyme residues through the steric and/or electronic effect. Finding the abortive bicyclic product may help us getting more information about the formation of B-ring. Site-saturated mutagenesis coupled with product characterization can help us elucidate the functional role of specific residues, and the mutation-induced product specificity/diversity profile also provides an insight into the catalytic mechanism.

Previously, based on the human OSC crystal structure, it was predicted that Tyr98 in human OSC (corresponds to Tyr99 in *S. cerevisiae* ERG7) will influence the B-ring of 2,3-oxidosqualene to form the energetically unfavorable boat conformation required for lanosterol formation by pushing the methyl group at C-8 (lanosterol numbering) below the molecular plane (Fig. 1-15).[6] However, our lab had proved that the exact function of *Sce*ERG7 Tyr99 is to affect both chair-boat tricyclic Markovnikov C-14 cation stabilization and the stereochemistry of the protons at the C-15 position for subsequent deprotonation, but not the B-ring formation.[74] Therefore, the information regarding which residue(s) in OSC is (are) involved in the chair-boat bicyclic intermediate formation is still unknown.

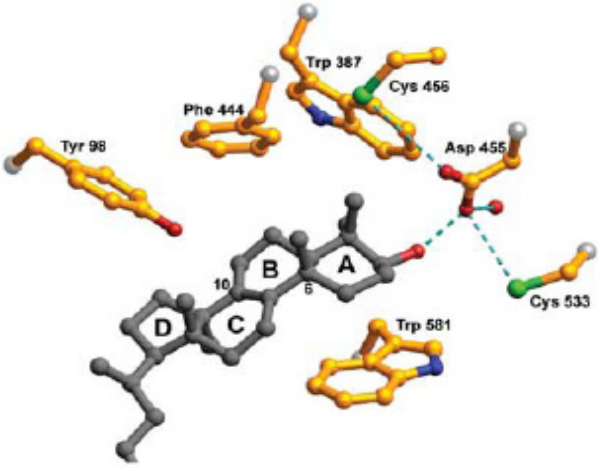

Figure 1-15 The human OSC strucute with lanosterol. The Tyr98 side chain was proposed to sterically hinder the B-ring from assuming the favorable chair conformation.

The Tyr707 residue of *S. cerevisiae* oxidosqualene-lanosterol cyclase (ERG7) corresponds to the Tyr704 residue in human OSC. The multiple sequence alignment revealed that the Tyr707 residue of *S. cerevisiae* ERG7 is highly conserved in both oxidosqualene cyclases and squalene-hopene cyclases (SHCs). According to the human OSC crystal structure, the position of Tyr704 is close to the C-8 of lanosterol (see Fig. 1-8), which is the location of the cation which formed after the B-ring formation. The π-electron rich side chain of Tyr707 was also expected to stabilize the electron-deficient cationic intermediates generated during polycyclization process through the cation-π interaction. In addition, bicyclic products had been produced in the mutants of Tyr609 in SHC, which corresponds to Tyr707 in *S. cerevisiae* ERG7, suggested that Tyr609 stabilized the bicyclic C-8 cation and led to subsequent C-ring formation.[19-22] For these reasons, Tyr707 is probably an important residue to influence the stability of C-8 cation and result in the formation of bicyclic triterpenoid products.

On the other hand, the Tyr710 residue of *S. cerevisiae* ERG7 is another highly conserved aromatic residue which corresponds to Tyr707 in human OSC and Tyr612 in SHC. It has been reported that there are monocyclic and bicyclic triterpene products been isolated in the

mutants of Tyr612Ala and Tyr612Leu in SHC, suggesting that Tyr612 works to stabilize both the C-10 and C-8 cabocation intermediates through intensifying the function of Asp377 and Phe365, which stabilized the C-10 and C-8 cation, respectively.[19-22] In the active site cavity, the position of Tyr710 is on the A-ring and B-ring side of lanosterol but is not very close to the C-10 and C-8 position of lanosterol. Therefore, we thought Tyr710 in OSC may have similar function as in SHC that can stabilize the C-8 cabocation through interaction with other residues nearby, even if SHC is only 19-25% identical to eukaryotic oxidosqualene cyclase.

In order to further investigate the functional role of Tyr707 and Tyr710 in *S. cerevisiae* ERG7, a series of site-saturated mutagenesis and the product profiles characterizations were carried out in this thesis. Hoping this study can elucidate the relationship of Tyr707 and Tyr710 to the chair-boat bicyclic intermediate formation and acquire truncated bicyclic products through their mutations.

Chapter 2 Materials and Methods

2.1 Materials

Chemicals and reagents:

Acetic acid (Merck)

Acetic anhydride (Sigma)

Acetone (Merck)

Adenine (Sigma)

Agarose-LE (USB)

95% Alcohol (Merck)

Ampicillin sulfate (Sigma)

Anisaldehyde (Mecrk)

Bacto™Agar (DIFCO)

Dichloromethane (Merck)

Dimethyl sulfoxide (MP Biomedicals)

DNA 10Kb Ladder (Bio Basic Inc., Tanwan)

D-Sorbitol (Sigma)

Ergosterol (Sigma)

Ethyl acetate (Merck)

Ethylenediamine-tetraacetic acid (Merck)

Ether (Merck)

G418 sulfate (Gibco)

Glycerol (Merck)

Glucose (Sigma)

Hemin Chloride (Merck)

Hexane (Merck)

Hisidine (Sigma)

LB Broth, Miller (DIFCO)

Lysine (Sigma)

Methanol (Merck)

Methioine (Sigma)

dNTP Set, 100mM Solutions (GE Healthcare)

Petroleum ether (TEDIA)

Primers (Bio Basic Inc.)

Potassium hydroxide (Merck)

Pyridine (Sigma)

Pyrogallol (Merck)

Restriction enzyme (New England BioLabs Inc.)

Sea sand (Merck)

Silica gel (Merck)

Silver nitrate (Merck)

Sodium sulfate (Merck)

Sulfonic Acid (Merck)

SYBR® Green I (Roche)

TLC plate (Merck)

Tris base (USB)

Trptophan (Sigma)

Tween 80 (Merck)

Trypton (DIFCO)

Yeast Extra (DIFCO)

Yeast Nitrogen Base w/o amino acid (DIFCO)

Uracil (Sigma)

Kits:

BigDye® Teminator v3.1 Cycle Sequencing Kit (Applied Biosystems)

GFX™ PCR DNA and Gel Band Purification Kit (GE Healthcare)

Plasmid Miniprep Purification Kit (GeneMark)

QuickChange Site-Directed Mutagenesis Kit (Stratagene Inc., La Jolla, CA)

Bacterial, yeast strains and vectors:

Escherichia coli XL-Blue (Novagen)

CBY57 (a yeast stain, MATa or MATα ERG7Δ:: LEU2 *ade*2-101 *his*3-Δ200 *leu2*-Δ1 *lys*2-801 *trp1*-Δ63 *ura3*-52 [pZS11])

TKW14C2 (a yeast stain, MATa or MATα ERG7Δ:: LEU2 *ade*2-101 *his*3-Δ200 *leu2*-Δ1 *lys*2-801 *trp1*-Δ63 *ura3*-52 *hem1*Δ::Kan^R)

Vector pRS314 (a shuttle vector with selection marker *Trp1*, New England BioLabs)

Equipments:

ABI PRISM® 3100 Genetic Analyzer (Applied Biosystems)

Allegra™ 21R Centrifuge (Beckman Coulter)

Avanti® J0E Centrifuge (Beckman Coulter)

Colling Circulator Bath Model B401L (Firstek Scientific)

Centrifuges 5415R (eppendorf)

DU 7500 UV-Vis Spectrophotometer (Beckman Coulter)

Durabath™ Water Bath (Baxter)

Electrophoresis Power Supply EPS 301 (GE healthcare)

EPSON® GT-7000 Scanner (EPSON)

GeneAmp® PCR System 9700 Thermal Cycler (Applied Biosystems)

Hoefer® HE 33 Mini Horizontal Submarine Unit (GE Healthcare)

Kodak Electrophoresis Documentation an Analysis System 120 (Kodak)

Orbital Shaking Incubator Model-S302R (Firstek Scintific)

Pulse Controller (BioRad)

Rotary Vaccum Evaporator N-N Series (EYELA)

Steritop™ 0.22μm Filter Unit (Millipore)

Rotary vacuum evaporator N-N series (EYELA)

Orbital shaking incubator Model-S302R (First Scientific)

Solutions:

Ampicillin stock solution (100mg/mL)

Dissolve 1 g ampicillin sulfate in 10 ml ddH_2O. Filter through 0.22 μm pore size filter and stock at -20 ℃.

50X TAE buffer

Dissolve Tris base 242 g, acetic acid 57.1 ml, and 0.5 M EDTA in 1 L dH_2O and adjust to pH 8.5. Store it at room temperature. Dilute to 1X with dH_2O and adjust pH to 7.5~7.8 before use.

50X ALTH solution

0.2% Adeine, 0.3% Lysine, 0.2% Tryptophan, 0.2% Hisidine were dissolved in dH_2O and sterilized. Store at 4 ℃.

50X ALH solution

0.2% Adeine, 0.3% Lysine, 0.2% Hisidine were dissolved in dH_2O and sterilized. Store at 4 ℃.

50X ALHU solution

0.2% Adeine, 0.3% Lysine, 0.2% Hisidine, 0.2% Uracil were dissolved in dH_2O and sterilized. Store at 4 ℃.

50X ALTHMU solution

0.2% Adeine, 0.3% Lysine, 0.2% Tryptophan, 0.2% Hisidine, 0.2% Methonine, 0.2% Uracil were dissolved in dH_2O and sterilized. Store at 4 ℃.

50X ALHMU solution

0.2% Adeine, 0.3% Lysine, 0.2% Hisidine, 0.2% Methonine, 0.2% Uracil was dissolved in dH_2O and sterilized. Store at 4 ℃.

50% Glucose solution

500g glucose was dissolved in 1 L dH_2O and sterilized.

80% Glycerol solution

80 ml glycerol was added in 20 ml dH_2O and sterilized. Store at 4 ℃.

LB medium

25 g LB Broth was dissolved in 1 L dH_2O and sterilized.

LB plate

25 g LB Broth and 20 g Bacto™ Agar was dissolved in 1 L dH_2O and sterilized. The sterile LB agar was poured and dispersed in Petri dishes before it coagulates.

G418 stock solution (1g/mL)

Dissolve 500 mg G418 in 500 μl sterile dH_2O. Store it in darkness at 4 ℃.

SD medium

0.17% Yeast nitrogen base was dissolved in dH_2O and sterilized.

20% EA developing solution

Add 20 ml ethyl acetate to 80 ml hexane and mix it.

TLC staining solution

40 ml of conc. H_2SO_4 is added into 800 ml ethanol slowly, followed by 12 ml acetic acid and 16 ml anisaldehyde.

1 M sorbitol solution

182.2 g D-sorbitol was dissolved in 500 ml dH_2O and sterilized. Store at 4 ℃.

5X sequencing buffer

Dissolve 4.85 g Tris base and 0.203 g $MgCl_2$ in 100 ml dH_2O and adjust to pH 9. Store at 4 ℃.

10X SYBR Green solution

10000X SYBR Green was diluted to 10X with DMSO. Store it in darkness.

6X DNA loading dye

0.25% bromophenol blue and 30% glycerol were dissolved in ddH_2O. Store at -20 ℃.

Hemin solution

0.5 g heme chloride was dissolved in 250 ml 0.2 N potassium hydroxide and thus mixes it with 250 ml 95% alcohol in aseptic condition. Store it at room temperature in darkness.

Ergosterol supplement solution

1 g Ergosterol was dissolved in 250 ml 95% alcohol and thus mixes with 250 ml Tween 80 in aseptic condition. Store it in darkness at room temperature.

ALHMU/Hemin/Ergosterol plate

0.67 g yeast nitrogen base, 2 g Bacto™ Agar was dissolved in 100ml dH_2O and sterilized. Add 2 ml 50X ALHMU solution, 4 ml 50% glucose solution, 2 ml hemin solution, 2 ml ergosterol supplement solution, and 100 μl G148 stock solution into the sterile SD medium. Then the mixture was poured and dispersed in Petri dishes before it coagulates. All of steps are in aseptic condition and stock in darkness at 4 ℃.

2.2 Methods

2.2.1 The Construction of Recombinant Plasmids

The mutations of ERG7^{Tyr707X} and ERG7^{Tyr710X} were constructed using the QuikChange site-directed mutagenesis kit and the strategies are shown in Figure 2-1. The ERG7$^{F699M/Y707H}$ and ERG7$^{F699M/Y707Q}$ double mutants were also constructed by the same strategies but using the RS314ERG7^{F699M} plasmid as template.

(1) **Primer design:**

For the ERG7^{Tyr707X} and ERG7^{Tyr710X} mutants:

TTW-OSCY707X-Pvu Ⅰ 1
5'- CAACCACTCTTgTgCgATCgAANNNCCAAgTTATCg-3'
TTW-OSCY707X-Pvu Ⅰ 2
5' – CgATAACTTggNNNTTCgATCgCACAAgAgTggTTg- 3'

TTW-OSCY710X-AvaI-1
5'-CAATTgAATACCCgAgTNNNCgATTCTTATTCCC -3'
TTW-OSCY710X-AvaI-2
5'-gggAATAAgAATCgNNNACTCgggTATTCAATTg -3'

For the ERG7$^{F699M/Y707H}$ and ERG7$^{F699M/Y707Q}$ double mutants:

TTW-OSCY707Q-PvuI 1
5'- CCAC**Ag**CTgTgCgATCgAACAACCAAgTTATCg-3'
TTW-OSCY707Q-PvuI 2
5'-CgATAACTTggTTgTTCgATCgCACA**gCT**gTgg -3'

TTW-OSCY707H-PvuI 1
5'- CCAC**Ag**CTgTgCgATCgAACATCCAAgTTATCg-3'
TTW-OSCY707H-PvuI 2
5'-CgATAACTTggATgTTCgATCgCACA**gCT**gTgg -3'

The gray background letters in the sequence line of primers show the target mutations, and "N" means A, T, C, G four bases, thereby 20 possible amino acids. The bold letter

indicates silent mutation for *Pvu* I or *Ava* I mapping analysis and construction are marked with underline. In addition, the recombination plasmid of $ERG7^{F699M}$ has been constructed previously in our laboratory. The other primers for specific mutation are listed in Appendix 1.

(2) QuikChange PCR:

Composition	Volume (μL)
Template	0.5
Primer 1	0.5
Primer 2	0.5
dNTP mix (2.5 mM each)	1.6
Pfu Ⅱ polymerase	0.4
Pfu Ⅱ buffer	2.0
ddH_2O	14.5
Total	20

Table 2-1 QuikChange Site-Directed Mutagenesis Kit PCR composition

Segment	Cycles	Temperature	Time
1	1	95 ℃	2 min
2	18	95 ℃	30 sec
		50~55 ℃	1 min
		68 ℃	16 min
3	1	4 ℃	pause

Table 2-2 Reaction conditions for PCR mutagenesis reaction

(3) *Dpn* I digest parental DNA template:

The digested reaction was incubated at 37 ℃ for 3 hours to digest the parental supercoiled DNA.

Reagents	Volume (μL)
PCR products	8
10× NE Buffer 4	1
Dpn I	1

Table 2-3 QuikChange Site-Directed Mutagenesis PCR products digestion

(4) Transformation into *E. coli* (heat shock) and enzyme mapping

The digested QuikChange products were added into 100 μl *E. coli* XL1-Blue competent cells and incubated on ice for 20 min. The cells were transformed by heat shock methods for 1 min at 42 ℃, following 1 min on ice. Then the cells were transferred to 1 ml Luria-Bertani (LB) medium immediately and then shaken in 200 rpm for 1 hour at 37 ℃ incubator. Then, the cells were centrifuged at 8,000 rpm for 1 min and propagated on LB plate containing 100 μg/ml ampicillin (LB_{amp}). Incubate these plates 16 hr at 37 ℃. Pick the colonies and culture in 3 ml LB medium containing 100 μg/ml ampicillin overnight at 37 ℃. The plasmid DNAs were isolated by Plasmid Miniprep Purification Kit, according to the manufacturer instructions. The plasmid DNAs were then digested with *Pvu* I for $ERG7^{Tyr707X}$ mutants, *Ava* I for $ERG7^{Tyr710X}$ mutants, and *Pvu* I for the $ERG7^{F699M/Y707H}$ and $ERG7^{F699M/Y707Q}$ double mutants to confirm the presence of the mutations.

(5) Sequencing analysis of the mutated genes

The exact amino acid substitution at Phe699, Tyr707 and Tyr710 positions were determined by sequencing of the DNA using ABI PRISM 3100 auto-sequencer. Nucleotide sequencing was performed using the dideoxynucleotide chain-termination method with only one forward of reverse primers (described on Appendix 1). Sequencing reactions were carried out with BigDye® Terminator v3.1 Cycle Sequencing Kit, according to the manufacturer protocol. Briefly, each of sample was performed with 1 μl each forward or reverse primer (Appendix 1), 2 μl plasmid DNA, 3μl 5X sequencing buffer, 0.5 μl premix and ddH_2O to create a final volume of 20 μl. Each of the reaction was performed on the ABI PRISM® 3100 Genetic Analyzer, following the manufacturer's guidelines.

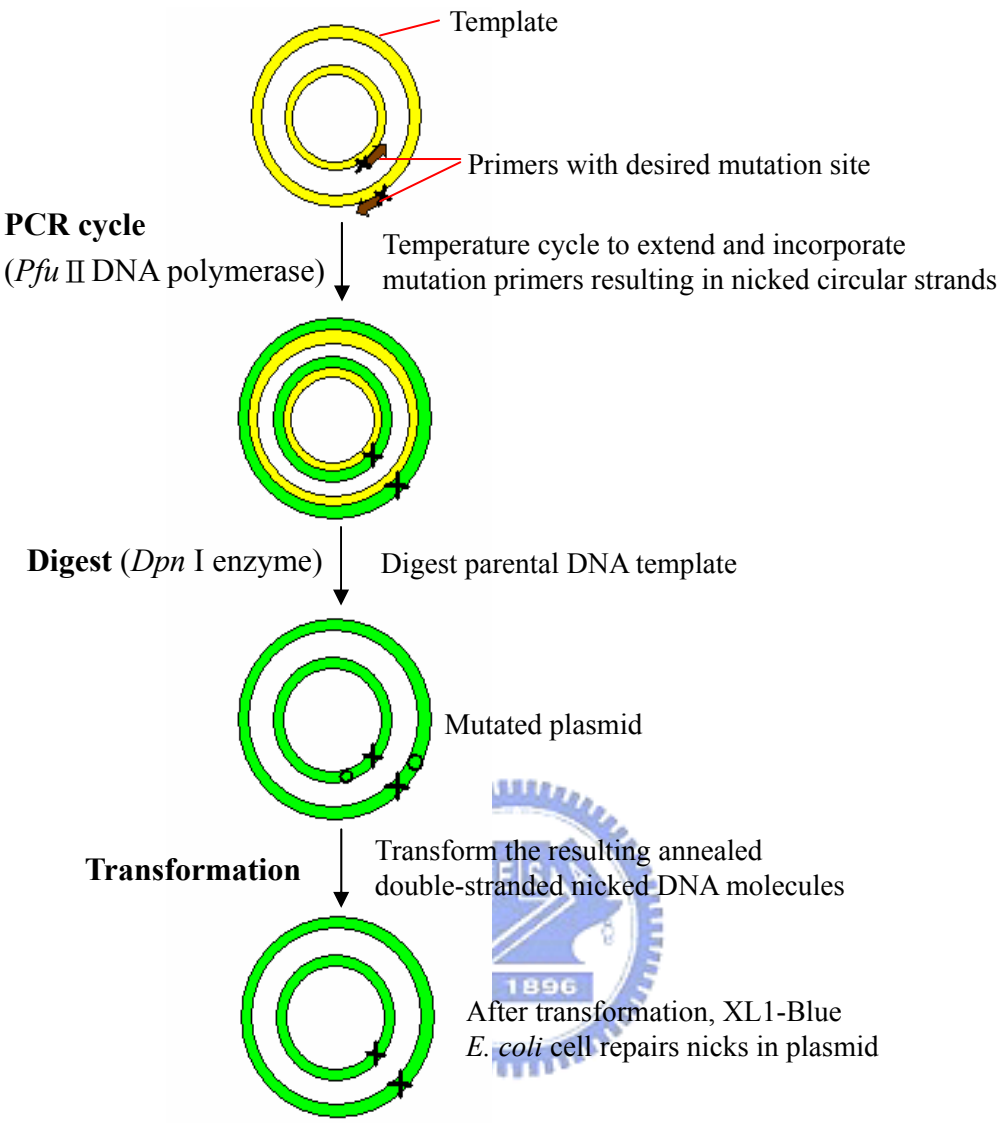

Figure 2-1 QuikChange site-directed mutagenesis strategies

2.2.2 Preparation of Competent Cell (CBY57 and TKW14C2)

Pick the yeast TKW14C2 stock into the 3 ml SD medium, containing 60 µl 50X ALTHMU solution, 120µl 50% glucose solution, 60 µl hemin solution and 60 µl ergosterol solution and then incubated at 30 ℃ for two to three days. When the cell grew well, transferred it to 100 ml SD medium with the same condition and incubated at 30 ℃ for 12-18 hours. After OD_{600} of it reaches 1.0~1.5, the cells were centrifuged to collect at 3,000

rpm, 10 min at 4 ℃ and the supernatant was discarded. Add 50 mL aseptic ddH_2O to resuspend the pellet and centrifuge it at 3000 rpm, 10 min at 4 ℃. Repeated this step but with 25 mL aseptic ddH_2O. Then add 25 ml of 1 M D-sorbitol solution to resuspend the pellet and centrifuge it at the same condition. Finally, add n × 50 μL (n is the number of samples) of 1 M D-sorbitol into the pellet and resuspend it gently. The volume of 50 μl competent cells was added into each 1.5 ml microtube with 5 μl recombinant plasmids, respectively. The preparation protocol of yeast CBY57 is the same as above mention except the yeast growth medium are ALTH solution and glucose solution.

2.2.3 Ergosterol Complementation (expression mutated ERG7 gene in yeast strain TKW14C2)

The pRS314-derived plasmids were transformed into TKW14C2, an ERG7-deficient yeast strain, by electroporation using a Gene Pulser with Pulse Controller (BioRad, Hercules, CA). Mixed 5μL plasmid DNA with 50μL competent cell, and put the mixture on ice for 5 min. Pipetted total of the mixture into cuvette and flick the cuvette to ensure the DNA and cell mixture on the bottom of cuvette. Set the conditions for transformation according to strains. For TKW14C2 cells, use 1.5k volt and the time constant should be 3-4 seconds. Dry off any moisture from cuvette outside and immediately place curette in white plastic holder. Slide holder into position and zap cells. If you hear a high constant tone, immediately add the 0.5 mL of D-sorbitol solution to cells. Aliquots of 120 μL of each culture were plated onto SD+Glu+ALHMU+hemin+Erg+G418 plates, and incubated at 30 ℃ for three to five days to select for the presence of pRS314-derived plasmids. The pRS314 and pRS314-ERG7 gene plasmids were transformed as negative and positive controls, respectively.

Several colonies form each of plate were picked to reselect on two kinds of selective plates, SD+ALHMU+hemin+Erg+G418 and SD+ALHMU+hemin+G418. The transformants

were incubated three to five days at 30℃to confirm the complementation effect. Ergosterol supplement is a selection marker for functional complementation of cyclase in ERG7 mutants.

2.2.4 Plasmid Shuffle and Counter Selection (expression mutated ERG7 gene in yeast strain CBY57)

The pRS314-derived ERG7 mutated plasmids were electroporated into a cyclase-deficient yeast haploid strain CBY57[PZS11]. The pRS314-derived plasmids, the TRP1 centrometric plasmids with no insert and with the mutated *S. cerevisiae* ERG7 gene, were plated onto SD+Glu+ALH+sorbitol plates at 30 ℃ for 3-5 days to determine the presence of both PZS11 and pRS314-derived plasmids. Individual colonies were grown in 10 ml SD+Glu+ALHU liquid culture. Aliquots of 100 μl of each culture were plated on the SD+Glu+ALHU and SD+Glu+ALHU+1mg/ml 5-FOA (5-fluoroorotic acid) plates and grown at 30 ℃ for 3-5 days to elucidate the complementation effect. Expression of the pRS314 and pRS314WT (pRS314-ERG7) in the same strain were treated as negative and positive control, respectively.

2.2.5 Extracting Lipids and Column Chromatography

In the small scale incubation, the mutant transformants were grown in the 2.5 L SD liquid culture medium containing Glu+ALHMU+hemin+Erg medium at 30 ℃ with 130 rpm shaking for five to seven days. The cells were harvested by centrifugation at 6000 rpm for 10 minutes, and saponified with 200 mg pyrogallol by refluxing them in 250 mL of a 15% KOH/ 50% EtOH for 2 hours. The hydrolysate was extracted three times with total 600 ml petroleum ether for extract the nonasponifiable lipid (NSL), the organic phase were collected and dehydrated by sodium sulfate and concentrated using a rotary evaporator. The extract was

fractionated by silica gel column chromatography using a 19:1 hexane/ethyl acetate mixture. Each of fractions was spotted on the thin-layer chromatography which developed with 4:1 hexane/ethyl acetate and the TLC plates were subjected to the stain buffer (5% Anisaldehyde, 5% H_2SO_4 in ethanol) and heated until the patterns appeared. According the TLC results, the fractions can be divided into five regions: OS (oxidosqualene), LA (lanosterol) up, LA, LA down, and Ergosterol. The fractions of LA up, LA, and LA down sections were performed on GC/MS analysis for examination the triterpene products with a molecule mass of *m/z* = 426.

2.2.6 Acetylating Modification and Argentic Column Chromatography

The dry triterpene alcohol fraction was first dissolved in 2 ml pyridine solvent, and then 1 ml acetic anhydride was added into solution. The solution was stirred overnight at room temperature. The acetylation reaction was monitored by TLC analysis. After 16 hours, 5 ml of water was added to terminate the reaction and three times extraction with 10 ml CH_2Cl_2 were carried out. The total organic phase was collected and dried over with sodium sulfate, then evaporated in a rotary evaporator.

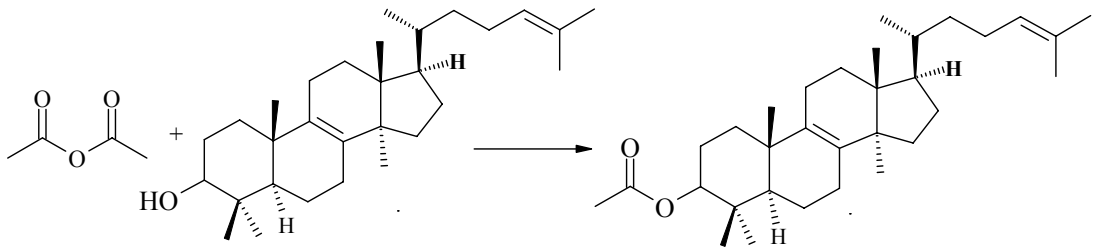

Figure 2-2 The acetylation modification.

2.2.7 $AgNO_3$-impregnated Silica Gel Chromatography

8.6 g $AgNO_3$ and 25 g silica gel dissolved in 50 ml water, stirred and kept them away from light in the oven under 110 ℃ for 16 hours. The gel was used to pack the column with hexane. The acetylated products were fractioned by $AgNO_3$-impregnated silica gel chromatography using 3% diethyl ether in hexane as the eluent. The fractions were analyzed by GC-MS to identify the products and collect the single compound.

2.2.8 Deacetylation Reaction of the Modified Compounds

The dry acetylation triterpene fraction was dissolved in 10 ml methanol, and 0.5 g potassium hydroxide (KOH) was added into the reaction. The reaction was performed with the closed system in the hood and stirred for 12-16 hours at room temperature. The deacetylation reaction was monitored by TLC analysis. After 16 hours, the reactant was dried by rotary evaporator and then 10 ml water was added to dissolve potassium hydroxide. The deacetylated products were extracted three times with dichloromethane. The total organic phase was collected and dried over with anhydrous sodium sulfate (Na_2SO_4), and then dried thoroughly in a rotary evaporator. The deacetylated products were separated by silica gel column chromatography using 19:1 hexane/ethyl acetate mixture. The structure of finally novel products were characterized and identified by NMR spectroscopy (^1H, ^{13}C, DEPT, COSY, HMQC, HMBC, and NOE).

2.2.9 GC-MS Column Chromatography Condition

GC analyses were performed with a Hewlett-Packard model 5890 series Ⅱ or Agilent 6890N chromatography equipped with a DB-5 column (30 m x 0.25 mm I.D., 0.25 μm film; oven gradient at 50 °C for 2 min, and then 20 °C per min until 300°C, held at 300°C for 20 min, 300 °C injector; 250 °C interface; 1/40 split ratio using helium carrier gas at 13 psi column head pressure). GC/MS was performed on a Hewlett-Packard model 5890 II GC (J &

W DB-5MS column, 30 m x 0.25 mm I.D., 0.25 μm film; oven 280 °C, injector 270 °C, GC-MS transfer line: 280 °C) coupled to a TRIO-2000 micromass spectrometer.

2.2.10 Molecular Modeling

Molecular-modeling studies were using the Insight II Homology program with the X-ray structure of lanosterol-complexd human OSC as the template. The MODELER program is designed to extract spatial constraints such as stereochemistry, main-chain and side-chain conformation, distance, and dihedral angle from the template structure. The resulting structure was optimized using an objective function that included spatial constraints and a CHARMM energy function. The objective function combines free energy perturbation, correlation analysis, and combined quantum and molecular mechanics (QM/MM) to obtain a better description of molecular level structure, interactions, and energetics. The homologous model structure, with the lowest objective function, was evaluated further using the Align2D algorithm for sequence-structure alignment.

Chapter 3 Results and Discussions

3.1 Functional Analysis of Tyr707 within *S. cerevisiae* ERG7

3.1.1 Site-Saturated Mutagenesis of Tyr707

To further determine the functional role of Tyr707 and to investigate the effects of substitutions of this residue, we genetically selected Tyr707 site-saturated mutants (Y707X) and characterized each mutant product. The $ERG7^{Y707X}$ site-saturated mutations were generated using QuikChange site-directed mutagenesis kit, and followed by restriction enzyme mapping (*Pvu* I) and DNA sequencing to verify the accuracy of the mutants (Table 3-1). The DNA agarose gel electrophoresis of the mapping results were shown in Appendix 2.

The recombinant plasmids were then transformed into a cyclase-deficient *S. cerevisiae* TKW14C2 strain (MATa/α ERG7Δ::LEU2 HEM1Δ::G418 *ade2-101 his3-Δ200 Leu2-Δ1 lys2-801 trp-Δ63*), a HEM1 ERG7 double-knockout strain which maintains cell viability through uptake of ergosterol from the medium. If the colony of ERG7 mutant grows in the environment without additional ergosterol, it represents that the mutant complemented the yeast viability through normal oxidosqualene-lanosterol cyclase function (Figure 3-1).

Another plasmid shuffle/counter selection method to check the yeast viability of $ERG7^{Y707X}$ mutants were carried out. The "plasmid shuffle" method of exchanging a mutant sequence for a wild type ERG7 containing plasmid (pZS11) was utilized in the analysis of site-directed mutants. The selectable marker of pZS11 is URA3, which is easily counterselected through the use of 5-fluorootic acid (5'-FOA). URA3 converts 5'-FOA into the toxic compound 5-fluorouracil. Yeast that lacks URA3 activity is therefore resistant to 5'-FOA.

CBY57 (MATa/α ERG7Δ::LEU2 *ade*2-101 *his*3-Δ200 *leu*2-Δ1 *lys*2-801 *trpl*-Δ63 [pZS11]) is another strain constructed by our lab, containing pZS11 thus be killed when

placed on media containing 5'-FOA. Therefore the yeast viability of CBY57 only depends on whether the ERG7^{Y707X} mutants complemented the cyclase activity, while the 1% randomly loss of the pZS11 plasmid every generation in the media with exogenous uracil (Figure 3-1).

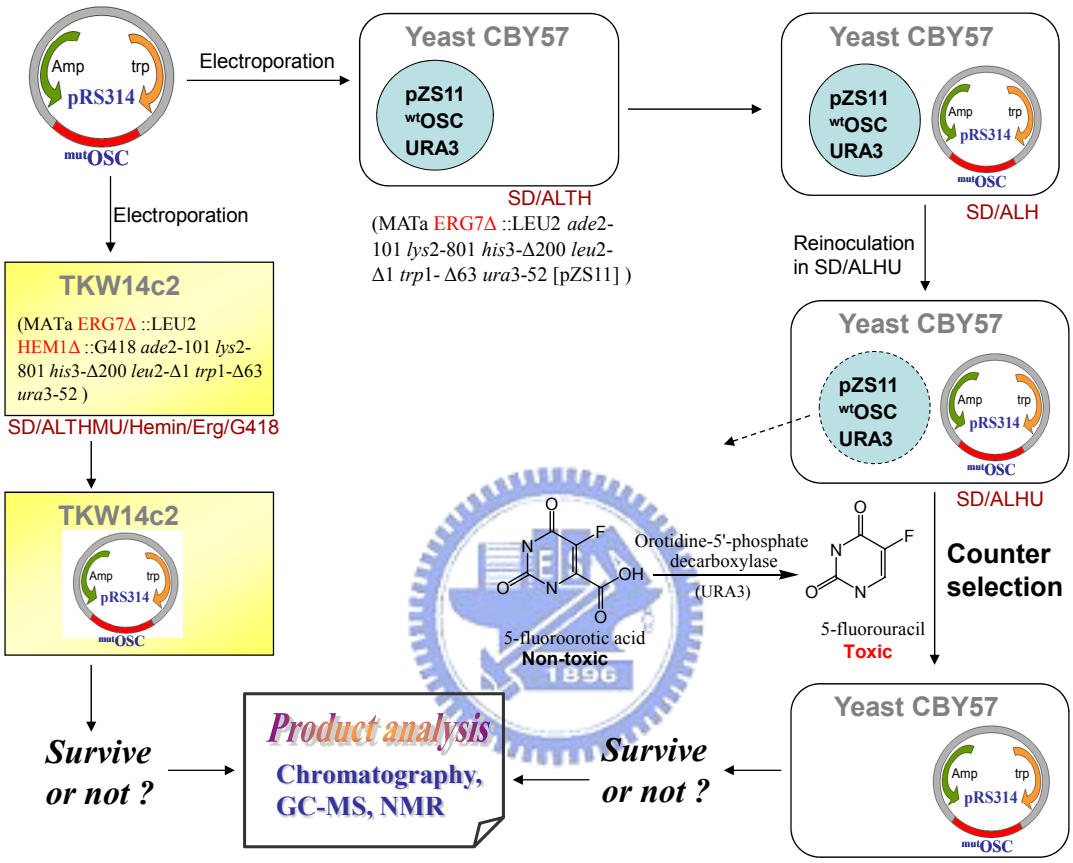

Figure 3-1 The strategies of two selection method using TKW14C2 and CBY57 strains.

The yeast viability of ERG7^{Y707X} mutants in both TKW14C2 (ergosterol complement) and CBY57 (counter selection) must show the same result. These two survival selection displayed that most mutations in Tyr707 cannot abolish the activity of ERG7 cyclase except Tyr707Arg (Table 3-1), indicating the Tyr707 mutations were not detrimental to essential activity of ERG7. However, the loss of the cyclase activity in ERG7$^{\Delta 707}$ mutant suggested that the existence of Tyr707 is crucial for the catalytic function of ERG7.

*Sce*ERG7^{mut}	**Restriction Enzyme Mapping**	**Sequence Confirmation**	**Ergosterol Complement (TKW14C2)**	**Counter Selection (CBY57)**
Y707**H (His)**	*Pvu* I	CAT	+	+
Y707**Q (Gln)**		CAG	+	+
Y707**E (Glu)**		GAA	+	+
Y707**D (Asp)**		GAT	+	+
Y707**T (Thr)**		ACA	+	+
Y707**S (Ser)**		AGC	+	+
Y707**C (Cys)**		TGC	+	+
Y707**G (Gly)**		GGT	+	+
Y707**A (Ala)**		GCC	+	+
Y707**L (Leu)**		CTC	+	+
Y707**I (Ile)**		ATT	+	+
Y707**F (Phe)**		TTT	+	+
Y707**V (Val)**		GTC	+	+
Y707**P (Pro)**		CCA	+	+
Y707**M (Met)**		ATG	+	+
Y707**N (Asn)**		AAT	+	+
Y707**W (Trp)**		TGG	+	+
Y707**K (Lys)**		AAG	+	+
Y707**R (Arg)**		CGA	−	−
Δ707		—	−	−

Table 3-1 The site-saturated mutants of *S. cerevisiae* ERG7^{Y707X} and its viability in TKW14C2 and CBY57 strains

Sce ERG7^{mut}	Product yield ratio (%)				
	(9*R*,10*S*)-polypoda-8(26),13*E*,17*E*,21-tetraen-3β-ol	Lanosterol	9*β*-Lanosta-7,24-dien-3β-ol	Parkeol	No product
Y707H	83.6	4.7	6.2	5.5	
Y707Q	82	4.3	–	13.7	
Y707E	12.3	70.8	10.5	6.4	
Y707D	21.8	67.3	7.6	3.3	
Y707T	9.8	65.1	13.5	11.6	
Y707S	21.3	42.9	20.5	15.3	
Y707C	6	47.1	42.6	4.3	
Y707G	28.3	48.2	16.3	7.2	
Y707A	18.9	56.9	19.9	4.3	
Y707L	–	85.3	14.7	–	
Y707I	–	87.9	12.1	–	
Y707F	–	89.2	7.7	3.1	
Y707V	–	100	–	–	
Y707P	–	100	–	–	
Y707M	–	100	–	–	
Y707N	–	100	–	–	
Y707W	–	100	–	–	
Y707K	–	100	–	–	
Y707R	–	–	–	–	**V**
Δ707	–	–	–	–	**V**

Table 3-2 The product profile of *S. cerevisiae* TKW14 expressing ERG7^{Y707X} site-saturated mutants

The TKW14C2[pERG7^{Y707X}] mutant strains were cultured in 2.5L culture medium and isolated the nonsaponifiable lipid (NSL) extracts for product characterization. Silica gel column chromatography coupled with thin layer chromatography (TLC) and gas chromatography-mass spectrometry (GC-MS) was used to analyze the triterpenoid products with a molecular mass of m/z = 426.

No products with m/z = 426 were observed in the nonviable mutants, ERG7^{Y707R} and

ERG7$^{\Delta Y707}$. However, in the viable mutants, most of them produced other products besides lanosterol, including two altered deprotonation products, 9β-lanosta-7,24-dien-3β-ol and parkeol, as well as a novel product, (9*R*,10*S*)-polypoda-8(26),13*E*,17*E*,21-tetraen-3β-ol. In the ERG7^{Y707Q} and ERG7^{Y707H} mutations, large amounts of (9*R*,10*S*)-polypoda-8(26),13*E*,17*E*,21-tetraen-3β-ol were generated as the sole product, while lanosterol is major in other viable mutants. The ERG7^{Y707L}, ERG7^{Y707I}, and ERG7^{Y707F} mutants produced only lanosterol, 9β-lanosta-7,24-dien-3β-ol, and a slight amount of parkeol. Six mutants (substitution with V, P, M, N, W, K) produced only lanosterol as wild-type ERG7. The product profiles of each mutant are summarized in Table 3-2. The relative retention time in GC column and the mass pattern of each product is shown in Figure 3-3 and Figure 3-4.

3.1.2 Identification and Characterization of the Novel Product

To obtain the pure unknown compound for further identification, 61 L of mutant yeast was cultured. The unknown compound was isolated and purified from NSL extracts by silica gel column chromatography, using 3~5% ethyl acetate in hexane as the eluent. The unknown compound is spotted on TLC using 20% ethyl acetate in hexane as the eluent, and its location is on the upper of lanosterol (Figure 3-2). The retention time of the unknown compound in GC is 22.86 min compare to 24.41 min of lanosterol (Figure 3-3), and its mass pattern is shown in Figure 3-4.

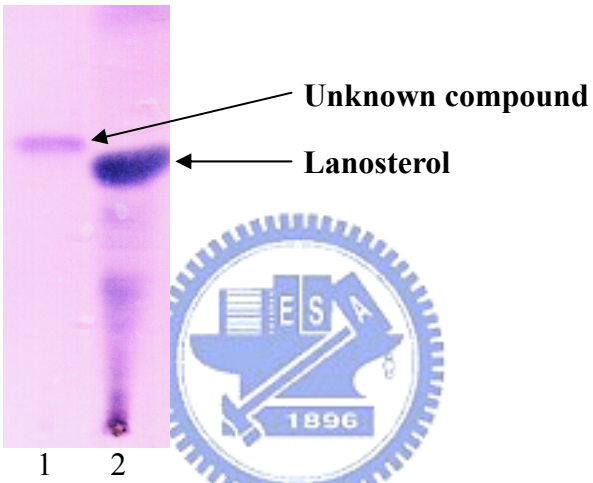

Figure 3-2 The TLC analysis of the unknown compound. Lane 1 is the unknown compound; lane 2 is the lanosterol standard.

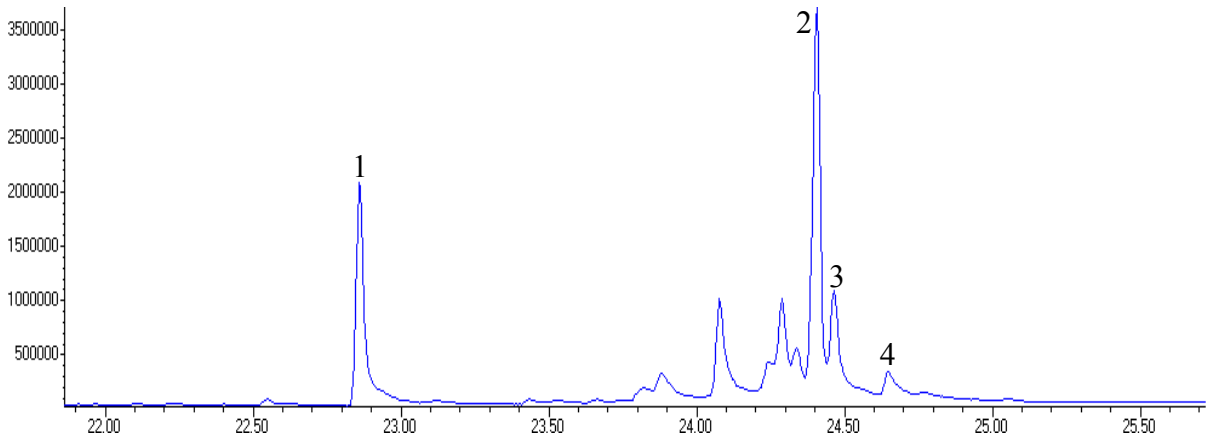

Figure 3-3 GC analysis of the NSL extracts derived from ERG7^{Y707Gly}. Peak 1 is the unknown compound; peak 2, 3 and 4 represent lanosterol, 9β-lanosta-7,24-dien-3β-ol, and parkeol, respectively. The retention time of 1, 2, 3, and 4 is 22.86, 24.41, 24.47, and 24.65, respectively.

Unknown compound

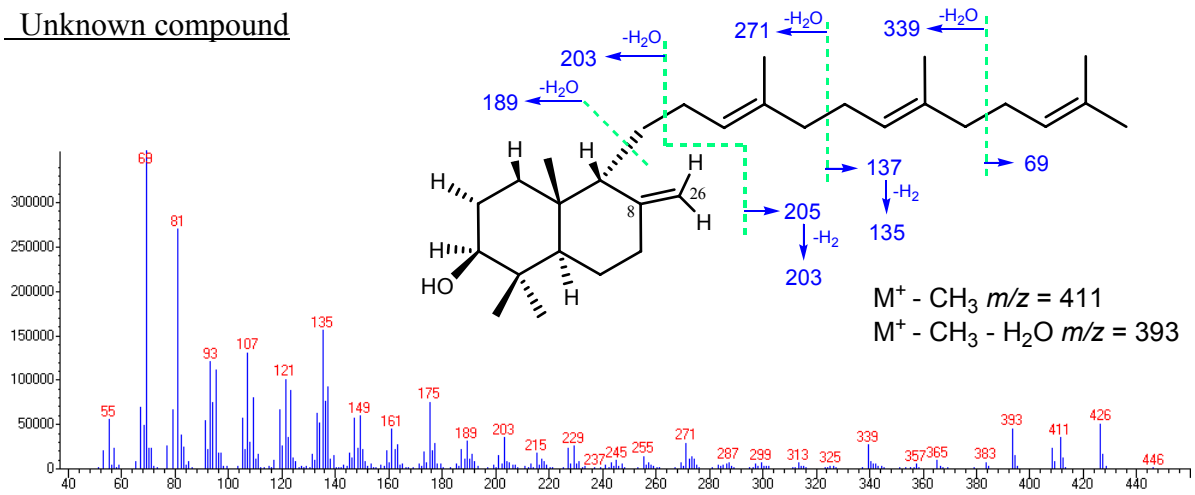

Lanosterol

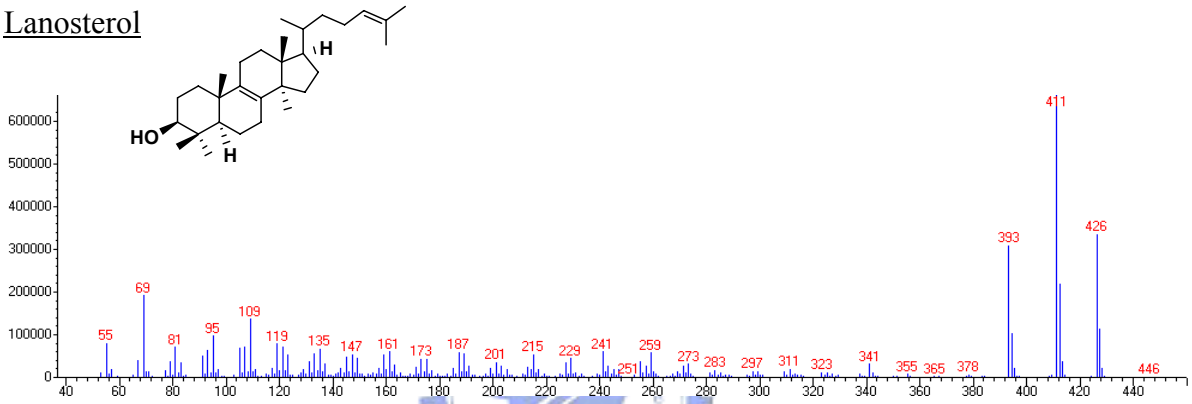

9β-lanosta-7,24-dien-3β-ol

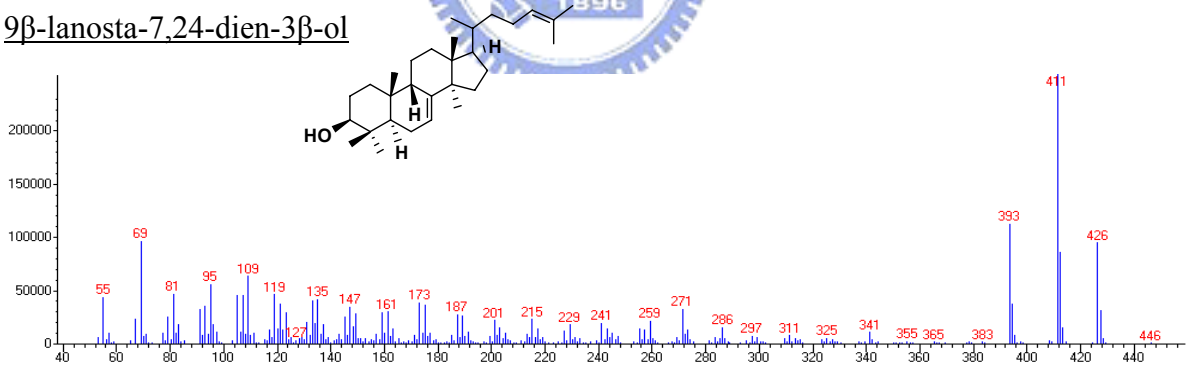

Parkeol

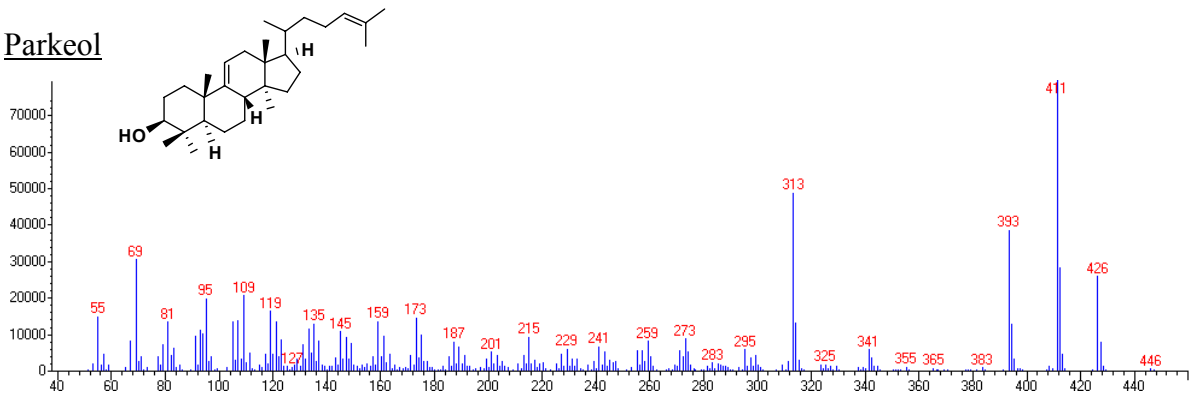

Figure 3-4 The mass spectra of all products of ERG7^{Y707X} mutants.

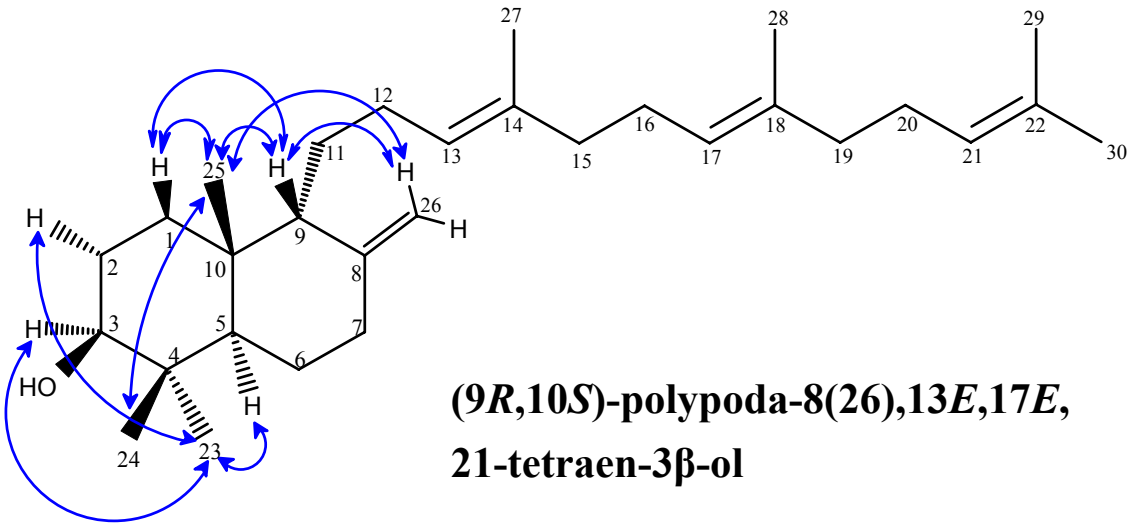

(9*R*,10*S*)-polypoda-8(26),13*E*,17*E*, 21-tetraen-3β-ol

Figure 3-5 The structure and the NOE correlation of the unknown compound.

	^{13}C(δ)	^{1}H(δ)		^{13}C(δ)	^{1}H(δ)
C-1	34.447	1.741, 1.138(dt,J=12.6, 3Hz)	C-16	26.778	2.102 (2H)
C-2	28.027	1.674 (2H)	C-17	124.448	5.163 (1H)
C-3	79.266	3.222 (1H)	C-18	135.047	-
C-4	38.953	-	C-19	39.934	2.02 (2H)
C-5	45.141	1.342(dd, J=12.6, 3Hz)	C-20	26.969	2.102
C-6	23.414	1.695, 1.418(dd, J=12.6, 4.8Hz)	C-21	124.540	5.163 (1H)
C-7	31.263	2.126, 2.218(dd, J=13.8, 3Hz)	C-22	131.344	-
C-8	149.26	-	C-23	28.264	1.023 (3H, s)
C-9	57.744	1.629 (1H)	C-24	15.532	0.802 (3H, s)
C-10	37.881	-	C-25	22.403	0.952 (3H, s)
C-11	26.729	1.364~1.39(m), 1.529~1.585(m)	C-26	109.42	4.576, 4.748
C-12	26.729	1.741~1.790(m), 1.900~1.960(m)	C-27	15.900	1.614 (3H, s)
C-13	124.960	5.163 (1H)	C-28	15.900	1.644 (3H)
C-14	134.943	-	C-29	17.562	1.644 (3H)
C-15	39.897	2.02 (2H)	C-30	25.591	1.72 (3H, s)

Table 3-3 NMR assignments for (9*R*,10*S*)-polypoda-8(26),13*E*,17*E*,21-tetraen-3β-ol for dilute CD_2Cl_2 solution.

The unknown compound was further characterized with NMR (^{1}H, ^{13}C NMR, DEPT, HMQC, HMBC, ^{1}H-^{1}H COSY and NOE) and demonstrated to be (9*R*,10*S*)-polypoda-8(26),13*E*,17*E*,21-tetraen-3β-ol, based on the following data (Figure 3-5 and Table 3-3). The spectra of this compound are shown in Appendix 3. The compound

showed a distinct ^{1}H NMR chemical shift with three unseparated olefinic protons (δ 5.163, 3H) and two methylene protons (δ 4.576, δ 4.748), as well as five methyl singlets (δ 0.802, 0.952, 1.023, 1.614, 1.720) and two unseparated methyl singlets (δ 1.644). The ^{13}C NMR spectrum revealed the presence of one secondary-quaternary (δ = 109.42, 149.26 ppm) and three tertiary-quaternary substituted double bond (δ = 124.960, 134.943; 124.448, 135.047; and 124.540, 131.344 ppm). The HMQC spectrum showed that the olefinic methylene protons at δ 4.576 and 4.748 are attached to the carbon at δ 149.26 ppm (C-8). The aforementioned NMR information indicated a bicyclic triterpene alcohol with three double bonds on the side chain as well as a double bond of two germinal protons. Furthermore, the presence of NOEs among Me-24/Me-25, Me-25/H-26, Me-25/H-1, Me-25/H-9, H-9/H-1, H-9/H-26, Me-23/H-3, Me-23/H-2, and Me-23/H-5, as well as the absence of NOEs among Me-23/H-9, Me-23/Me-25, Me-24/H-3, Me-24/H-5, Me-25/H-5, and H-5/H-1, were uniquely consistent with the stereochemistry of the chair-boat 6-6 bicyclic nucleus with a C-9α hydrocarbon side chain and $\Delta^{8(26),13,17,21}$ double bonds. Structural assignment was also confirmed by comparison of the ^{1}H and ^{13}C NMR spectra with a stereoisomer polypoda-8(26),13,17,21-tetraen-3β-ol which has a C-9β hydrocarbon side chain configuration. [59]

This is the first time to isolate the bicyclic triterpene alcohol derived from a chair-boat bicyclic cation. In particular, the product profile showed the surprisingly high percentage of the bicyclic product in Y707Q and Y707H (82% in Y707Q and 83.6% in Y707H) mutants (Table 3-2), indicating that the Tyr707 residue may play an important role for cation stabilization at C-8 position.

3.1.3 Proposed Cyclization/Rearrangement Mechanism of TKW14C2 Expressing ERG7^{Y707X}

The product profile shows a truncated bicyclic product and two altered deprotonation products as well as lanosterol accumulate in the ERG7^{Y707X} mutants (Table 3-2). The proposed cyclization/rearrangement mechanism is shown in Scheme Ⅳ. First, protonation of the expoxide moiety of oxidosqualene initiates opening of the oxirane ring and the subsequent ring annulations. A bicyclic C-8 cation (lanosterol numbering) was formed without disruption at the monocyclic C-10 cation position, and it is followed by deprotonation of Me-26 to produce (9*R*,10*S*)-polypoda-8(26),13*E*,17*E*,21-tetraen-3β-ol. Further cyclization of the C- and D-ring proceeds to produce a tetracyclic protosteryl C-20 cation. Then skeletal rearrangement of two hydrides and two methyl groups, H-17α→20α, H-13α→17α, Me-14β→13β, Me-8α→14α, and/or one hydride shift from H-9β to H-8β generated lanosteryl C-8/C-9 cation, which undergoes deprotonation at C-7, C-8, and C-11 to result in 9β-lanosta-7,24-dien-3β-ol, lanosterol, and parkeol, respectively.

During the enzymatic cyclization/rearrangement reaction process, several high energetically cationic intermediates will be generated. In general, they proceed to the next step and form lanosterol accurately through the assist of residues within oxidosqualene-lanosterol cyclase. The mutations of ERG7^{Y707} result in the formation of truncated bicyclic product, (9*R*,10*S*)-polypoda-8(26),13*E*,17*E*,21-tetraen-3β-ol, indicates that the energy of the bicyclic C-8 cationic intermediate has been changed and so the reaction will early deprotonate in the bicyclic stage rather than proceed on the normal pathway. It suggested that Tyr707 participated in the B-ring formation of lanosterol by affecting the stability of bicyclic C-8 cationic intermediate. The formation of 9β-lanosta-7,24-dien-3β-ol and parkeol also indicated the influence of Tyr707 to the lanosteryl C-8/C-9 cationic intermediate.

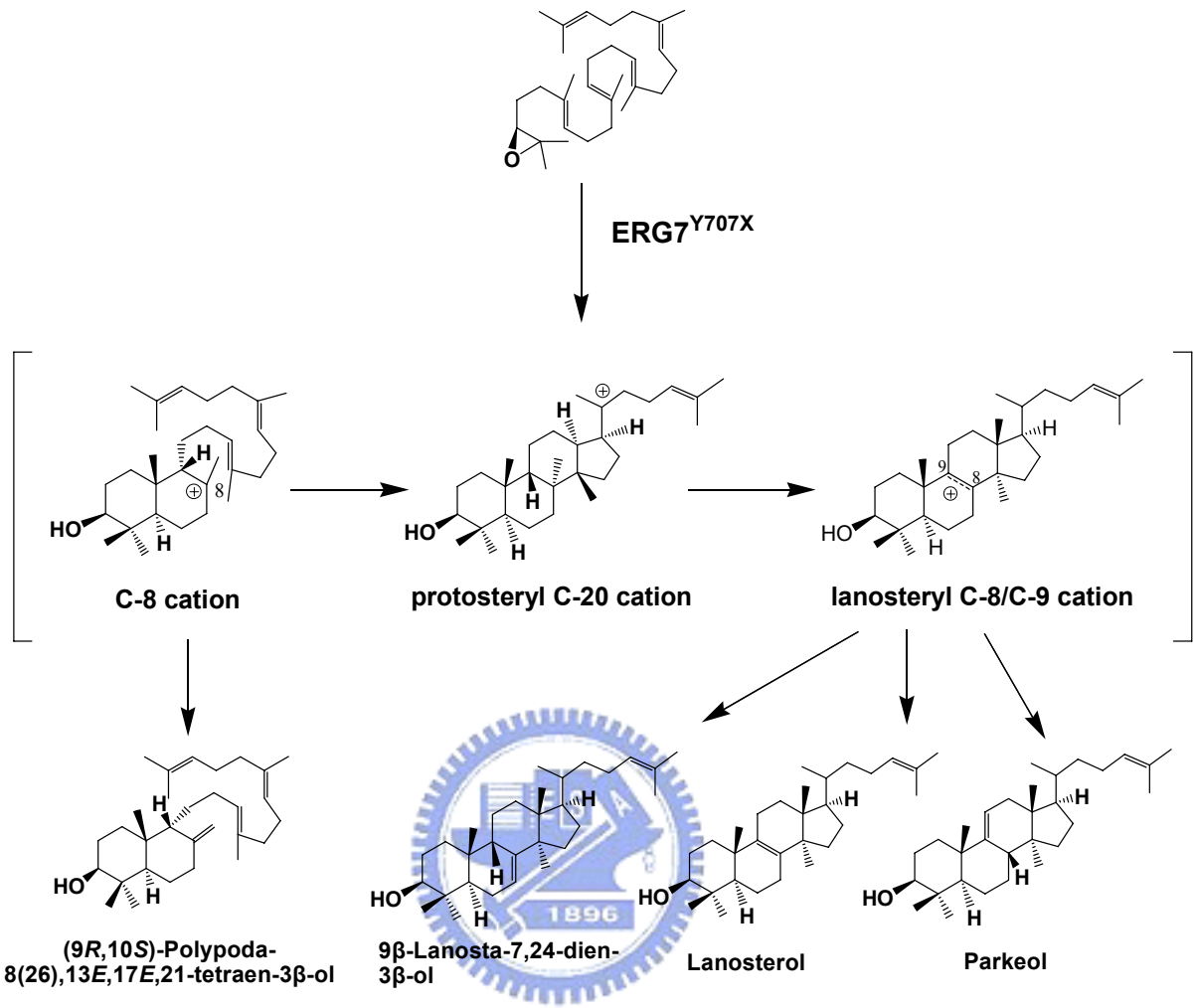

Scheme Ⅳ The proposed cyclization/rearrangement mechanism occurred in the ERG7^{Y707X} site-saturated mutants.

3.1.4 Analysis of the ERG7^{Y707X} Mutants with the ERG7 Homology Modeling

Due to the lack of a high-resolution crystal structure of *S. cerevisiae* wild-type and mutated ERG7 proteins, we used homology models derived from the human OSC X-ray crystal structure and complexed with lanosterol and bicyclic C-8 cation, together with product profiles, to investigate how the ERG7^{Y707X} mutants results in truncated bicyclic and altered deprotonation products. The homology model of ERG7 revealed that Tyr707 is spatially proximal to both C-10 and C-8 positions of lanosterol, and its hydroxyl group points toward the B-ring that is suitable to stabilize the bicyclic cationic intermediate (Fig. 3-6a). The aromatic side chain is also predicted to form a π-electron-rich pocket with nearby aromatic residues that are optimal for the stabilization of the electron-deficient cationic intermediates.[43] (Only the homology models of *Sce*ERG7 complexed with lanosterol are shown here, but the models of *Sce*ERG7 complexed with bicyclic C-8 cation also represented similar results as that complexed with lanosterol.)

The product profile of ERG7^{Y707X} mutants showed that nine amino acid substitutions (H, Q, E, D, T, S, C, G, A) affect the stability of bicyclic C-8 cation, thus produced the truncated bicyclic product. Among those mutants which produced the bicyclic product, most of them are replaced with polar or acidic side chain groups. Substitutions of Tyr707 with the polar or acidic side chain groups possibly change the interaction of Tyr707 to the bicyclic C-8 cation or to other residues nearby. Actually, the human OSC X-ray crystal structure showed that Tyr704 (Tyr707 in *S. cerevisiae* ERG7) is hydrogen bonded to the backbone carbonyl group of Trp581 (Trp587 in *S. cerevisiae* ERG7) through a water bridge (Fig. 3-6b). [6,8] These polar groups may destroy the hydrogen-bonding of Tyr707 to the water molecule and alter the interaction to other residues due to their different orientation and intensity of the dipoles, thus changes the electron distributions for stabilizing the bicyclic cation (Fig. 3-6c).

Interestingly, there are significant accumulations of the bicyclic product in the mutants of Tyr707His and Tyr707Gln, whereas no any truncated or altered deprotonation product appeared in Tyr707Asn. Various factors were possibly involved in the enzyme-substrate interaction to lead to the contrasting result. One reason might be the additional hydrogen bonding site of His and Gln compare to Tyr, which altered the H-bonding around Tyr707. Further, Asn has an amide group as Gln but the length of the side-chain and the spatial orientation relative to the cation position are different; it is likely that these differences produced a deviation of the electron density distribution (Fig. 3-6d).

On the other hand, substitution with small aliphatic side chains such as Gly and Ala possibly enlarged the cavity of active site to make the substrate more flexible. This may shift the substrate to inappropriate orientation that incapable to form lanosterol accurately, and lost the protection to C-8 cation for further cyclization, giving the chance of the catalytic base to attack the bicyclic cationic intermediate and generated the truncated bicyclic product.

Based on human OSC X-ray structure, it has been suggested that the active site has a higher π-electron density near C-8/C-9 positions of lanosterol with seven aromatic residues, which might be responsible for the equilibrium shift from C-20 cation toward the C-8/C-9 cation and for the subsequent formation of lanosterol.[6] Because Tyr707 is spatially proximal to the C-8 position of lanosterol, it may provide the π-electron density to affect the stability of the lanosteryl C-8/C-9 cation and the steric bulk also assist the cationic intermediate in the appropriate position to form lanosterol accurately. Therefore, substitution of Tyr707 with polar and small aliphatic side chains may disturb the electron density distribution around the C-8/C-9 cation and alter the deprotonation site of lanosteryl C-8/C-9 cation to produce 9β-lanosta-7,24-dien-3β-ol and parkeol.

The $ERG7^{Y707K}$ and $ERG7^{Y707R}$ mutants, which Tyr was substituted with positively

charged side chains, showed radically different results that ERG7^{Y707K} synthesize lanosterol normally but ERG7^{Y707R} lost cyclase activity completely. The mutation of ERG7^{Y707R} cannot complement yeast viability perhaps due to the strong positive charge and the long side chain of Arg that generated a significant repulsion to the cation and thus abolished the total reaction processes. However, homology models revealed that when substitution with Lys, its ε-amino group didn't point toward the C-8 cation and the farther distance to C-8 perhaps reduced the electrostatic repulsion of the positive charge of Lys to C-8 (Fig. 3-6e).

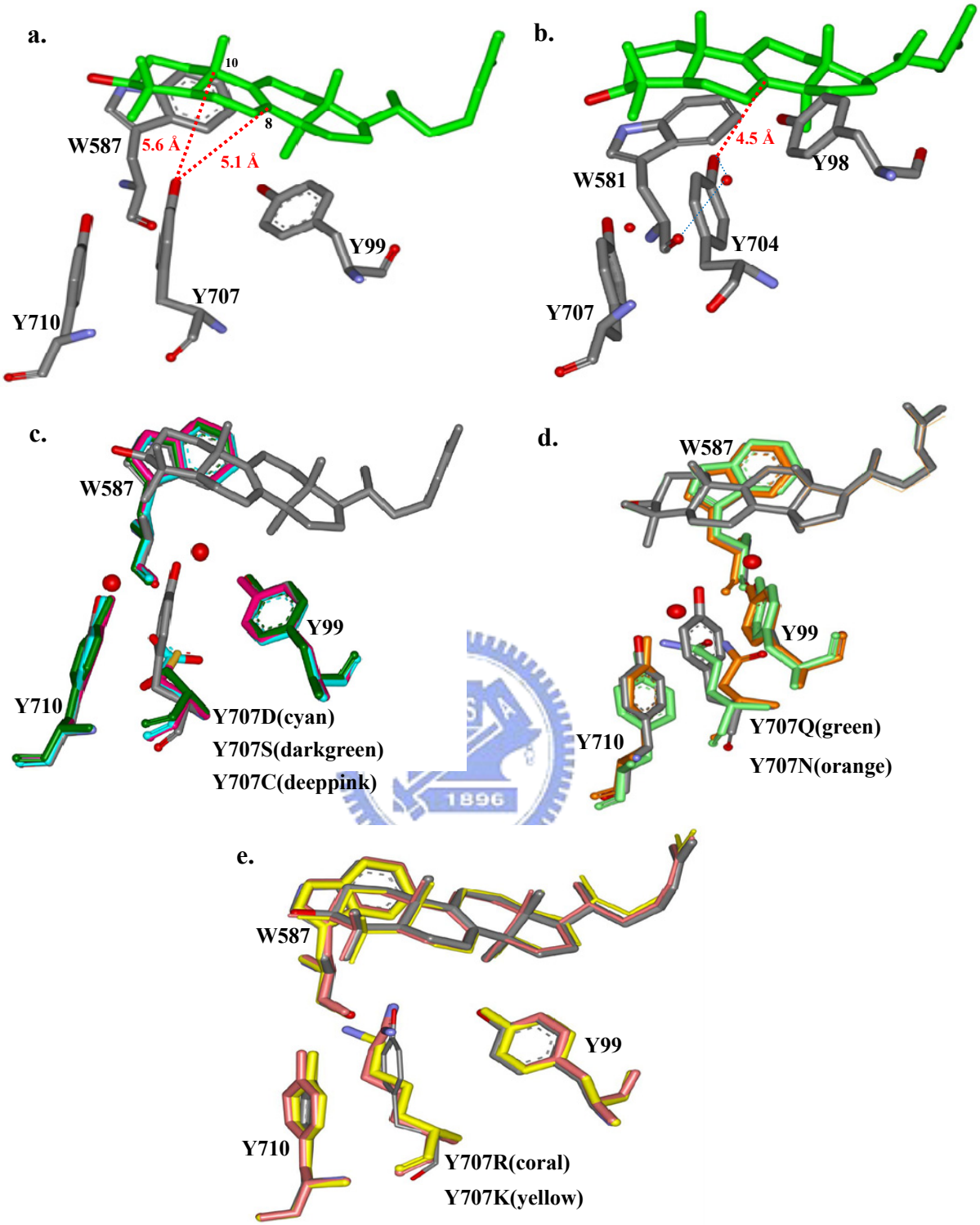

Figure 3-6 (a)The homology model of wild-type ERG7 complexed with lanosterol. The distance of Tyr707 to C-10 and C-8 position of lanosterol is 5.6 Å and 5.1 Å, respectively. (b)The human OSC X-ray structure: water molecules near Tyr704 (corresponds Tyr707 in *S. cerevisiae* ERG7) are shown. (c-e)The homology models of $ERG7^{Y707X}$ mutants coupled with wild-type ERG7 (gray). Color cord: Y707D (cyan); Y707S (darkgreen); Y707C (deeppink); Y707Q (green); Y707N (orange); Y707K (yellow); Y707R (coral).

To our surprise, most nonpolar amino acid substitutions formed lanosterol normally without any truncated cyclization product, indicating the loss of H-bonding did not cause obvious interference in the reaction process. The oxidosqualene-lanosterol cyclase can tolerate this difference when Tyr707 was substituted with nonpolar amino acids, perhaps because other residues nearby will complement the function of Tyr707 somehow. But the exact interaction remains unclear.

It is difficult to explain why the mutations of Y707I, Y707L, and Y707F also produced altered deprotonation products but no truncated bicyclic product. Perhaps the bulky side chains of Ile, Leu, and Phe still pulled the water molecule in an appropriate position for stabilization of the bicyclic cationic intermediate, although they cannot form hydrogen bonds with the water molecule. However, these mutations are not very adequate for the cyclase that caused some perturbation of the active site and so result in the altered deprotonation products.

Interestingly, the homology model displayed that the distance between Tyr707 and C-8 position in wild-type ERG7 when complexed with bicyclic C-8 cation (6.2Å) is farther than the human OSC crystal structure complexed with lanosterol shown (4.5Å) (Table 3-4). Therefore, we also examined the distance of Tyr707 to C-8 position in the homology model which complexed with lanosterol. It showed the distance of 5Å, that still farther than the human OSC crystal structure shown but shorter than that in the homology model complexed with bicyclic C-8 cation. The same results were also shown in the homology models of other mutants (Table 3-4). This difference perhaps is the deviation raised from the computational calculation; however, it also provided a possibility that the relative position between the enzyme and the substrate was changed during the cyclization process and the distance became farther when the moment the bicyclic cation intermediate formed.

Amino acid substitution	Distance to C-8 of the bicyclic C-8 cation (Å)	Distance to C-8 of lanosterol (Å)	
WT	6.18	5.07	
Q	8.45(N); 8.94(O)	7.98(N); 7.73(O)	Bicyclic and altered deprotonation
H	8.08 (N)	6.73 (N)	
E	7.51 (O)	6.51 (O)	
D	9.14 (O)	7.88 (O)	
C	9.3 (S)	8.06 (S)	
S	10.41 (nearest) ; 11.38(O)	9.23 (nearest) ; 10.13(O)	
T	10.5 (O)	9.32 (O)	
A	10.86	9.85	
G	11.94	10.65	
F	7.16	6.02	Altered deprotonation
L	8.63	7.9	
I	9.08	8.01	
W	7.73 (N)	6.38 (N)	LA only
M	7.17 (nearest)	6.06 (nearest)	
P	10.08	8.75	
N	8.85(N); 9.01(O)	7.55(N); 7.69(O)	
K	8.17	6.83	
R	5.99	4.71	No product

Table 3-4 The distance of Tyr707 to C-8 in the homology models complexed with bicyclic C-8 cation and lanosterol, respectively.

3.2 The Double Mutagenesis of ERG7$^{F699M/Y707H}$ and ERG7$^{F699M/Y707Q}$

Recently, the Phe699 of *S. cerevisiae* ERG7 has been identified to be an important plasticity residue with diverse product profiles that can be applied to protein redesign.[51] Besides, a chair-chair-chair tricyclic product, malabarica-14*E*-trien-3β-ol, was isolated from the ERG7^{F699M} and ERG7^{F699N} mutants, indicated a conformational change of the substrate from chair-boat-chair to chair-chair-chair prefolded conformation.[75] In addition, the Tyr707 of *S. cerevisiae* ERG7 has been demonstrated to be an important residue to stabilize the bicyclic C-8 cationic intermediate in this study. Because of the uncommon conformational change of B-ring in ERG7^{F699M} mutant and the stabilization ability of bicyclic C-8 cation of Tyr707 in ERG7, combination of these two mutations may provide the possibility to produce chair-chair bicyclic products. Therefore, two mutations Try707His and TyrY707Gln, which produce the bicyclic triterpene alcohol as the sole product, were selected to combine with the mutation of F699M for further analysis.

*Sce*ERG7^{mut}	**Restriction Enzyme Mapping**	Ergosterol supplement	Product pattern (%)
F699M/Y707H	*Pvu* I	−	No product
F699M/Y707Q	*Pvu* I	−	No product

Table 3-5 The genetic selection results and the product profiles of the ERG7$^{F699M/Y707H}$ and ERG7$^{F699M/Y707Q}$ double mutants

The double mutations of F699M/Y707H and F699M/Y707Q of *S. cerevisiae* ERG7 were constructed using QuikChange site-directed mutagenesis strategies. The recombinant plasmids of ERG7$^{F699M/Y707H}$ and ERG7$^{F699M/Y707Q}$ were then transformed into the TKW14C2 strain to check the yeast viability and for further analysis of their products, following the same

strategies described in Chapter 2 and Section 3.1.1. The genetic selection results revealed that both mutants cannot complement the yeast viability. Further analysis of their products showed that no product with a molecular mass of m/z = 426 was accumulated in the ERG7$^{F699M/Y707H}$ and ERG7$^{F699M/Y707Q}$ mutants (Table 3-5). The inactivity of these two mutations indicated that the double mutation of F699M/Y707H or F699M/Y707Q may cause a large perturbation around the active site, thus abolished the lanosterol biosynthesis. In fact, the single mutation of either F699M or Y707H and Y707Q has a significant disturbance in the catalytic function of ERG7 that produced large amounts of truncated cyclization/rearrangement products and only a little amount of lanosterol. However, these two mutations didn't show any product in GC-MS analysis. Perhaps, mutation of these two residues which have important catalytic function in *S. cerevisiae* ERG7 collectively may destroy the structural integrity of active site for substrate binding or intermediate stabilization and result in the total vanish of the cyclase function.

3.3 Functional Analysis of Tyr710 within *S. cerevisiae* ERG7

3.3.1 Generation of Site-Saturated Mutants of Tyr710

Tyrosine 710 of the *S. cerevisiae* ERG7 gene was substituted with other 19 amino acids by using the QuikChange site-directed mutagenesis strategies with the respective mutagenic primers. A silent mutation was introduced to easily screen the desired mutants, according to a restriction enzyme (*Ava* I) mapping confirmation. The DNA agarose gel electrophoresis of the mapping results were shown in Appendix 2. The presence of the mutations was verified by sequence determination (Table 3-6).

The recombinant plasmids were transformed into TKW14C2 and CBY57 by the same strategies as previously described in Chapter 2 and Section 3.1.1. The genetic selection and counter selection results of the $ERG7^{Y710X}$ mutants were shown in Table 3-4. The genetic selection revealed that only one mutant, Tyr710Pro, cannot allow for ergosterol-independent growth. Other mutants all complemented the yeast viability. These results indicated that the mutations of Tyr710 were not detrimental to the essential activity of ERG7.

*Sce*ERG7^{mut}	**Restriction Enzyme Mapping**	**Sequence Confirmation**	**Ergosterol Complement (TKW14C2)**	**Counter Selection (CBY57)**
Y710**G (Gly)**		GGG	+	+
Y710**A (Ala)**		GCC	+	+
Y710**V (Val)**		GTC	+	+
Y710**I (Ile)**		ATC	+	+
Y710**L (Leu)**		CTA	+	+
Y710**E (Glu)**		GAA	+	+
Y710**D (Asp)**		GAC	+	+
Y710**Q (Gln)**		CAA	+	+
Y710**N (Asn)**		AAC	+	+
Y710**H (His)**	*Ava* I	CAT	+	+
Y710**K (Lys)**		AAA	+	+
Y710**R (Arg)**		CGC	+	+
Y710**M (Met)**		ATG	+	+
Y710**C (Cys)**		TGT	+	+
Y710**S (Ser)**		TCC	+	+
Y710**T (Thr)**		ACC	+	+
Y710**F (Phe)**		TTC	+	+
Y710**W (Trp)**		TGG	+	+
Y710**P (Pro)**		CCT	−	−

Table 3-6 The site-saturated mutants of *S. cerevisiae* ERG7^{Y710X} and its viability in TKW14C2 and CBY57 strains

3.3.2 Lipid Extraction, Column Chromatography and Product Characterization

The recombinant TKW14C2[pERG7^{Y710X}] mutant strains were cultured in 2.5L culture medium and the NSL extracts were isolated for product characterization. In the inviable mutant, Tyr710Pro, there is no product with molecular mass of *m*/*z* = 426 compared with the product pattern of negative control, TKW14C2. Four viable TKW14C2[pERG7^{Y710X}] mutants, Tyr710Gly, Tyr710Ser, Tyr710Ile, and Tyr710Arg revealed other products with molecular mass of *m*/*z* = 426 in addition to lanosterol. These product compounds were identified with authentic lanosterol, 9β-lanosta-7,24-dien-3β-ol, parkeol, achilleol A, and camelliol C standards by GC-MS. In Tyr710Ser and Tyr710Gly mutants, visible amounts of 9β-lanosta-7,24-dien-3β-ol were produced; while parkeol appeared in the Tyr710Ile mutant. Besides, in the Tyr710Arg mutant, achilleol A and camelliol C as well as lanosterol were produced. The GC analysis and their mass patterns were shown in Figure 3-7. The product profiles of each mutant are summarized in Table 3-7.

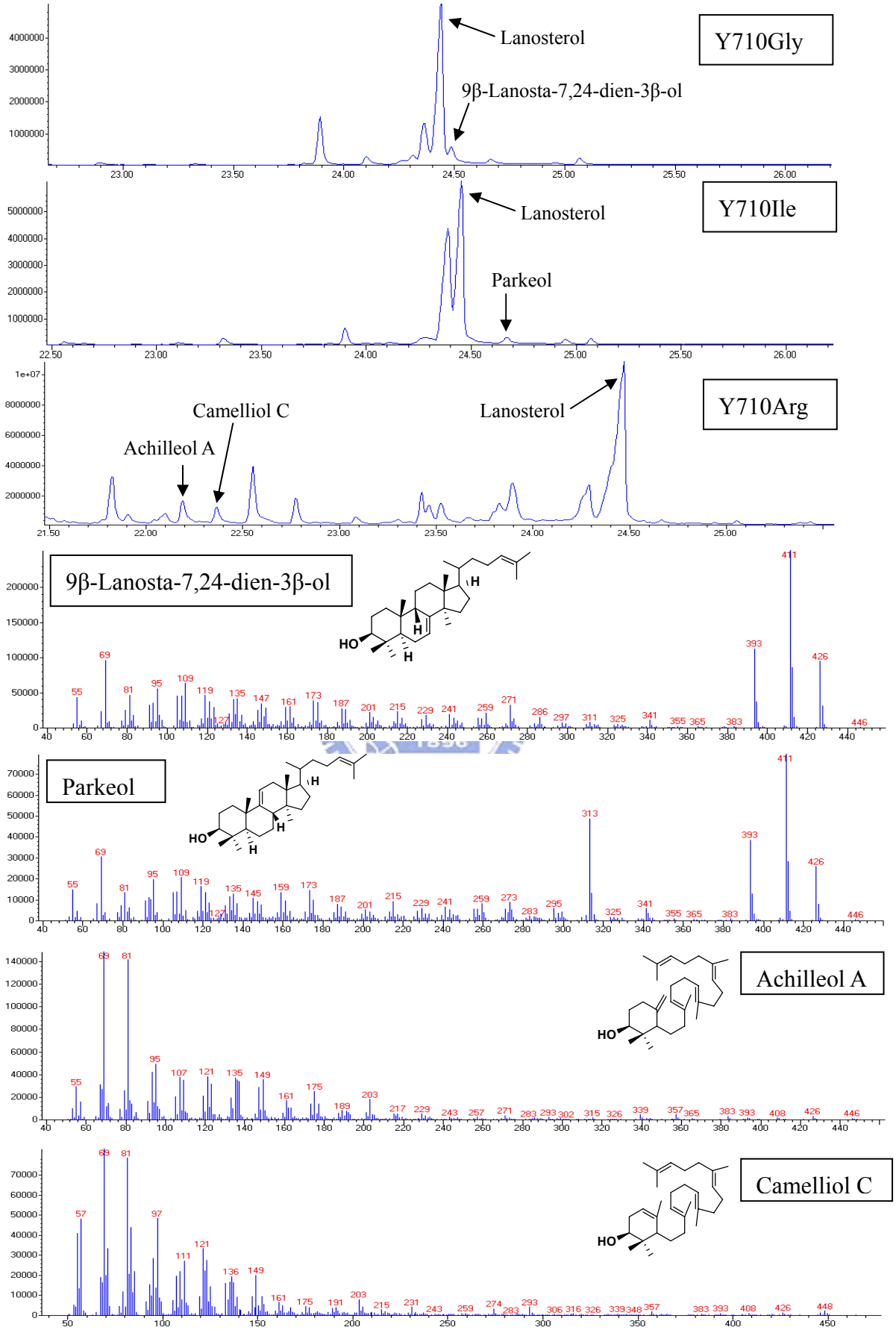

Figure 3-7 The product patterns of ERG7^{Y710Gly}, ERG7^{Y710Ile} and ERG7^{Y710Arg} mutants GC analysis and their mass patterns.

Sce ERG7^{mut}		Ergosterol supplement	Product yield ratio (%)					
			Achilleol A	Camelliol C	Lanosterol	9β-Lanosta-7,24-dien-3β-ol	Parkeol	No product
Aliphatic	**Y710G**	+	–	–	88.8	11.2	–	
	Y710A	+	–	–	100	–	–	
	Y710V	+	–	–	100	–	–	
	Y710I	+	–	–	93.7	–	6.3	
	Y710L	+	–	–	100	–	–	
Acidic and amide	**Y710E**	+	–	–	100	–	–	
	Y710D	+	–	–	100	–	–	
	Y710Q	+	–	–	100	–	–	
	Y710N	+	–	–	100	–	–	
Basic	**Y710H**	+	–	–	100	–	–	
	Y710K	+	–	–	100	–	–	
	Y710R	+	7.6	6.1	86.3	–	–	
Sulfur-containing	**Y710M**	+	–	–	100	–	–	
	Y710C	+	–	–	100	–	–	
Hydroxyl group	**Y710S**	+	–	–	90	10	–	
	Y710T	+	–	–	100	–	–	
Aromatic	**Y710F**	+	–	–	100	–	–	
	Y710W	+	–	–	100	–	–	
Imino	**Y710P**	–	–	–	–	–	–	**V**

Table 3-7 The product profile of *S. cerevisiae* TKW14 expressing ERG7^{Y710X} site-saturated mutants

3.3.3 Proposed Cyclization/Rearrangement Mechanism of TKW14C2 Expressing ERG7^{Y710X}

Scheme V showed the proposed cyclization/rearrangement mechanism in the ERG7^{Y710X} mutants. In most of the ERG7^{Y710X} mutants, the cyclization reaction proceeded to the tetracyclic protosteryl C-20 cation without any disruption, and followed by a series of skeletal rearrangements to generate lanosteryl C-8/C-9 cation. In some cases, the cation stayed in the C-9 position and deprotonation at C-8 or C-11 to form lanosterol and parkeol. While in the Tyr710Gly and Tyr710Ser mutants, the cation stayed in the C-8 position and abstract the proton at C-9 or C-7 to produce lanosterol and 9β-lanosta-7,24-dien-3β-ol. However, the Tyr710Arg mutant produced two monocyclic products, achilleol A and camelliol C, meaning the premature truncation of the monocyclic C-10 cation intermediate and the proton abstraction from Me-25 or C-1 position.

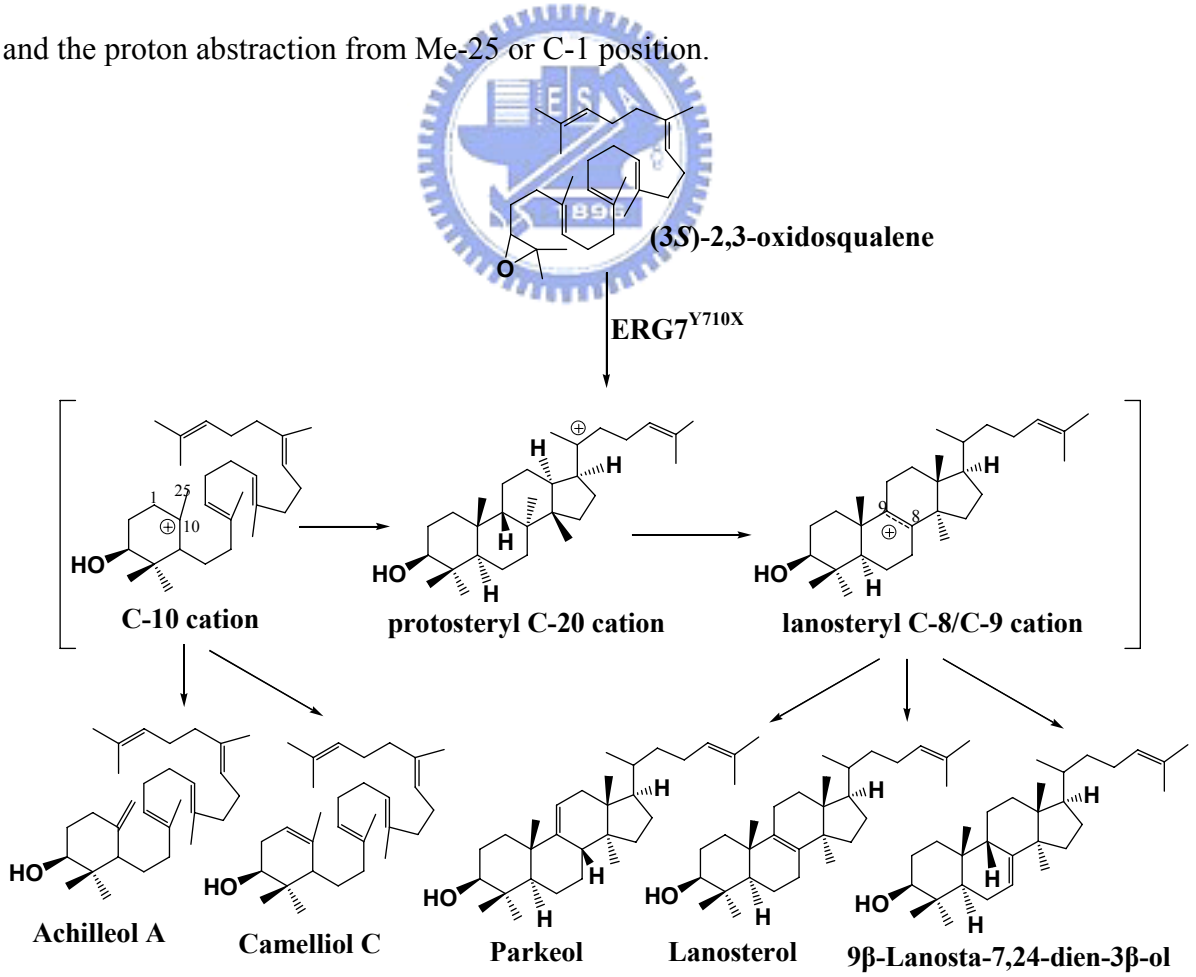

Scheme V The proposed cyclization/rearrangement mechanism occurred in the ERG7^{Y710X} site-saturated mutants

3.3.4 Analysis of the ERG7^{Y710X} Mutants with the ERG7 Homology Modeling

The multiple sequence alignment analysis showed that the Tyr710 residue of *S. cerevisiae* ERG7 is highly conserved in most cyclases, it corresponds to the Tyr612 in *A. acidocaldarius* SHC and to Tyr707 in *H. sapiens* OSC. This highly conserved aromatic residue was considered as an important residue during the catalytic cyclization mechanism. However, the functional role of Tyr710 in *S. cerevisiae* ERG7 was not consisting with what we thought or reported before based on our experiment results.

According to the previous studies, the Tyr612Ala and Tyr612Leu mutants in SHC produced little amounts of mono- and bicyclic products, thus Tyr612 was thought to intensify the function of both Asp377 and Phe365, by placing Asp377 and Phe365 at the correct positions in the enzyme cavity and enriching the negative charge of Asp377 and the π-electrons of Phe365.[54,70] But the function of Tyr612 has not been clearly referred to by the X-ray analysis of *A. acidocaldarius* SHC.[11,12]

In the X-ray analysis of human OSC, Tyr707 (corresponds to Tyr710 in *S. cerevisiae* ERG7) still not to be mentioned to have an important catalytic function.[6] However, examined the human OSC X-ray structure, Tyr707 is on the top of the active site cavity and forms a hydrogen-bonding network with Trp581 (corresponds to Trp587 in *S. cerevisiae* ERG7) and Tyr587 (corresponds to Tyr593 in *S. cerevisiae* ERG7) *via* water-bridges. In our homology modeling of *S. cerevisiae* ERG7, Tyr710 is proximal to the Tyr707, and the distance of Tyr710 is 8.8 Å to the C-10 of lanosterol and 8.7 Å to the C-8 of lanosterol. Although the position of Tyr 710 is far from the substrate, we thought that it still has opportunity to influence the mono- or bicyclic cation through the interaction with other residue(s) nearby as Tyr612 did in SHC.

However, our mutagenesis studies to the Tyr710 of *S. cerevisiae* ERG7 showed different results from what we predicted. No bicyclic product was produced in the ERG7^{Y710X} mutants and most of the mutants just produced the natural product lanosterol. Only the Tyr710Arg mutant produced two monocyclic products. But the altered deprotonation products, parkeol and 9β-Lanosta-7,24-dien-3β-ol were produced in Tyr710Ile or Tyr710Ser and Tyr710Gly, respectively. Specially, only the Tyr710Pro mutant lost the catalytic activity and no product was produced.

The homology models of mutated ERG7 proteins may provide us some information. The Tyr710 residue is located at the end of an α-helix structure. When it was mutated to Pro, the α-helix may be distorted and changed the position of the following residues thus destabilized the structure of the active site (Fig. 3-8a). It was suggested that Tyr710 may play a role in preserving the cyclase structure. On the other hand, computer models have shown that the mutation of Try710 to the side chain of Gly enlarges the cavity of the active site and causes a displacement of the residues around the active site, especially of Ile705 (Fig. 3-8b). The position of Ile705 in the ERG7^{Y710G} mutant is closer to the substrate and the steric bulk of Ile may push the substrate to the incorrect position, thus changes the deprotonation site of the lanosteryl C-8/C-9 cation. Mutation of Try710 to Ser also caused the displacement of the active site residue and shifted the deprotonation site to generate 9β-lanosta-7,24-dien-3β-ol, perhaps due to the small size and the dipole of Ser. In addition, the ERG7^{Y710I} mutant produced lanosterol as well as parkeol, perhaps due to the steric effect of Ile that caused a subtle change in the conformation of the top of the cavity, thus shifts the substrate away from the correct deprotonation site (Fig. 3-8c).

Further, the accumulation of monocyclic achilleol A and camelliol C in the ERG7^{Y710R} mutant suggested that Tyr710 has an influence to the monocyclic C-10 cation intermediate. The mutation of Tyr710 to Arg caused a marked perturbation around the active site by both

steric and electrostatic effects, thus terminating the cyclization at the monocyclic reaction stage. Tyr710 should not interact with Cys457 (corresponds Asp377 in SHC) as expected previously because the distance of Tyr710 to Cys457 is too far (9.3 Å in our homology model). Instead, the homology model showed a dramatic displacement of Trp390 when Tyr710 was mutated to Arg (Fig. 3-8d). In fact, our homology modeling of wilt-type ERG7 shows the distance of Tyr710 to Trp390 is 3.0 Å. The result indicated that Tyr710 may work to place Trp390 at the correct position to assist the cyclization/rearrangement reaction process.

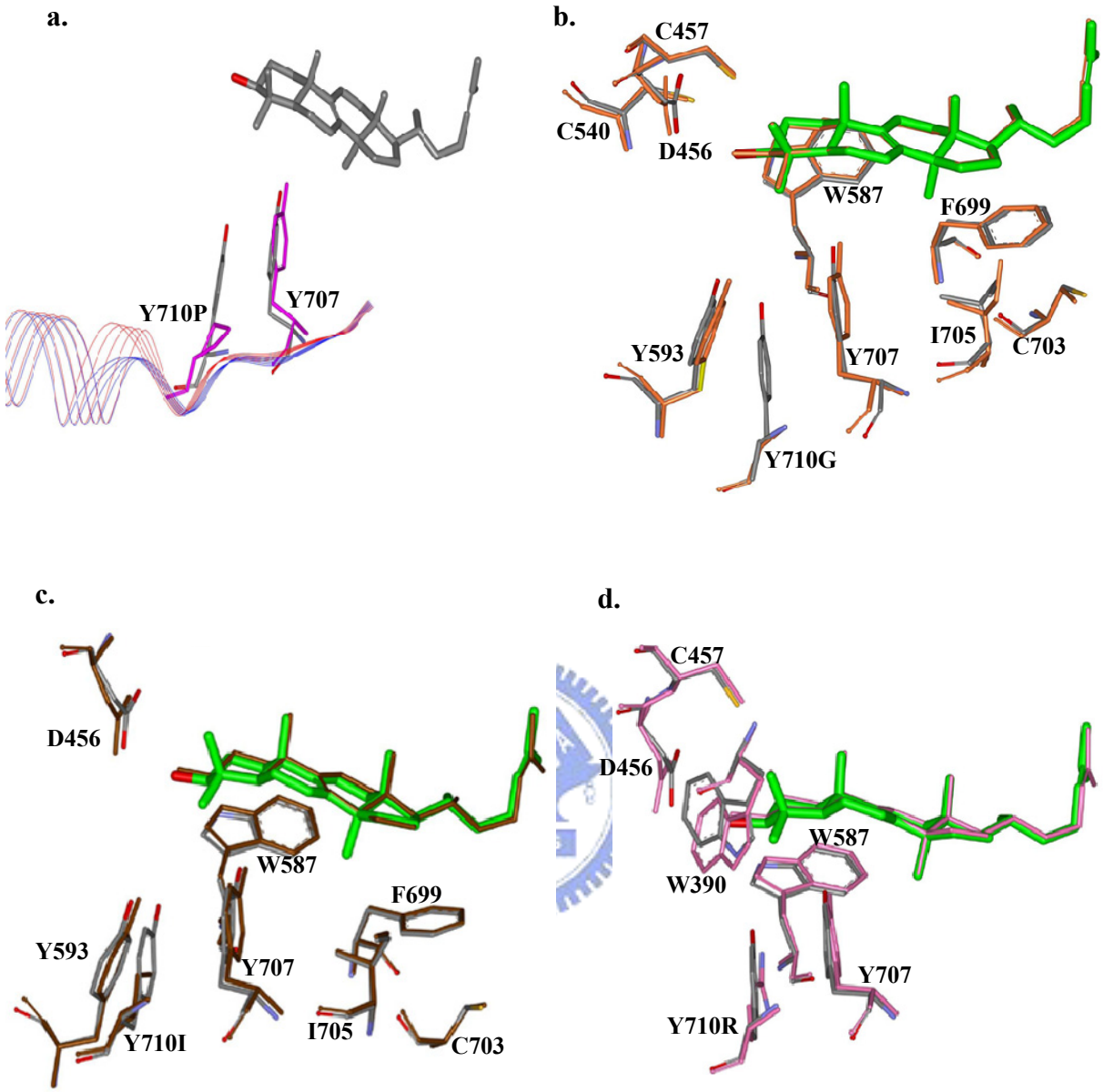

Figure 3-8 The homology models of ERG7^{Y710X} mutants (colored) coupled with wild-type ERG7 (gray). (a) ERG7^{Y710P}, the secondary structure of Y710P (red) and wild-type ERG7 (blue) were also shown. (b) ERG7^{Y710G} (c) ERG7^{Y710I} (d) ERG7^{Y710R}.

Chapter 4 Conclusion

Site-saturated mutagenesis, an approach to replace the target residue with other 19 proteinogenic amino acids, is applied to give the detailed understanding of the electrostatic and steric effects of a specific residue. The structure of the abortive products produced by the mutants provides an evidence of the functional role of the residue in the cyclization/rearrangement reaction mechanism.

In our studies, the site-saturated mutagenesis coupled with product isolation strategy were preformed in the Tyr707 and Tyr710 within *S. cerevisiae* oxidosqualene-lanosterol cyclase to analyze the functional role and the relationship to the bicyclic cationic intermediate of these highly conserved aromatic residues in the putative active site of cyclases.

In the part of *Sce*ERG7^{Y707X} mutants:

1. We have constructed the saturated mutants of ERG7^{Y707} from *S. cerevisiae* and analyzed all of them by genetic selection and product characterization. The genetic selection results showed that most mutations in Tyr707 cannot abolish the activity of ERG7 cyclase except Tyr707Arg and the deletion of Tyr707, indicating that the Tyr707 mutations were not detrimental to essential activity of ERG7. However, the loss of the cyclase activity in ERG7$^{\Delta 707}$ mutant suggested that the existence of Tyr707 is crucial for the catalytic function of ERG7.

2. A novel product, which was produced in several mutants including Y707H, Y707Q, Y707E, Y707D, Y707T, Y707S, Y707C, Y707G, and Y707A, was identified as (9*R*,10*S*)-polypoda-8(26),13*E*,17*E*,21-tetraen-3β-ol, a bicyclic triterpene alcohol with a chair-boat conformation, by ^{1}H and ^{13}C NMR for the first time.

3. The product profile revealed that a bicyclic intermediate, (9*R*,10*S*)-polypoda-8(26),13*E*,17*E*,21-tetraen-3β-ol, coupled with two altered deprotonation products, 9β-lanosta-7,24-dien-3β-ol and parkeol, as well as lanosterol were produced in ERG7^{Y707X} mutants. These results suggested that the Tyr707 residue may play an important role in stabilizing both the bicyclic C-8 cation and the final lanosteryl C-8/C-9 cationic intermediates. Tyr707 participated in the B-ring formation of lanosterol by affecting the stability of bicyclic C-8 cationic intermediate after B-ring formation thus for subsequent cyclization.

4. The Tyr707 residue of *S. cerevisiae* ERG7 corresponds to the Tyr609 residue in *A. acidocaldarius* SHC. This finding also demonstrated that the strictly conserved tyrosine residue within OSC has the similar function as in SHC that affects the bicyclic cation stability and thus the subsequent cyclization reaction.

5. The homology model of ERG7 revealed that Tyr707 is spatially proximal to C-8 positions of lanosterol, and its hydroxyl group points toward the B-ring that is suitable to stabilize the bicyclic cationic intermediate. Replaced Tyr707 to other polar side chains may alter the hydrogen-bonding of Tyr707, due to their different orientation and intensity of the dipoles, thus changes the electron distributions for stabilizing the bicyclic cationic intermediate. However, most nonpolar amino acid substitutions formed lanosterol normally without any truncated cyclization product, perhaps because other residues nearby will complement the function of Tyr707 somehow. Nevertheless, the exact interaction remains unclear.

6. In order to acquire a novel bicyclic product with chair-chair conformation from *Sce*ERG7 through the protein redesign, the double site-specified mutagenesis of ERG7$^{F699M/Y707H}$ and ERG7$^{F699M/Y707Q}$ was performed. However, the double mutations of F699M/Y707H

and F699M/Y707Q of *Sce*ERG7 lost the cyclase activity and both didn't generate any product with a molecular mass of *m*/*z* = 426. Perhaps mutation of these two residues may collectively destroy the structural integrity of the active site for substrate binding or intermediate stabilization and result in the total vanish of the cyclase function.

In the part of *Sce*ERG7^{Y710X} mutants:

1. The genetic selection of ERG7^{Y710X} mutants revealed that only one mutant, Tyr710Pro, cannot allow for ergosterol-independent growth. Other mutants all complemented the yeast viability. These results indicated that Tyr710 is not a crucial residue for the catalytic activity of ERG7.

2. The Tyr710 residue of *S. cerevisiae* ERG7 corresponds to the Tyr612 residue in *A. acidocaldarius* SHC. The previous studies revealed that the mutations of Tyr612 in SHC produced mono- and bicyclic products; therefore Tyr612 was thought to influence the C-10 and C-8 cation stability by intensifying the function of both Asp377 and Phe365.

3. In our mutagenesis studies of *Sce*ERG7, however, showed different result with the previous studies. The product profile of ERG7^{Y710X} saturated mutants showed no bicyclic product but the altered deprotonation products, parkeol and 9β-lanosta-7,24-dien-3β-ol as well as lanosterol in several mutants. Only the Tyr710Arg mutant produced two monocyclic products, achilleol A and camelliol C, and no product was produced in the inactive Tyr710Pro mutant.

4. The product distribution of ERG7^{Y710X} indicated that Tyr710 is irrelevant to the bicyclic cationic intermediate but influence the monocyclic C-10 cationic intermediate by placing Trp390 at the correct position to assist the cyclization/rearrangement reaction process. The inactivity of the ERG7^{Y710P} mutant and the prodution of 9β-lanosta-7,24-dien-3β-ol

and parkeol in other mutants also suggested that Tyr710 may play a role in preserving the cyclase structure and the conformation of the active site.

5. According to the human OSC X-ray structure, the Tyr710 residue is located at the end of an α-helix structure and forms a hydrogen-bonding network with Trp587 and Tyr593 *via* water-bridges. The result indicated that Tyr710 may preserve the cyclase structure and the conformation of the active site through the hydrogen-bonding network.

Chapter 5 Future Perspective

In our mutagenesis experiments, the recombinant plasmid was transformed into an HEM1 ERG7 double knockout strain, TKW14C2, for the *in vivo* assay. However, despite of the deletion of oxidosqualene-lanosterol cyclase (ERG7) in the strain, the squalene epoxidase (ERG1) and lanosterol 14 α-demethylase (ERG11) which were located in the upstream and downstream of oxidosqualene-lanosterol cyclase, respectively, still influence the reaction by adding the substrate (oxidosqualene) and removing the product (lanosterol). The incessant consumption of the native product lanosterol and accumulation of other products will result in an inaccuracy of the proportion of products. Therefore, in order to quantify the real amount of the metabolite in *S. cerevisiae* ERG7, we developed an HEM1 ERG1 ERG7 triple knockout yeast strain for the *in vitro* analysis of the mutated oxidosqualene cyclase *via* the addition of the substrates. The *in vitro* analysis can control the reaction away from other regulatory pathways in the living organism and thus can reach the real equilibrium state of the reaction. In addition, we will further develop a HEM1 ERG7 ERG11 knockout strain for *in vivo* assay. The strain will prevent the interference due to the downstream enzymes and consequently ensure the more detailed understanding for the catalytic function of the putative active sites.

On the other hand, we have been demonstrated that the functional role of Tyr707 within *Sce*ERG7 is to stabilize the bicyclic C-8 cationic intermediate in this study, but how oxidosqualene-lanosterol cyclase controls the prefolding of the substrate to the B-ring boat rather than B-ring chair conformation is still unclear. The Tyr707 residue is also highly conserved in some oxidosqualene cyclases such as β-amyrin synthase and lupeol synthase, which pre-folded the substrate into B-ring chair conformation. Using site-directed mutagenesis approach to investigate the function of the residues which correspond to the Tyr707 of *Sce*ERG7 in β-amyrin synthase or lupeol synthase, respectively, may provide us a more comprehensive view for the cyclization mechanism of triterpene synthases.

Chapter 6 Reference

1. Solomons, T. W. G.; Fryhle, C. B. Organic Chemistry, eighth ed., John Wiley and Sons, Inc., 2004.
2. Istvan, E. S.; Deisenhofer, J. *Science* **2001**, 292, 1160-1164.
3. Grundy, S. M.; Cleeman, J. I.; Merz, C. N. B.; Brewer, H. B., Jr; Clark, L. T.; Hunninghake, D. B.; Pasternak, R. C.; Smith, S. C., Jr; Stone, N. J., *J. Am. Coll. Cardiol*. **2004**, 44, 720-732.
4. Bellosta, S.; Paoletti, R.; Corsini, A., *Circulation* **2004**, 109, III50-III57.
5. Pederson, T. R.; Tobert, J. A., *Drug Saf*. **1996**, 14, 11-24.
6. Thoma, R.; Schulz-Gasch, T.; D'Arcy, B.; Benz, J.; Aebi, J.; Dehmlow, H.; Hennig, M.; Stihle, M.; and Ruf, A., *Nature* **2004**, 432, 118-122.
7. Connolly, J. D.; Hill, R. A., *Nat. Prod. Rep*. **2002**, 19, 494-513.
8. Wendt, K. U., *Chem. Int. Ed*. **2005**, 44, 3966-3971.
9. Kannenberg, E. L.; Poralla, K., *Naturwissenschaften* **1999,** 86, 168-176.
10. Ochs, D.; Kaletta, C.; Entian, K.-D.; Beck-Sickinger, A.; Poralla, K., *J. Bacteriol.* **1992**, 174, 298-302.
11. Wendt, K. U.; Poralla, K.; Schulz, G. E., *Science* **1997**, 277, 1811-1815.
12. Wendt, K. U.; Lenhart, A.; Schulz, G. E., *J. Mol. Biol.* **1999**, 286, 175-187.
13. Wendt, K. U.; Schulz, G. E.; Corey, E. J.; Liu, D. R., *Angew. Chem. Intl. Ed.* **2000,** 39, 2812-2833.
14. Hoshino, T.; Sato, T., *Chem. Commun.* **2002,** 291-301.
15. Ruzicka, L.; Eschenmoser, A.; Heusser, H., *Experientia* **1953,** 357-367.
16. Eschenmoser, A.; Ruzicka, L.; Jeger, O.; Arigoni, D., *Helv. Chim. Acta*. **1955,** 38, 1890-1904.
17. Arigoni, D. Biogenesis of terpenes in molds and higher plants. In: Ciba Foundation Symposium Biosynthesis of Terpenes and Sterols, **1959**, 1958, 231-243.
18. Ruzicka, L., *Pure Appl. Chem.* **1963**, 6, 493-522.
19. Xu, R.; Fazio, G. C.; Matsuda, S. P. T., *Phytochemistry* **2004**, 65, 261-291.
20. Honig, B.; Dinur, U.; Nakanishi, K.; Balogh-Nair, V.; Gawinowicz, M.; Arnaboldi, M.; Motto, M., *J. Am. Chem. Soc.* **1979**, 101, 7084-7086.
21. Johnson, W. S.; Telfer, S. J.; Cheng, S.; Schubert, U., *J. Am. Chem. Soc.* **1987**, 109, 2517-2518.
22. Johnson, W. S.; Lindell, S. D.; Steele, J., *J. Am. Chem. Soc*. **1987**, 109, 5852-5853.
23. Johnson, W. S.; Buchanan, R. A.; Bartlett, W. R.; Thaqt, F. S.; Kullnigt, R. K., *J. Am.*

Chem. Soc. **1993,** 115, 504-515.

24. Dougherty, D. A., *Science* **1996**, 271, 163-168.
25. Zacharias, N.; Dougherty, D. A., *TRENDS in Pharmacological Sciences* **2002**, 23, 281-287.
26. Buntel, C. J.; Griffin, J. H., *J. Am. Chem. Soc.* **1992,** 114, 9711-9713.
27. Shi, Z.; Buntel, C. J.; Griffin, J. H., *Proc. Natl. Acad. Sci. U.S.A.* **1994**, 91, 7370-7374.
28. Abe, I.; Tomesch, J. C.; Wattanasin, S.; Prestwich, G. D., *Nat. Prod. Rep.* **1994**, 11, 279.
29. Corey, E. J.; Virgil, S. C., *J. Am. Chem. Soc.*, **1991**, 113, 4025-4026.
30. E. J. Corey, S. C. Virgil; S. Sarshar, *J. Am. Chem. Soc.*, **1991**, 113, 8171-8172.
31. Abe, I., *Nat. Prod. Rep.* **2007**, 24, 1311-1331.
32. Barton, D. H. R.; Jarman, T. R.; Watson, K. C.; Widdowson, D. A.; Boar, R. B.; Damps, K., *Perkin Trans.* **1975**, 1, 1134-1138.
33. Corey, E. J.; Staas, D. D., *J. Am. Chem. Soc.* **1998**, 120, 3526-3527.
34. Corey, E. J.; Cheng, H.; Baker, C. H.; Matsuda, S. P. T.; Li, D.; Song, X., *J. Am. Chem. Soc.* **1997**, 119, 1277-1288.
35. Corey, E. J.; Cheng, H.; Baker, C. H.; Matsuda, S. P. T.; Li, D.; Song, X., *J. Am. Chem. Soc.* **1997**, 119, 1289-1296.
36. Gandour, R. D., *Bioorg. Chem.* **1981**, 10, 169-176.
37. Gao, J.; Pavelites, J. J., *J. Am. Chem. Soc.* **1992**, 114, 1912-1914.
38. van Tamelen, E. E., *J. Am. Chem. Soc.* **1982**, 104, 6480-6481.
39. Gao, D.; Pan, Y. K., *J. Am. Chem. Soc.* **1998,** 120, 4045-4046.
40. Hess, B. A.; Smentek, L., *Molecular Physics.* **2004**, 102, 1201-1206.
41. Corey, E. J.; Virgil, S. C.; Cheng, H.; Baker, C. H.; Matsuda, S. P. T.; Singh, V.; Sarshar, S., *J. Am. Chem. Soc.*, **1995**, 117, 11819-11820.
42. Wu, T. K.; Liu, Y. T.; Chang, C. H., *Chembiochem* **2005**, 6, (7), 1177-1181.
43. T. K. Wu, Y. T. Liu, F. H. Chiu; Chang, C. H., *Org. Lett.* **2006**, 8, (21), 4691-4694.
44. Hess, B. A.; Jr., *J. Am. Chem. Soc.*, **2002**, 124, 10286-10287.
45. B. A. Hess, Jr., *Org. Lett.*, 2003, **5**, 165-167.
46. Abe, I.; Rohmer, M.; Prestwich, G. D., *Chem. Rev.* **1993**, 93, 2189-2206.
47. Blobel, G., *Proc. Natl Acad. Sci. USA* **1980**, 77, 1496-1500.
48. Wu, T. K.; Chang, C. H., *Chembiochem* **2004**, 5, 1712-1715.
49. Wu, T. K.; Yu, M. T.; Liu, Y. T.; Chang, C. H.; Wang, H. J.; Diau, E. W. G., *Org. Lett.* **2006**, 8, 1319-1322.
50. Wu, T. K.; Liu, Y. T.; Chang, C. H.; Yu, M. T.; Wang, H. J., *J Am Chem. Soc.* **2006**, 128, 6414-6419.

51. Wu, T. K.; Wen, H. Y.; Chang, C. H.; Liu, Y. T., *Org. Lett*. **2008**, 10, 2529-2532.
52. Poralla, K.; Hewelt, A.; Prestwich, G. D.; Abe, I.; Reipen I.; Sprenger, G., *Trends Biochem. Sci.*, **1994**, 19, 157-158.
53. Sato, T.; Hoshino, T., *Biosci. Biotechnol. Biochem.*, **1999**, 63, 1171-1180.
54. Sato, T.; Hoshino, T., *Biosci. Biotechnol. Biochem.*, **2001**, 65, 2233–2242.
55. Godzina, S. M.; Lovato, M. A.; Meyer, M. M.; Foster, K. A.; Wilson, W. K.; Gu, W.; de Hostos, E. L.; Matsuda, S. P. T., *Lipids*, **2000**, 35, 249-255 and references cited therein.
56. Feil, C.; Sussmuth, R.; Jung, G.; Poralla, K., *Eur. J. Biochem.* **1996**, 242, 51-55.
57. Sato, T.; Hoshino, T., *Biosci. Biotechnol. Biochem.*, **1999**, 63, 2189-2198.
58. Reinert, D. J.; Balliano, G.; Schulz, G. E., *Chem. Biol.* **2004**, 11, 121-126.
59. Bennett, G. J., Harrison, L. J., Sia, G.-L., Sim, K.-Y., *Phytochemistry* **1993**, 32, 1245-1251.
60. Nguyen, L. H. D.; Harrison, L. J., *Phytochemistry* **1998**, 50, 471-476.
61. Boar, R. B.; Couchman, L. A.; Jaques, A. J.; Perkins, M. J., *J. Am. Chem. Soc.* **1984**, 106, 2476-2477.
62. Shiojima, K.; Arai, Y.; Masuda, K.; Kamada, T.; Ageta, H., *Tetrahedron Lett.* **1983**, 24, 5733-5736.
63. Arai, Y.; Hirohara, M.; Ageta, H.; Hsu, H. Y., *Tetrahedron Lett*. **1992**, 33, 1325-1328.
64. Sato, T.; Hoshino, T., *Chem. Commun.* **1999**, 2005-2006.
65. Toyota, M.; Masuda, K.; Asakawa, Y., *Phytochemistry* **1998**, 48, 297-299.
66. Kinoshita, M.; Ohtsuka, M.; Nakamura, D.; Akita, H., *Chem. Pharm. Bull.* **2002,** 50, 930-934.
67. Nishizawa, M.; Takenaka, H.; Hayashi, Y., *J. Am.* Chem. *Soc.* **1985**, 107, 522-523.
68. Kronja, O.; Orlovic, M.; Humski, K.; Borčić, S., *J. Am. Chem. Soc.* **1991,** 113, 306-2308.
69. Füll, C.; Poralla, K., *FEMS Microbiology Letters* **2000**, 183, 221-224.
70. Füll, C., *FEBS Letters* **2001**, 509, 361-364.
71. Pale-Grosdemange, C.; Merkofer, T.; Rohmer, M.; Poralla, K., *Tetrahedron Lett.* **1999**, 40, 6009-6012.
72. Sato, T.; Sasahara, S.; Yamakami, T.; Hoshino, T., *Biosci. Biotechnol. Biochem.* **2002**, 66, 1660-1670.
73. Schmitz, S.; Füll, C.; Glaser, T.; Albert, K.; Poralla, K., *Tetrahedron Lett.* **2001**, 42, 883-885.
74. 李文暄，利用飽和定點突變方法研究酵母菌氧化黨烯環化酵素內的假設活性區胺基酸對於催化環化/重組反應的影響，國立交通大學生物科技研究所，碩士論文，中華

民國九十六年。

75. 溫晧宇，利用飽和定點突變對氧化黨烯環化酵素內假設活性區域殘基進行結構—反應關係之研究，國立交通大學生物科技研究所，碩士論文，中華民國九十六年。

Appendix 1

Primers used in this thesis

For mutagenesis

TTW-OSC-Y707RQKM-Pvu I-1	5’-CAACCACTCTTgTgCgATCgAA(A/C)(g/A/T)gCC AAgTTATCg- 3’
TTW-OSC-Y707RQKM-Pvu I-2	5’ -CgATAACTTggC(C/T/A)(T/g)TTCgATCgCACAA gAgTggTTg- 3'
TTW-OSC-Y707CV-Pvu I-1	5’-CAACCACTCTTgTgCgATCgAA(g/U)(g/U)CCCA AgTTATCg-3'
TTW-OSC-Y707CV-Pvu I-2	5’-CgATAACTTggg(C/A)(C/A)TTCgATCgCACAAgA gTggTTg-3'
TTW-OSC-Y707R-Pvu I-1	5’-CAACCACTCTTgTgCgATCgAACgACCAAgTTA TCg-3’
TTW-OSC-Y707R-Pvu I-2	5’-CgATAACTTggTCgTTCgATCgCACAAgAgTggTTg -3’
TTW-OSC-Y707K-Pvu I-1	5’-CAACCACTCTTgTgCgATCgAAAAgCCAAgTTA TCg-3’
TTW-OSC-Y707K-Pvu I-2	5’-CgATAACTTggCTTTTCgATCgCACAAgAgTggTTg -3’
TTW-OSC-Y710F-Ava I-1	5’-CAATTgAATACCCgAgTTTCCgATTCTTATTCCC-3’
TTW-OSC-Y710F-Ava I-2	5’-gggAATAAgAATCggAAACTCgggTATTCAATTg-3’
TTW-OSC-Y710M-Ava I-1	5’-CAATTgAATACCCgAgTATgCgATTCTTATTCCC -3’
TTW-OSC-Y710M-Ava I-2	5’-gggAATAAgAATCgCATACTCgggTATTCAATTg -3’

For sequencing

HJW-W657-A1	5’-gTT CAA ACC gCA gCg gCg CTA ATT -3’

Appendix 2

DNA electrophoresis of site-directed mutagenesis

(a)

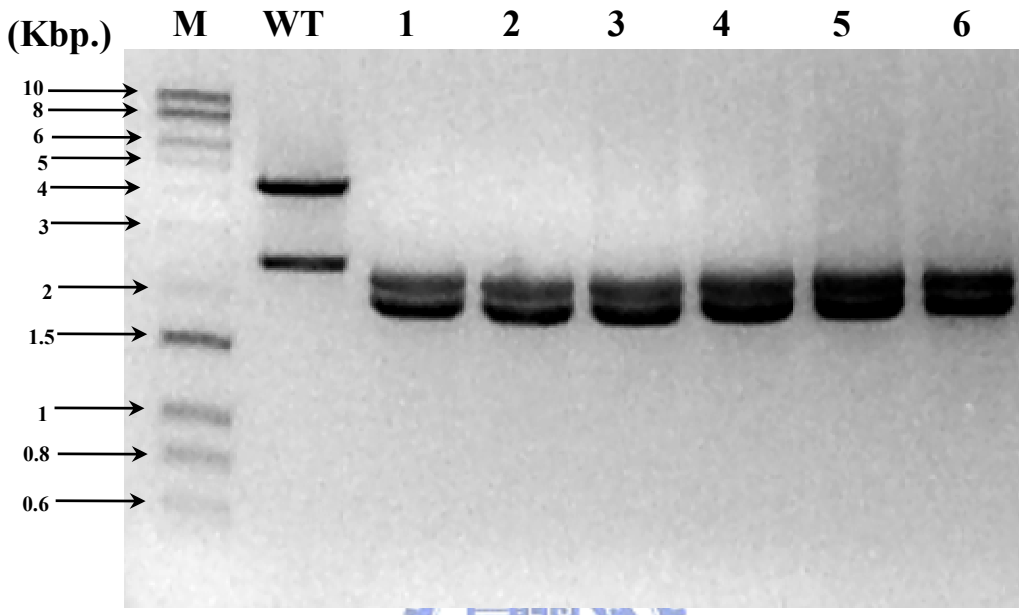

(b)

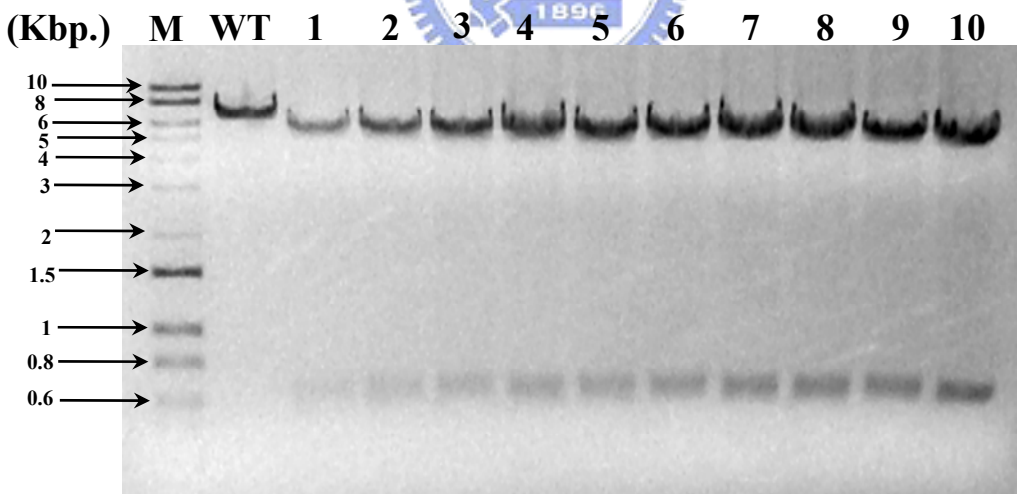

Appendix 2. DNA agarose gel electrophoresis of site-directed mutated plasmid checked by restriction enzymes. Lane M, 10kb-100 bp. DNA marker. Lane WT, pRS314+ERG7. (a) Lane 1-6: pRS314+ERG7Y707X. (b) Lane 1-10: pRS314+ERG7Y710X.

Appendix 3

^{1}H NMR of (9*R*,10*S*)-polypoda-8(26),13*E*,17*E*,21-tetraen-3β-ol

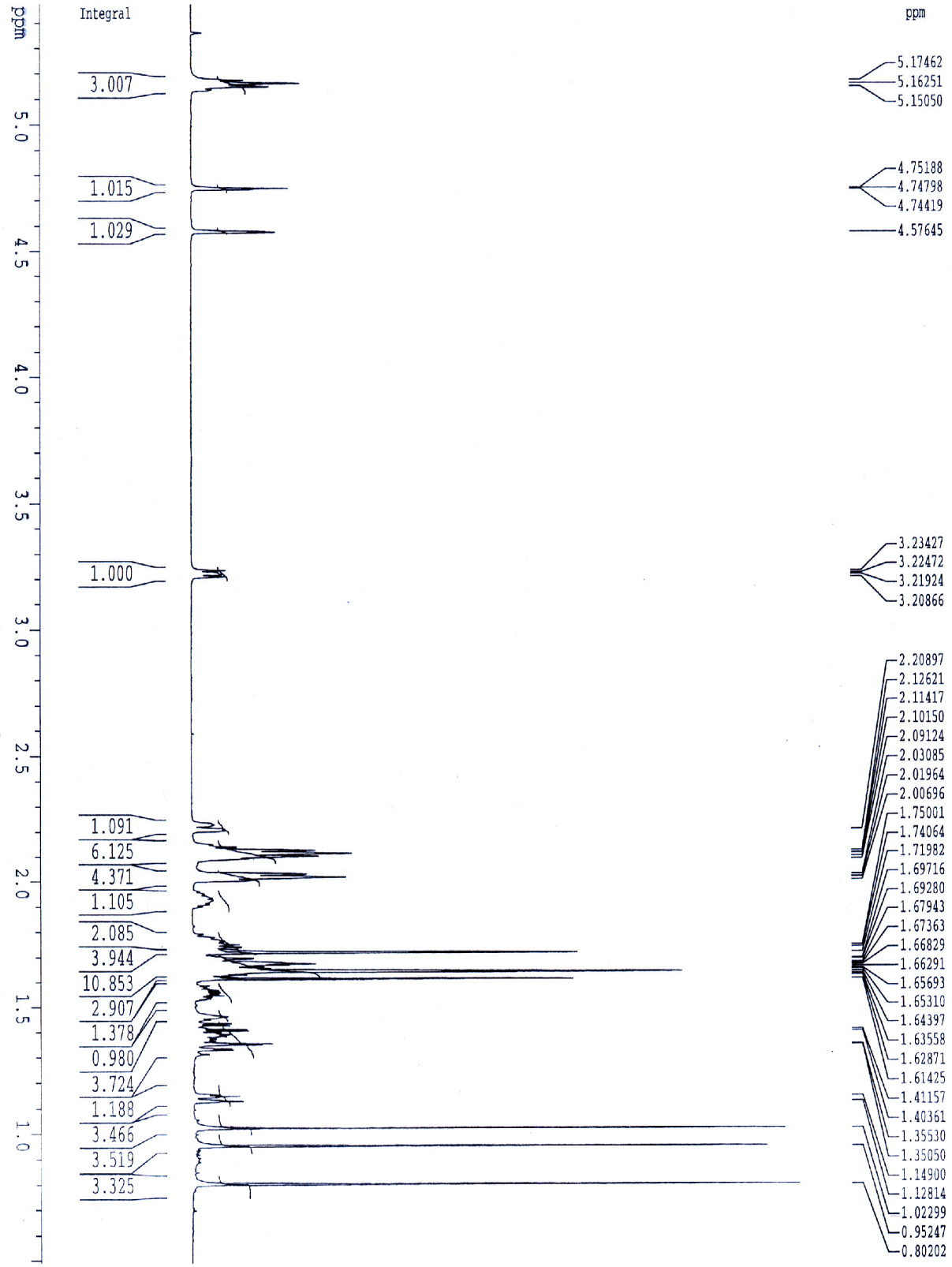

^{13}C NMR and DEPT of (9*R*,10*S*)-polypoda-8(26),13*E*,17*E*,21-tetraen-3β-ol

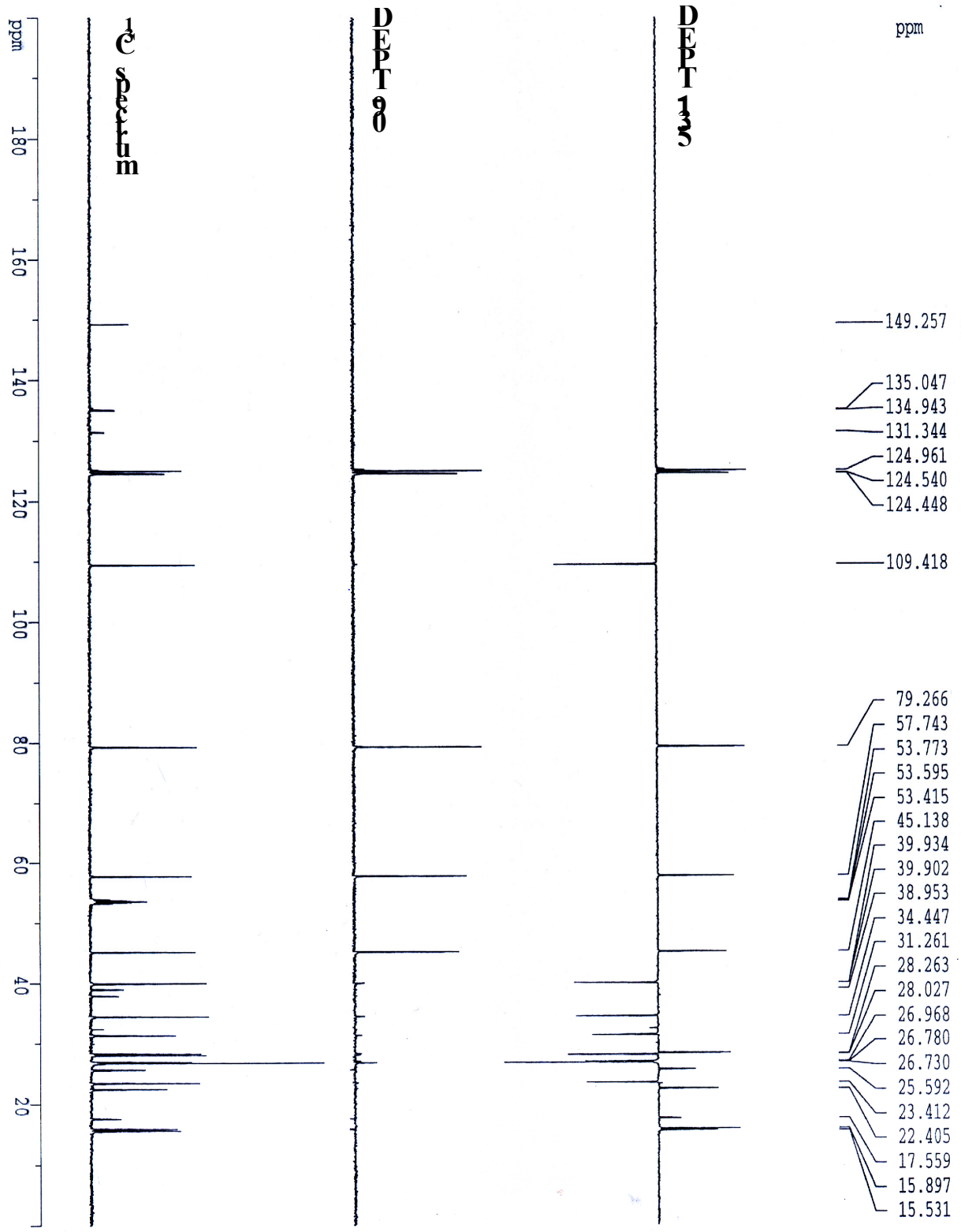

HMQC of (9*R*,10*S*)-polypoda-8(26),13*E*,17*E*,21-tetraen-3β-ol

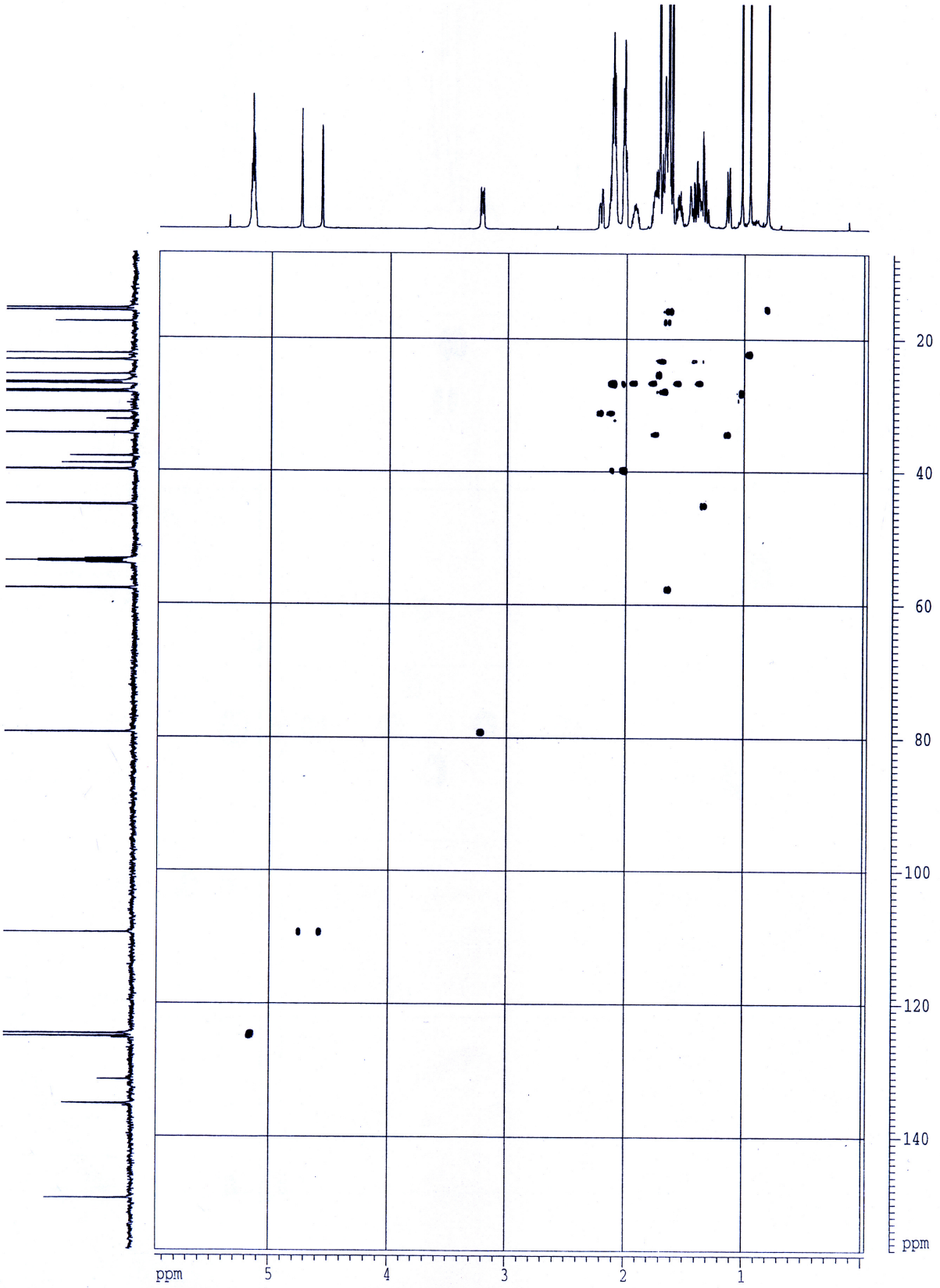

HMBC of (9*R*,10*S*)-polypoda-8(26),13*E*,17*E*,21-tetraen-3β-ol

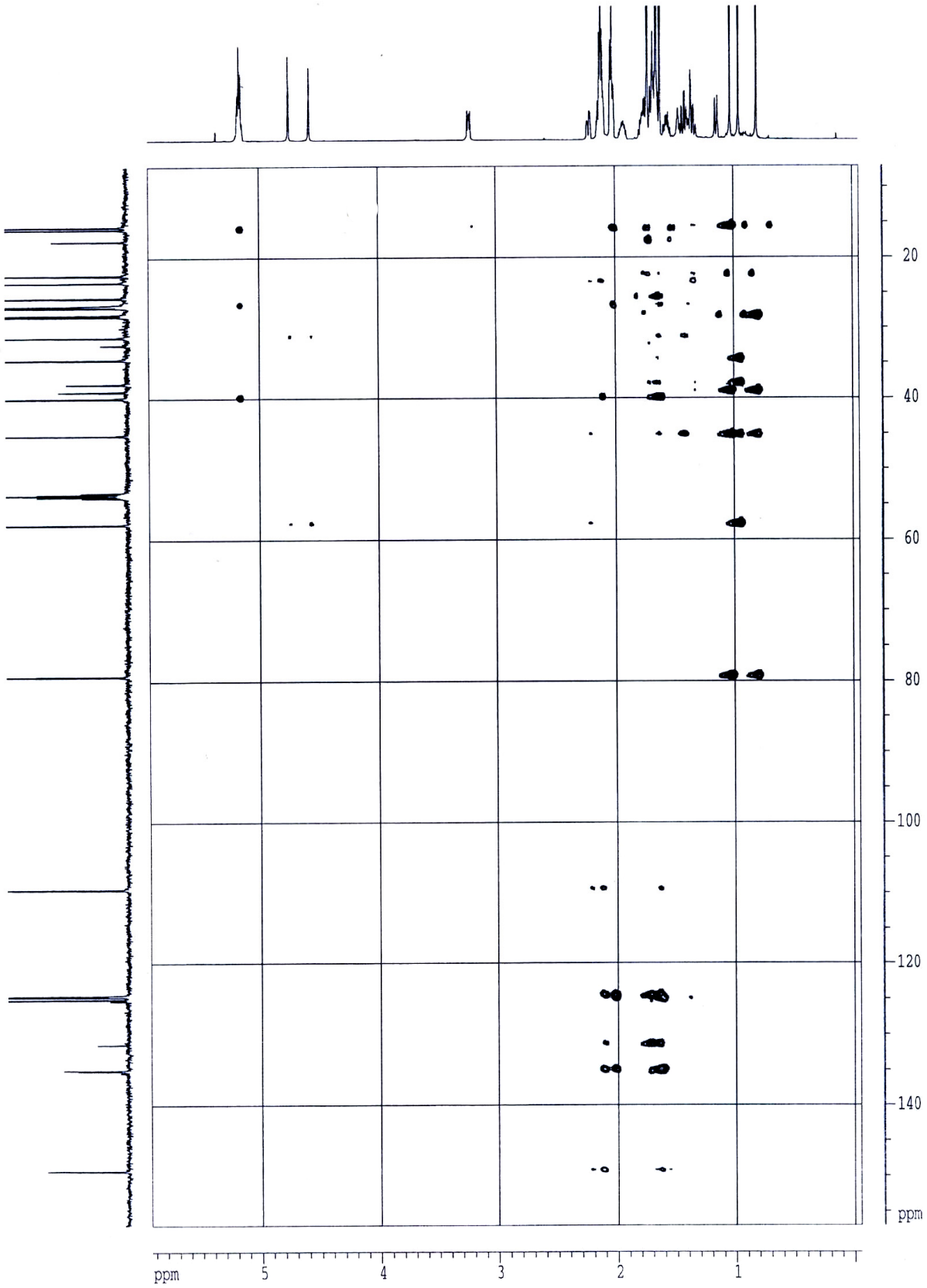
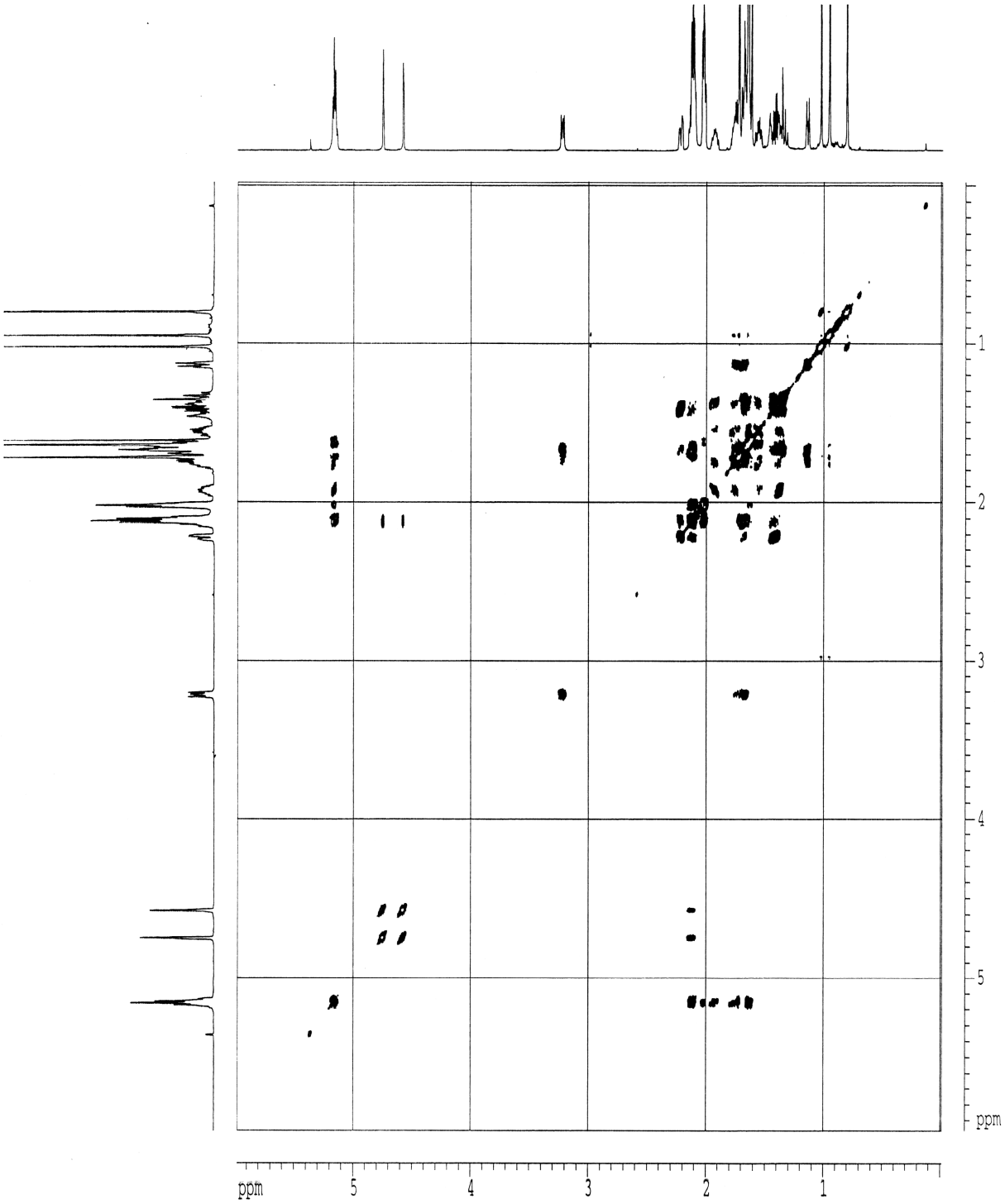
^{1}H-^{1}H COSY of (9*R*,10*S*)-polypoda-8(26),13*E*,17*E*,21-tetraen-3β-ol